MEMORANDUM REPORT

[redacted] MR No. L6D15

WIND-TUNNEL TESTS OF A 1/5-SCALE MODEL OF THE REPUBLIC XP-84 AIRPLANE (ARMY PROJECT MX-578)

II - LATERAL STABILITY AND CONTROL

By Clarence L. Gillis and
Seymour J. Deitchman

1946

NATIONAL ADVISORY COMMITTEE
FOR
AERONAUTICS

NACA LANGLEY MEMORIAL AERONAUTICAL LABORATORY

MEMORANDUM REPORT

 for the

Air Materiel Command, Army Air Forces

[redacted] MR No. L6D15

WIND-TUNNEL TESTS OF A 1/5-SCALE MODEL OF THE REPUBLIC XP-84 AIRPLANE (ARMY PROJECT MX-578) II - LATERAL STABILITY AND CONTROL

By Clarence L. Gillis and
Seymour J. Deitchman

SUMMARY

At the request of the Air Technical Service Command, Army Air Forces, a 1/5-scale powered model of the Republic XP-84 airplane was tested in the Langley 7- by 10-foot tunnel. The results of the lateral stability and control investigation are presented in the present report.

On the basis of low-speed wind-tunnel data, the model is directionally stable at all lift coefficients in the cruising and landing configurations. It has positive effective dihedral for all conditions tested except at the stall. The application of power or the external modification of the jet exit nozzle have little effect on the directional stability and effective dihedral. Rudder lock did not occur on the model for any condition tested. The directional control is satisfactory, and the aileron effectiveness with a limit of 30 pounds stick force will probably be satisfactory up to at least 500 miles per hour at sea level, according to the estimation from low-speed data, with no corrections for compressibility effects.

INTRODUCTION

At the request of the Air Technical Service Command, Army Air Forces, a series of wind-tunnel tests was made

of a 1/5-scale model of the Republic XP-84 airplane (Army Project MX-578). The object of these tests was to determine, and improve if necessary, the stability and control characteristics of the model.

The present report includes the results of the lateral stability and control investigation made on the model. The results of the longitudinal stability and control investigation have been presented in reference 1.

COEFFICIENTS AND SYMBOLS

The results of the tests are presented as standard NACA coefficients of forces and moments. Rolling-, yawing-, and pitching-moment coefficients are given about the center-of-gravity location shown in figure 1 (26.45 percent of the mean aerodynamic chord). The data are referred to the stability axes, which are a system of axes having their origin at the center of gravity and in which the Z-axis is in the plane of symmetry and perpendicular to the relative wind, the X-axis is in the plane of symmetry and perpendicular to the Z-axis, and the Y-axis is perpendicular to the plane of symmetry. The positive directions of the stability axes, of angular displacements of the airplane and control surfaces, and of hinge moments are shown in figure 2.

The coefficients and symbols are defined as follows:

C_L lift coefficient (Lift/qS)

C_X longitudinal-force coefficient (X/qS)

C_Y lateral-force coefficient (Y/qS)

C_l rolling-moment coefficient (L/qSb)

C_m pitching-moment coefficient (M/qSc')

C_n yawing-moment coefficient (N/qSb)

C_h hinge-moment coefficient ($H/qb'\overline{c}^2$)

T_c' effective thrust coefficient based on wing area (T_e/qS)

Lift = -Z

X, Y, Z	forces along axes, pounds
L, M, N	moments about axes, pound-feet
H	hinge moment of control surface, pound-feet
T_e	effective thrust, pounds
q	free-stream dynamic pressure, pounds per square foot $\left(\frac{\rho V^2}{2}\right)$
q_t	effective dynamic pressure at tail, pounds per square foot
S	wing area (10.40 sq ft on model)
c	airfoil section chord, feet
c'	wing mean aerodynamic chord (M.A.C.) (1.48 ft on model)
h	distance from the center of gravity to the thrust axis (0.0165 ft on the model) (positive if the thrust axis is above the center of gravity)
$\overline{c}$	root-mean-square chord of a control surface back of hinge line, feet
b	wing span (7.28 ft on model)
b'	control-surface span along hinge line, feet
V	air velocity, feet per second
V_i	average air velocity at the duct inlet, feet per second
p	rolling velocity, radians per second

and

ρ mass density of air, slugs per cubic foot

α angle of attack of fuselage center line, degrees

ψ angle of yaw, degrees

i_t angle of stabilizer with respect to fuselage center line, degrees; positive when trailing edge is down

δ control-surface deflection, degrees

Subscripts:

a aileron (a_R, a_L, right and left aileron)

r rudder

f flap

V vertical tail

b control-surface balance

MODEL AND APPARATUS

The XP-84 airplane is a jet-propelled fighter-type aircraft. The model was supplied by the Republic Aviation Corporation. A three-view drawing of the model is shown in figure 1, and photographs of the model with the flaps and landing gear retracted and extended are shown in figures 3(a) and 3(b), respectively. The physical characteristics of the full-scale airplane are listed in table I. The model was not checked for accuracy of construction.

After the testing was begun, the vertical tail was modified slightly to correspond to a change which was made on the full-scale airplane. A drawing of the vertical tail and the modification is presented in figure 4, and a photograph of the modified vertical tail is shown in figure 5. Figure 6 shows the plan form and cross section of the aileron. Both rudder and aileron were sealed completely, including the hinge cut-outs and the ends of the balance back to the hinge line.

Power was simulated in the model by means of a two-stage, electrically driven, axial-flow blower mounted in the hollow fuselage. The blower, designed and constructed at Langley, is shown in figure 7. Figure 8 shows a schematic diagram of the fuselage duct with the blower installed. The jet-exit nozzle supplied with the model (fig. 9(a)) was found to have an adverse effect on the longitudinal stability (reference 1), and was replaced by a modified nozzle assembly, designated revision No. 1 and shown in figure 9(b). A further modified tail-pipe and nozzle assembly, revision No. 2, was supplied a short time later by the Republic Corporation, and was the one used for most of these tests. The tail pipe in its final form is shown in figure 9(c).

The wing flaps were fixed to the model by means of two sets of fittings, which held them either in the retracted position or the deflected position. The rudder and aileron angles were set with the aid of templets furnished with the model. A templet used for setting the rudder tab angle was constructed at Langley. Aileron and rudder hinge moments were determined by means of electric strain-gage installations in the model. These installations were made at Langley.

TESTS AND RESULTS

Test conditions.- The tests were made in the Langley 7- by 10-foot tunnel at dynamic pressures of 16.37, 9.21, and 6.39 pounds per square foot, which correspond to airspeeds of about 80, 60, and 50 miles per hour, respectively. The test Reynolds numbers were about 1,100,000, 830,000, and 690,000, respectively, based on the wing mean aerodynamic chord of 1.48 feet.

Test procedure.- Tests were run for three power conditions: power off, idling power, and full power. During the power-off tests, the duct was open to the air stream and the blower was allowed to windmill with no power input. Power-on tests were run duplicating the full-scale airplane inlet velocity ratio V_1/V for the full-power and idling-power conditions. The thrust coefficient T_c' could not be duplicated at the same time, since the inlet and exit areas were fixed for the model, and were not in the proper ratio to give the correct jet

velocity for a cold jet. The investigations of reference 1 showed that it was more desirable to reproduce the effects on stability of the air flow through and around the nose of the model, which are determined by the ratio V_i/V, than the effects due to the thrust, since the latter are small and can easily be calculated.

The average air velocity at the inlet to the fuselage duct was determined by means of a survey rake across the duct inlet (fig. 10, reference 1) for the tests to determine the rudder characteristics and from the readings of a pitot-static tube at the jet exit for all the other tests. The inlet velocity was varied by varying the blower speed, which was measured by an electric tachometer accurate to within ±0.2 percent.

The variation of V_i/V with lift coefficient for the full-scale airplane at sea level was determined from data supplied by the Republic Corporation, and is shown in figure 11. Blower calibrations were made at the different values of dynamic pressure used, measuring the velocity of the air entering the duct and the thrust, with flaps and landing gear retracted and tail off, at an angle of attack of 0°, for a range of blower speeds.

The results of the calibrations were used with figure 11 to determine the variation of blower speed with model lift coefficient.

Tests to determine the characteristics in yaw were run by yawing the model through a range of angles from -10° to 40° with constant angle of attack. At each angle of attack, the blower speed was held constant throughout the yaw range at the value necessary to give the correct V_i/V ratio at 0° angle of yaw. Since the V_i/V ratios vary with yaw when the blower speed and angle of attack are held constant, the V_i/V ratio is known to be correct only at zero yaw. The variation with angle of yaw will probably be similar for the model and airplane, however, and therefore will probably have no effect on the validity of the results.

Data were taken for the angles of yaw from -10° to 40°, rather than ±40°, since the model was symmetrical and there were no asymmetric power conditions. Only those rudder deflections (up to the maximum) were tested

which were needed to trim the model through the test yaw range; for the rudder tab tests, the tab was deflected to trim the rudder. The direction of the yaw range was inadvertently reversed for the tests of the fuselage alone and the tests to determine the effect of nozzle shape, but because of the symmetry of the model there were probably no adverse effects on the results.

Lateral-stability parameters were obtained by running the model through the angle-of-attack range at angles of yaw of $\pm 5^\circ$, and assuming a straight-line variation of C_n, C_l, and C_Y with angle of yaw between these angles.

Aileron characteristics were determined by running the model through the angle-of-attack range, at zero angle of yaw, with the right aileron alone deflected. For the estimation of the wing-tip helix angle, $Pb/2V$, the differential linkage obtained from the Republic Corporation and shown in figure 12 was assumed.

Corrections.- Corrections for the tares caused by the model support strut and jet-boundary corrections to the angles of attack, longitudinal-force coefficients, and the tail-on pitching-moment coefficients were applied in all cases, except for the tests of the fuselage alone and the tests to determine the effect of nozzle shape. The jet-boundary corrections for those tests were negligible, and the lack of tares was not considered to have any significant effect on the validity of the results. Jet-boundary corrections were also applied to the rolling-moment coefficients for the aileron tests.

The jet-boundary corrections were made by adding to the test data the following increments, determined by the methods of reference 2:

$$\Delta\alpha = 1.00C_L$$

$$\Delta C_X = -0.0175C_L^2$$

$$\Delta C_m = -8.65C_L\left(\frac{0.216}{\sqrt{qt/q}} - 0.116\right)\left(\frac{\partial C_m}{\partial i_t}\right)$$

$$\Delta C_l = -0.0255C_l$$

where $\Delta\alpha$ is in degrees, and $\partial C_m/\partial i_t$ is the variation of the pitching-moment coefficient with stabilizer angle, and is taken from reference 1.

Corrections were added to the longitudinal-force data for the full- and idling-power conditions to account for the fact that the thrust coefficient for the full-scale airplane was not reproduced for these tests. The correction is

$$\Delta C_X = \Delta T_c'$$

where $\Delta T_c'$ is the difference between the full-scale airplane and the model thrust coefficients at the same lift coefficient. Figure 10 shows the required variation of thrust coefficient with lift coefficient. The actual thrust data for the model were obtained from calibrations of the model blower unit.

Corrections to account for the effect of the thrust force were also applied to the pitching-moment coefficients as follows:

$$\Delta C_m = - \left(\frac{h}{c'}\right) \Delta T_c'$$

Results.- The results were obtained for the following model configurations:

1. Cruising configuration
   Flaps retracted
   Landing gear retracted

2. Landing configuration
   Flaps deflected 40°
   Landing gear extended

The results of the lateral-stability and control investigation for these configurations are presented in the following figures:

	Figure no.
A. Lateral-stability parameters	
Power off	13
Full power	14
B. Aerodynamic characteristics in yaw	
Power off	15
Full power	16
Fuselage alone, power off	17
Effect of tail-pipe shape, power off	18

DISCUSSION

Stability

Rudder-fixed directional stability.- The results of the parameter tests (figs. 13 and 14) indicate that the model is directionally stable at all lift coefficients at angles of yaw between ±5°, and the tests to determine the aerodynamic characteristics in yaw show directional stability at all angles of yaw for which the rudder can trim the model. The values of $\partial C_n/\partial \psi$ from the yaw tests for angles of yaw between ±5° are shown on figures 13 and 14 by the large symbols. Since the data from the yaw tests show no change in stability between ±5° angle of yaw, the results of the parameter tests may be taken as valid for purposes of discussion at angles of yaw near zero. There is fairly good agreement between the results of the yaw tests and the parameter tests. The vertical tail was modified as previously described after the parameter tests of figure 13 were run and the modification maintained for the remainder of the investigation. The increased directional stability in the yaw tests might be attributed to the slightly larger vertical tail.

A comparison of the data for power effects at any lift coefficient in each configuration shows that the effect of power on the directional stability is negligible. Analysis of the data has shown that such a comparison must be made for the model at very nearly the

same angles of attack power on and power off in any configuration, since changes in the sidewash over the vertical tail occur which will affect the stability differently at different angles of attack.

Effective dihedral.- The model has positive effective dihedral $\left(\text{approximately } \frac{\partial C_l / \partial \psi}{0.0002}\right)$ in all cases, the values for the model with the tail on ranging between about 6° and 9° for all conditions, except at the stall. The variation of effective dihedral with lift coefficient is small, as is the variation with yaw up to about 15° angle of yaw. The effective dihedral is smaller at higher angles of yaw; this might be partially ascribed to stalling of the vertical tail. The values at zero yaw from the yaw tests show fair agreement with those from the parameter tests, though in general the yaw tests show slightly higher effective dihedral. There is no apparent reason for this difference. The application of power has little effect on the effective dihedral.

The results show that the tail makes a substantial contribution to the effective dihedral at low to intermediate lift coefficients. The values of effective dihedral for the complete model remain relatively constant, while the effective dihedral of the wing-fuselage combination increases with lift coefficient, showing that the contribution of the tail decreases with increasing angle of attack, as might be expected.

The data from the yaw tests show that for many of these tests the rolling-moment curves did not pass through zero at zero yaw. Upon examination of the test program it was discovered that all the tests for which the curves do pass through zero were made at the same time, and the remainder of the tests were made later, after the model had been taken apart and reassembled. This indicates that the failure to trim was probably due to a change in the adjustment of the model. There would be no effect on the validity of the lateral stability data, however.

Rudder-free stability.- The rudder-free data (figs. 15 and 16) do not show rudder lock, though the directional stability at angles of yaw above 10° is less when the rudder is free than when it is fixed. During the power-off tests the rudder was not free to deflect the maximum amount (±25°), but was stopped about 3° before the maximum deflection. The differences between the power-off and the

power-on rudder-free characteristics are therefore mainly due to different values of maximum rudder deflection and not to the effect of power.

The yawing-moment curve fails to pass through zero yawing-moment at zero angle of yaw in all cases when the rudder is freed. It is believed that this failure to trim is due to some unknown asymmetry of the vertical tail.

The slope of the rudder hinge-moment curves, $\partial C_h/\partial\psi$, at small angles of yaw tends to be irregular and fluctuates around zero. If full-scale constructional errors or Reynolds number effects result in appreciable positive values of $\partial C_h/\partial\psi$ there is a possibility of developing steady-state hunting oscillations unless the friction in the rudder control system is kept low.

Effect of nozzle shape.- The tests made with the original and modified nozzles (fig. 18) show that the external shape of the nozzle has a negligible effect on the lateral and directional stability, particularly at small angles of yaw.

Control

Rudder effectiveness.- Values of the rudder effectiveness $\partial C_n/\partial\delta_r$ for the different configurations and power conditions are presented in the following table:

Model configuration	Power	α (deg)	C_I	$\partial C_n/\partial\delta_r$ $\psi = 0$
Cruising	Idling	10.1	0.84	-0.0017
Landing	Idling	6.1	1.07	-.0017
Cruising	Full	6.3	.54	-.0018
Cruising	Full	1.4	.17	-.0017
Landing	Full	5.6	1.01	-.0016

The rudder is powerful enough at maximum deflection to trim the model at a maximum of about 12° angle of yaw in the cruising configuration, and about 15° in the landing configuration, with the wings level. The rudder effectiveness decreases considerably in most cases after about

20° rudder deflection. The application of power appears to have little effect on the rudder characteristics.

Rudder tab effectiveness.- Following are the values of rudder tab effectiveness, $\partial C_{h_r}/\partial \delta_t$, obtained from figures 21 and 22 for the model in the cruising configuration:

Power	α	$\frac{\partial C_{h_r}}{\partial \delta_t}$, $\psi = 0$
Idling	10.1	-0.0019
Full	6.3	-.0016
Full	1.4	-.0015

The tab is powerful enough at maximum deflection to reduce the rudder hinge moment to zero when the model is trimmed at about 5° angle of yaw in the cruising configuration.

Aileron characteristics.- Computations were made according to the method of reference 3 to determine the variation of wing-tip helix angle, pb/2V, with airspeed at sea level as limited by the maximum aileron deflection or by a maximum stick force of 30 pounds. This variation is presented in figure 24 as an indication of the aileron effectiveness. The values of pb/2V have been corrected for wing twist by the method of reference 4, using a value of wing stiffness obtained from a Republic Corporation representative at Langley. The computations for pb/2V and stick force were carried to 500 miles per hour at sea level since that is the highest specific speed at which the Army Air Forces specifications state a requirement for pb/2V. No corrections have been made for compressibility effects, but it is believed the estimate will reflect the approximate order of magnitude of the pb/2V characteristics of the airplane over the range indicated, inasmuch as the speed at which force-break occurs on the wing is well above 500 miles per hour at sea level. Stick-force computations were made using a boost ratio of 10:1, to correspond to that used on the airplane.

These calculations indicate that the aileron effectiveness with a limit of 30 pounds stick force will

probably be satisfactory throughout the speed range in both configurations.

Deflecting the ailerons produced favorable yawing moments up to about 7° angle of attack in the cruising configuration and about 9° in the landing configuration, after which the yawing moments became unfavorable. Sufficient data were not available to determine why the ailerons should produce favorable yawing moments. However, the tail-off data in figure 13 indicate that the deflection of a flap can produce marked effects on the yawing-moment characteristics of the model. It is possible, therefore, that the deflection of the aileron on this model would alter the field of flow about the fuselage and vertical tail in such a manner as to overshadow the direct contribution of the aileron to the yawing moment.

CONCLUSIONS

The following conclusions may be drawn from the results of the low-speed wind-tunnel tests to determine the lateral and directional stability and control characteristics of the Republic XP-84 airplane:

1. The model is directionally stable at all lift coefficients in the cruising and landing configurations.

2. The model has positive effective dihedral for all conditions tested, except at the stall. The variation of effective dihedral with lift coefficient is small.

3. The application of power or the external modification of the nozzle have little effect on the directional stability and control and effective dihedral.

4. Rudder lock did not occur on the model for any condition tested.

5. The rudder is powerful enough at maximum deflection to trim the model at a maximum of about 12° angle of yaw in the cruising configuration, and about 15° in the landing configuration, with the wings level.

6. The rudder tab is powerful enough at maximum deflection to reduce the rudder hinge moment to zero when the model is trimmed at about 5° angle of yaw in the cruising configuration.

7. The aileron effectiveness with a limit of 30 pounds stick force as estimated from low-speed data with no compressibility correction, will probably be satisfactory up to at least 500 miles per hour at sea level.

8. Deflecting the ailerons produces favorable yawing moments up to about 10° angle of attack after which the yawing moments become unfavorable.

Langley Memorial Aeronautical Laboratory
National Advisory Committee For Aeronautics
Langley Field, Va.

Clarence L. Gillis
Aeronautical Engineer

Seymour J. Deitchman
Aeronautical Engineer

Approved.

Hartley A. Soulé
Chief of Stability Research Divisc

CB

REFERENCES

1. Gillis, Clarence L., and Andrews, Thomas B., Jr.: Wind-Tunnel Tests of a 1/5-Scale Model of the Republic XR-84 Airplane (Army Project MX-578). I - Longitudinal Static Stability and Control. NACA MR No. L6D05, Army Air Forces, 1946.

2. Gillis, Clarence L., Polhamus, Edward C., and Gray, Joseph L., Jr.: Charts for Determining Jet-Boundary Corrections for Complete Models in 7- by 10-Foot Closed Rectangular Wind Tunnels. NAC ARR No. L5G31, 1945.

3. Swanson, Robert S., and Toll, Thomas A.: Estimation of Stick Forces from Wind-Tunnel Aileron Data. NACA ARR No. 3J29, 1943.

4. Pearson, Henry A., and Aiken, William S., Jr.: Charts for the Determination of Wing Torsional Stiffness Required for Specified Rolling Characteristics or Aileron Reversal Speed. NACA ACR No. L4L13, 1944.

TABLE I

PHYSICAL CHARACTERISTICS OF THE REPUBLIC XP-84 AIRPLANE

Type	Jet-propelled fighter
Wing:	
Area, sq ft	260
Span, ft	36.42
Aspect ratio	5.1
Taper ratio	0.57
Dihedral, deg	5
Incidence at station 27 in. from center line	0
Sweepback, 25-percent-chord line, deg	3.08
Geometric twist, deg (washin)	2
Mean aerodynamic chord (M.A.C.), ft	7.39
Station zero to 50-percent chord of M.A.C., ft	16.5
Airfoil section	Republic R-4, 45-15-12-.9
Horizontal tail:	
Area, sq ft	43.5
Span, ft	15.9
Aspect ratio	4.6
Elevator area behind hinge line, sq ft	13
Root-mean-square chord of elevator, ft	0.990
Airfoil section	Republic R-4, 40-010
Vertical tail:	
Total area, sq ft	35.80
Rudder area behind hinge line, sq ft	7.39
Height, from center line of fuselage, ft	8.10
Root-mean-square chord of rudder, ft	1.21
Airfoil section	Republic R-4, 40-010
High-lift device (slotted flap):	
Chord	0.26c
Location	Extends from wing-fuselage juncture to 0.51 b/2
Weight and balance:	
Normal gross weight, lb	12,500
Wing loading, lb/sq ft	48.1
Normal center-of-gravity position, percent M.A.C.	26.45
Center-of-gravity range, percent M.A.C.	26.45 to 30.00

NATIONAL ADVISORY
COMMITTEE FOR AERONAUTICS

FIGURE LEGENDS

Figure 1.- Three-view drawing of the 1/5-scale model of the Republic XP-84 airplane. (All of the dimensions are given in inches.)

Figure 2.- System of axes and control-surface hinge moments and deflections. Positive values of forces, moments, and angles are indicated by arrows. Positive values of tab hinge moments and deflections are in the same directions as the positive values for the control surfaces to which the tabs are attached.

Figure 3.- Three-quarter front view of the 1/5-scale model of the Republic XP-84 airplane mounted in the Langley 7- by 10-foot tunnel.

(a) Cruising configuration.

Figure 3.- Concluded.

(b) Landing configuration.

Figure 4.- Original and modified vertical tails tested on the 1/5-scale model of the Republic XP-84 airplane. (All dimensions are given in inches.)

Figure 5.- Vertical tail of the 1/5-scale model of the Republic XP-84 airplane.

Figure 6.- Plan form of wing and aileron, and typical aileron section of the 1/5-scale model of the Republic XP-84 airplane.

Figure 7.- Axial-flow blower used in the 1/5-scale model of the Republic XP-84 airplane.

Figure 8.- Schematic longitudinal section of the fuselage of the 1/5-scale model of the Republic XP-84 airplane.

Figure 9.- Original and modified nozzles for the 1/5-scale model of the Republic XP-84 airplane.

(a) Original nozzle.

Figure 9.- Continued.

(b) Revision no. 1.

FIGURE LEGENDS - Continued

Figure 9.- Concluded.

(c) Revision no. 2.

Figure 10.- Variation of effective thrust coefficient with lift coefficient for the full-scale Republic XP-84 airplane at sea level. w/s = 48.1 lb/sq ft.

Figure 11.- Variation of inlet velocity ratio with lift coefficient for the full-scale Republic XP-84 airplane.

Figure 12.- Aileron and stick geometry for the right aileron of the Republic XP-84 airplane.

Figure 13.- Lateral-stability parameters for the 1/5-scale model of the Republic XP-84 airplane. Power off.

(a) Cruising configuration.

Figure 13.- Concluded.

(b) Landing configuration.

Figure 14.- Lateral-stability parameters for the 1/5-scale model of the Republic XP-84 airplane. Full power; $i_t = 0°$.

(a) Cruising configuration.

Figure 14.- Concluded.

(b) Landing configuration.

Figure 15.- The aerodynamic characteristics in yaw of the 1/5-scale model of the Republic XP-84 airplane. Power off; $i_t = 0°$.

(a) Cruising configuration, $\alpha = 10.8°$.

Figure 15.- Continued.

(a) Concluded.

FIGURE LEGENDS - Continued

Figure 15.- Continued.

(b) Cruising configuration, $\alpha = 0.1^{\circ}$.

Figure 15.- Continued.

(b) Concluded.

Figure 15.- Continued.

(c) Landing configuration, $\alpha = 6.0^{\circ}$.

Figure 15.- Continued.

(c) Concluded.

Figure 15.- Continued.

(d) Landing configuration; $\alpha = -1.5^{\circ}$; $\delta_r = 0^{\circ}$.

Figure 15.- Concluded.

(d) Concluded.

Figure 16.- The aerodynamic characteristics in yaw of the 1/5-scale model of the Republic XP-84 airplane. Full power; $i_t = 0^{\circ}$.

(a) Cruising configuration; $\alpha = 6.0^{\circ}$.

Figure 16.- Continued.

(a) Concluded.

Figure 16.- Continued.

(b) Cruising configuration, $\alpha = 2.0^{\circ}$.

Figure 16.- Continued.

(b) Concluded.

Figure 16.- Continued.

(c) Landing configuration, $\alpha = 7.6^{\circ}$.

FIGURE LEGENDS - Continued

Figure 16.- Concluded.

(c) Concluded.

Figure 17.- The aerodynamic characteristics in yaw of the fuselage of the 1/5-scale model of the Republic XP-84 airplane. Power off.

Figure 17.- Concluded.

Figure 18.- The effect of nozzle shape on the aerodynamic characteristics in yaw of the 1/5-scale model of the Republic XP-84 airplane. Cruising configuration. Power off. $\alpha = 1.2^\circ$.

Figure 18.- Concluded.

Figure 19.- Effect of rudder deflection on the aerodynamic characteristics in yaw of the 1/5-scale model of the Republic XP-84 airplane. Idling power; $i_t = 1^\circ$.

(a) Cruising configuration, $\alpha = 10.1^\circ$.

Figure 19.- Continued.

(a) Continued.

Figure 19.- Continued.

(a) Continued.

Figure 19.- Continued.

(a) Concluded.

Figure 19.- Continued.

(b) Landing configuration, $\alpha = 6.1^\circ$.

Figure 19.- Continued.

(b) Continued.

FIGURE LEGENDS - Continued

Figure 19.- Continued.

(b) Continued.

Figure 19.- Concluded.

(b) Concluded.

Figure 20.- The effect of rudder deflection on the aerodynamic characteristics in yaw of the 1/5-scale model of the Republic XP-84 airplane. Full power, $i_t = 1^\circ$.

(a) Cruising configuration, $\alpha = 6.3^\circ$.

Figure 20.- Continued.

(a) Continued.

Figure 20.- Continued.

(a) Continued.

Figure 20.- Continued.

(a) Concluded.

Figure 20.- Continued.

(b) Cruising configuration, $\alpha = 1.4^\circ$.

Figure 20.- Continued.

(b) Continued.

Figure 20.- Continued.

(b) Continued.

Figure 20.- Continued.

(b) Concluded.

Figure 20.- Continued.

(c) Landing configuration, $\alpha = 5.6^\circ$.

FIGURE LEGENDS - Continued

Figure 20.- Continued.

(c) Continued.

Figure 20.- Continued.

(c) Continued.

Figure 20.- Concluded.

(c) Concluded.

Figure 21.- Effect of rudder tab deflection on the aerodynamic characteristics in yaw of the 1/5-scale model of the Republic XP-84 airplane. Cruising configuration; Idling power; $\delta_r = 0$; $\alpha = 10.1^\circ$; $i_t = 1^\circ$.

Figure 21.- Continued.

Figure 21.- Concluded.

Figure 22.- Effect of rudder tab deflection on the aerodynamic characteristics in yaw of the 1/5-scale model of the XP-84 airplane. Full power; $\delta_r = 0$; $i_t = 1^\circ$. Cruising configuration.

(a) $\alpha = 6.3^\circ$.

Figure 22.- Continued.

(a) Continued.

Figure 22.- Continued.

(a) Concluded.

Figure 22.- Continued.

(b) $\alpha = 1.4^\circ$

Figure 22.- Continued.

(b) Continued.

FIGURE LEGENDS - Concluded

Figure 22.- Concluded.

(b) Concluded.

Figure 23.- Aileron characteristics of the 1/5-scale model of the Republic XP-84 airplane. Power off; $i_t = 0^\circ$.

(a) Cruising configuration.

Figure 23.- Continued.

(a) Concluded.

Figure 23.- Continued.

(b) Landing configuration.

Figure 23.- Concluded.

(b) Concluded.

Figure 24.- Estimated variation of wing-tip helix angle with airspeed at sea level for the full-scale Republic XP-84 airplane. Maximum aileron deflection with stick force limit of 30 lbs.; $\delta_r = 0$.

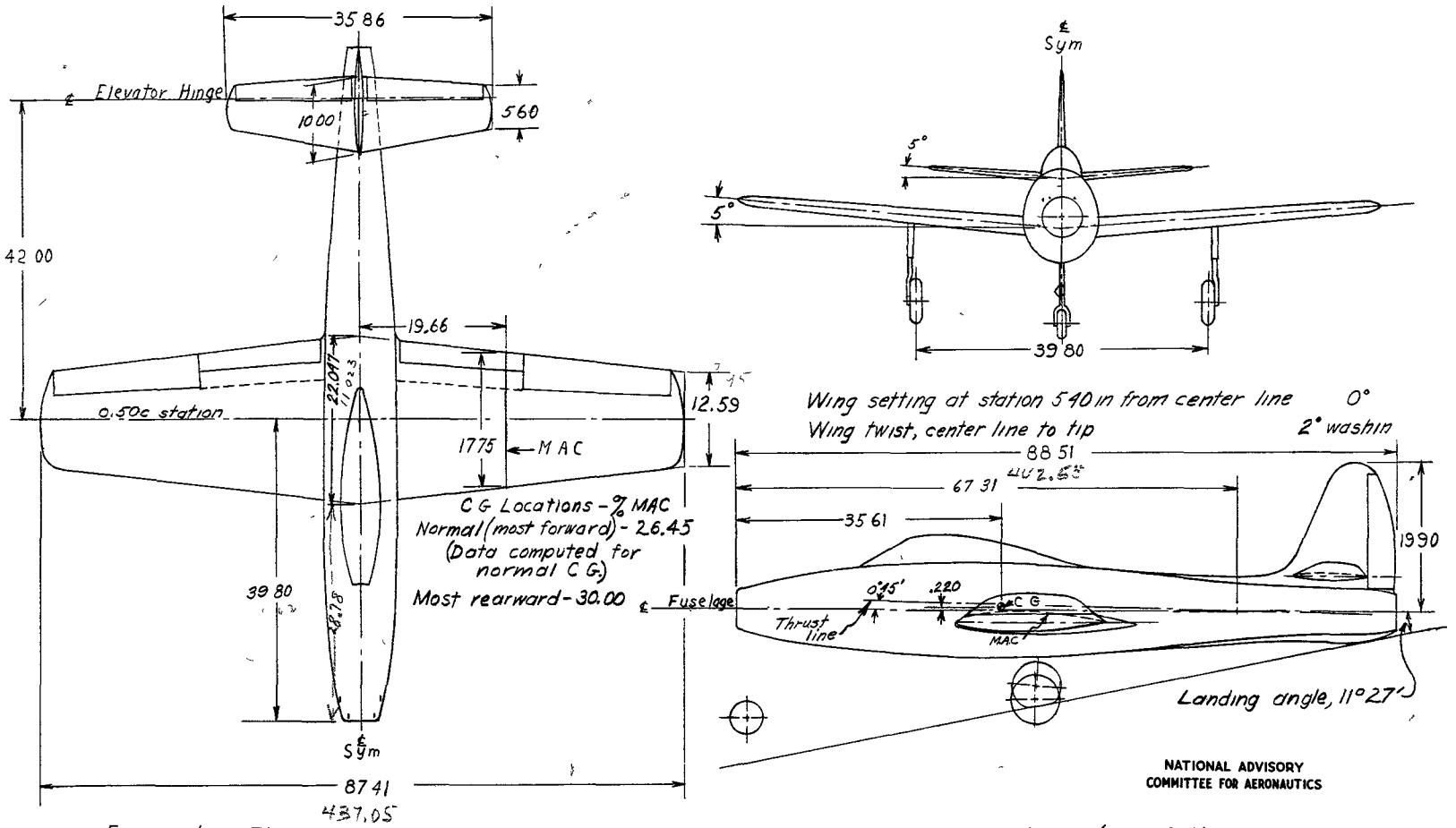

Figure 1 - Three-view drawing of the 1/5-scale model of the Republic XP-84 airplane (All of the dimensions are given in inches)

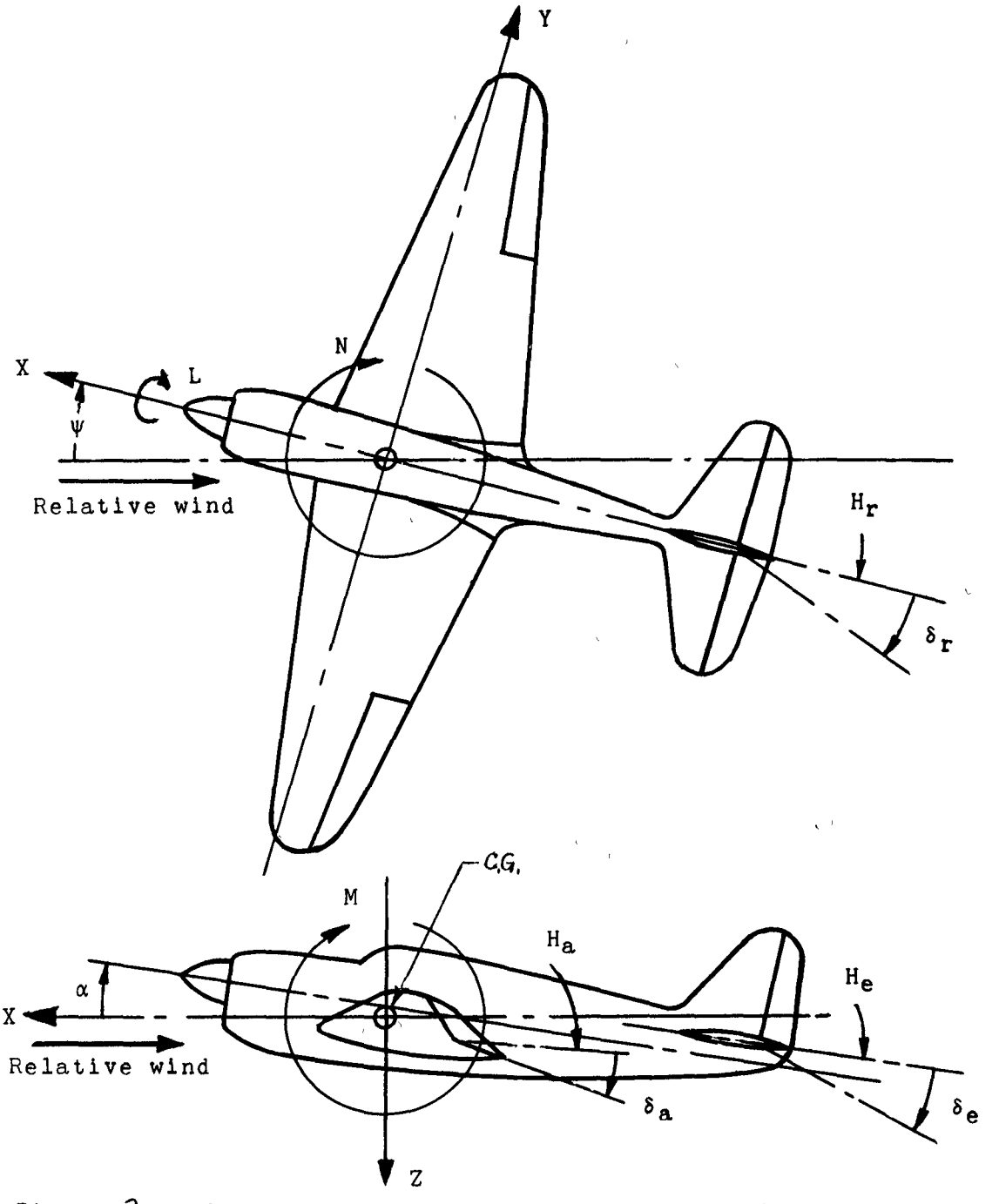

Figure 2 .- System of axes and control-surface hinge moments and deflections. Positive values of forces, moments, and angles are indicated by arrows. Positive values of tab hinge moments and deflections are in the same directions as the positive values for the control surfaces to which the tabs are attached.

NATIONAL ADVISORY
COMMITTEE FOR AERONAUTICS

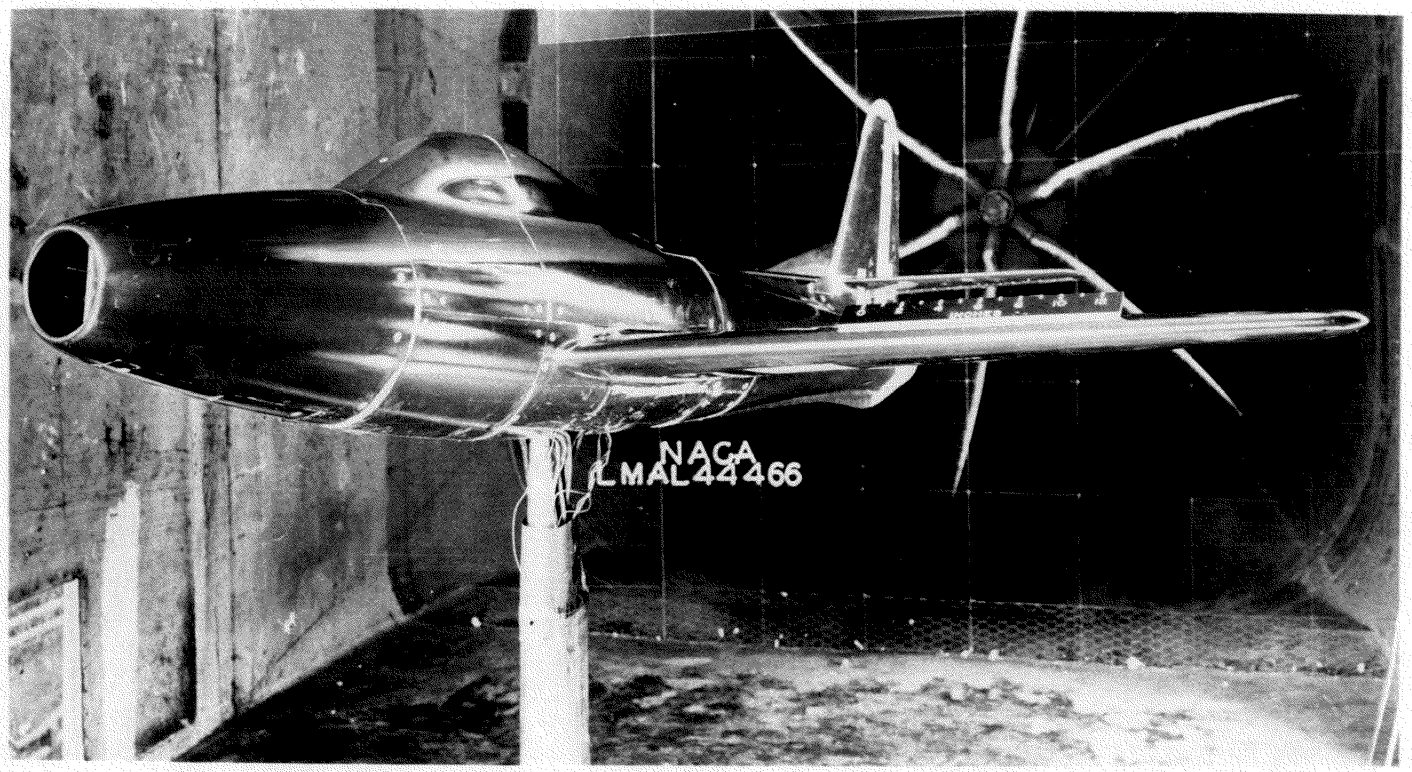

(a) Cruising configuration.

Figure 3.- Three-quarter front view of the $\frac{1}{5}$-scale model of the Republic XP-84 airplane mounted in the Langley 7- by 10-foot tunnel.

NATIONAL ADVISORY COMMITTEE FOR AERONAUTICS
LANGLEY MEMORIAL AERONAUTICAL LABORATORY - LANGLEY FIELD, VA.

MR No. L6D15

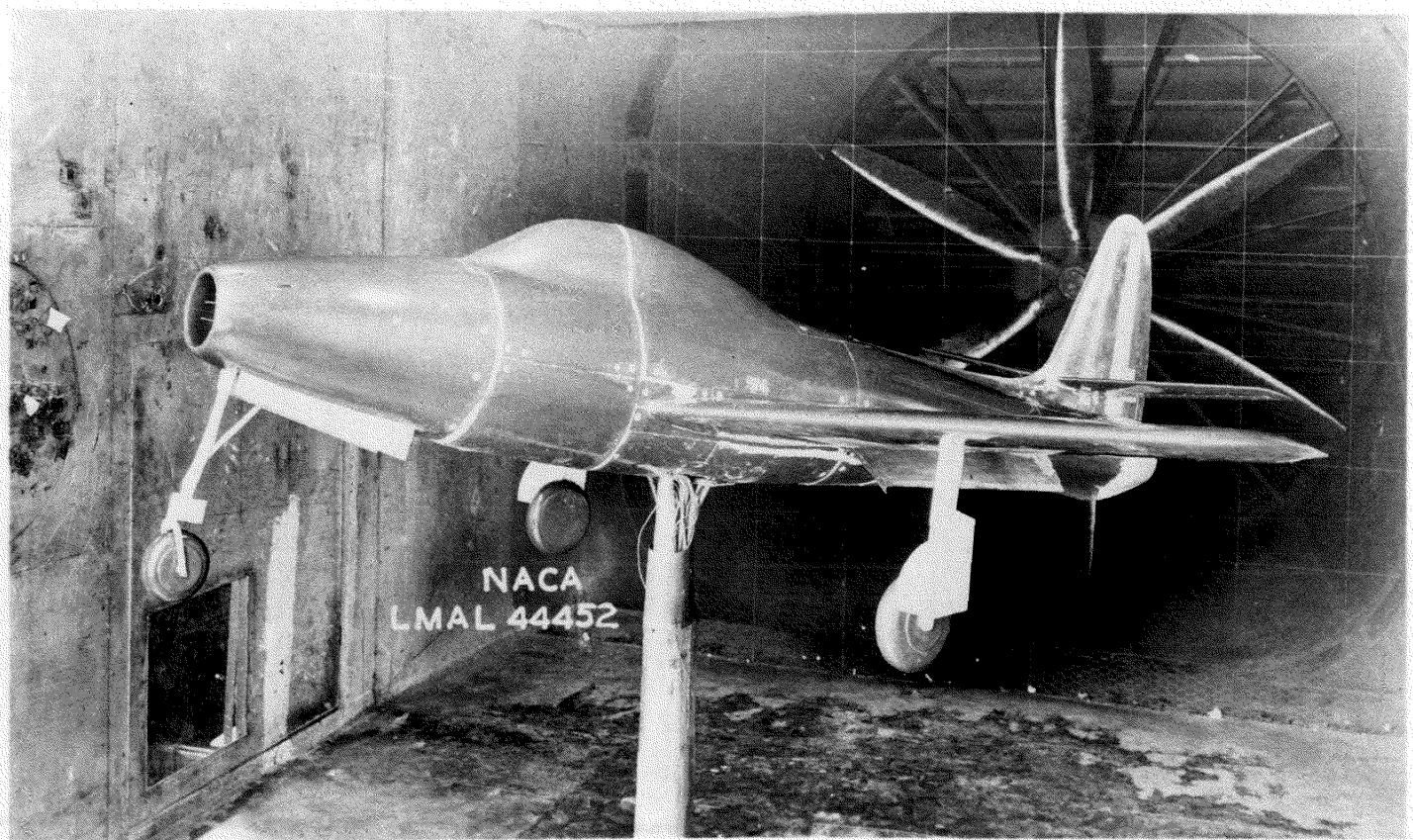

(b) Landing configuration.

Figure 3.- Concluded.

NATIONAL ADVISORY COMMITTEE FOR AERONAUTICS
LANGLEY MEMORIAL AERONAUTICAL LABORATORY - LANGLEY FIELD, VA.

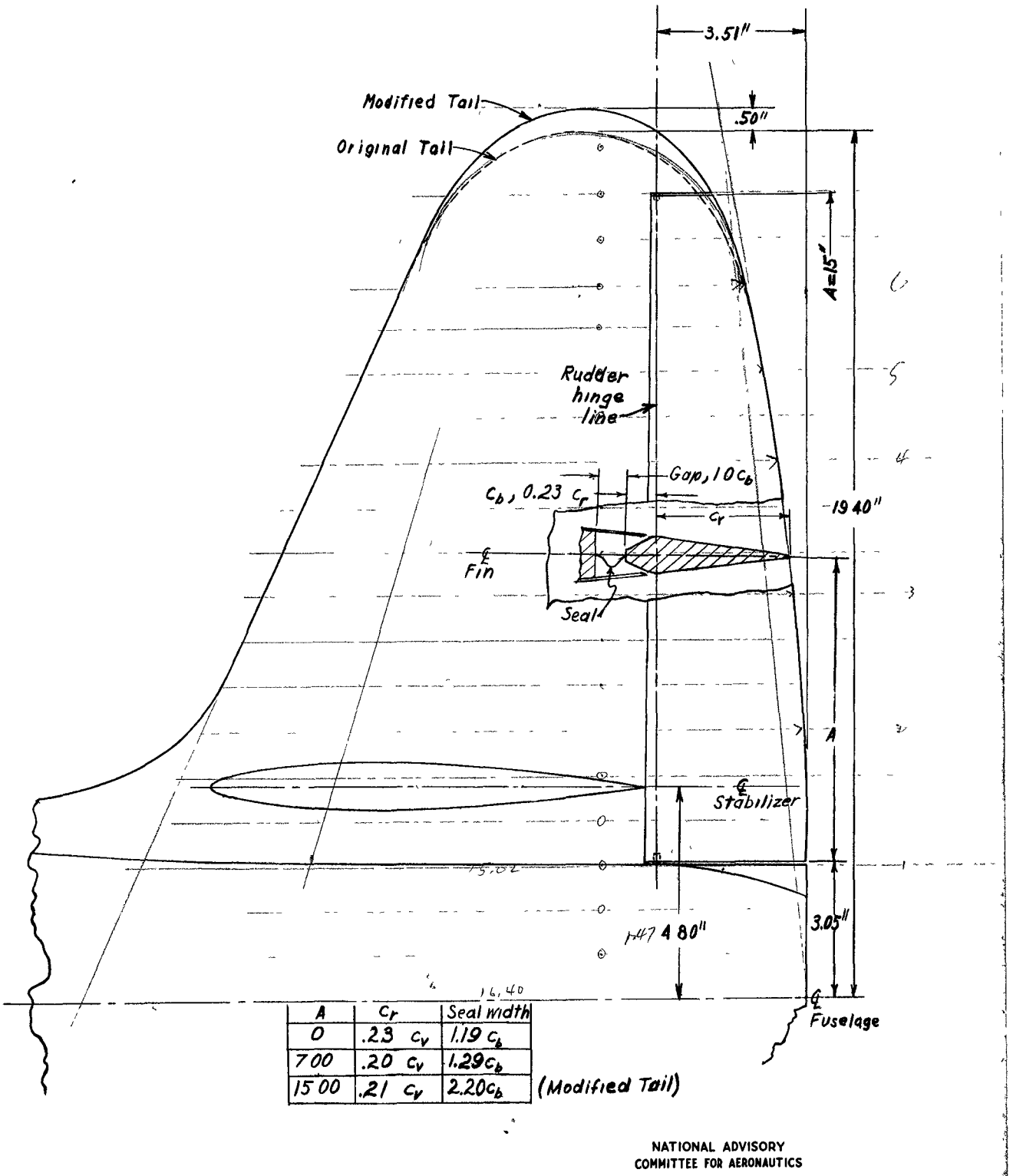

A	c_r	Seal width
0	.23 c_v	1.19 c_b
700	.20 c_v	1.29 c_b
1500	.21 c_v	2.20 c_b

(Modified Tail)

NATIONAL ADVISORY COMMITTEE FOR AERONAUTICS

Figure 4 - Original and modified vertical tails tested on the 1/5-scale model of the Republic XP-84 airplane (All dimensions are given in inches.)

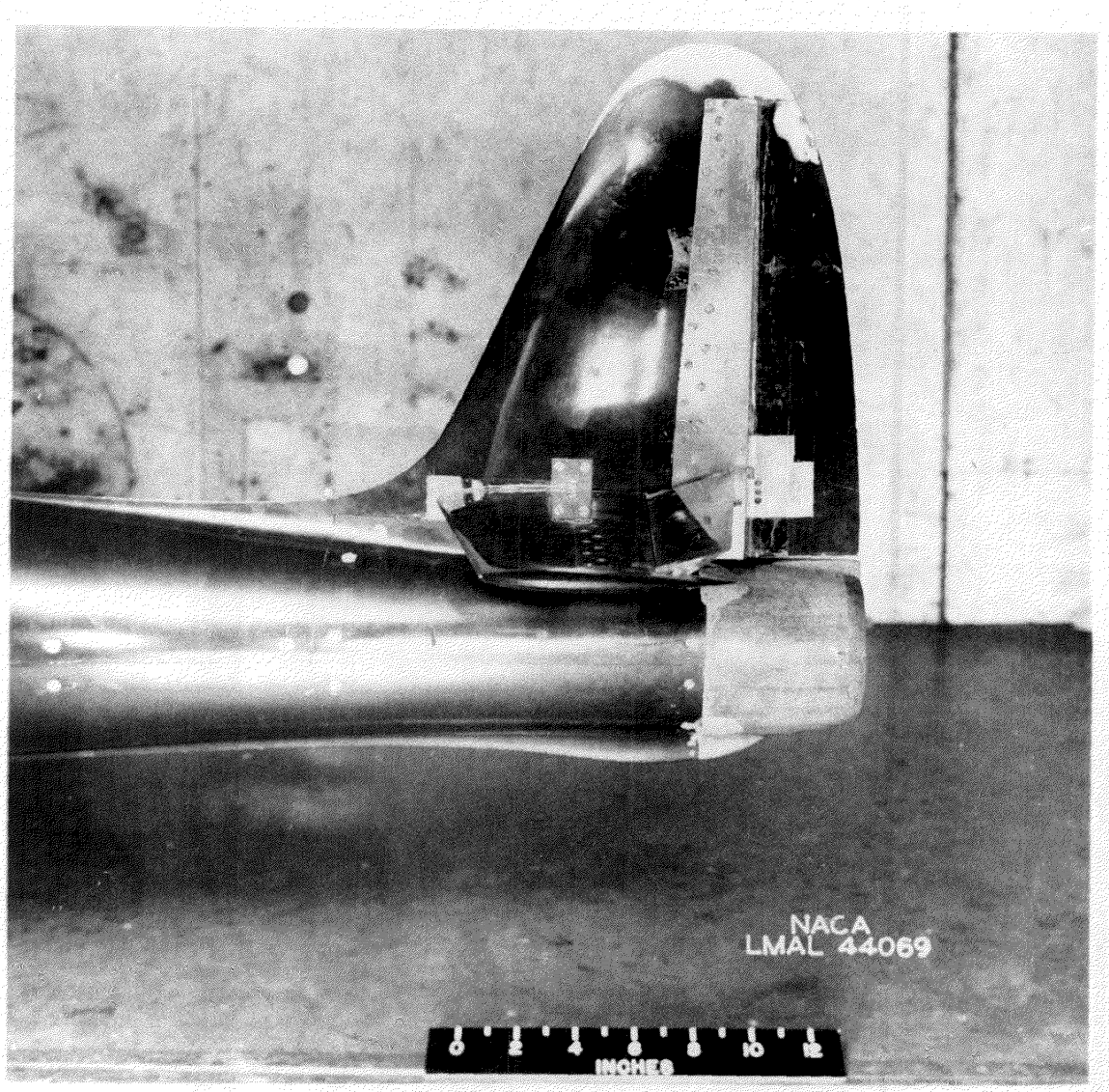

Figure 5.- Vertical tail of the $\frac{1}{5}$-scale model of the Republic XP-84 airplane.

NATIONAL ADVISORY COMMITTEE FOR AERONAUTICS
LANGLEY MEMORIAL AERONAUTICAL LABORATORY - LANGLEY FIELD, VA.

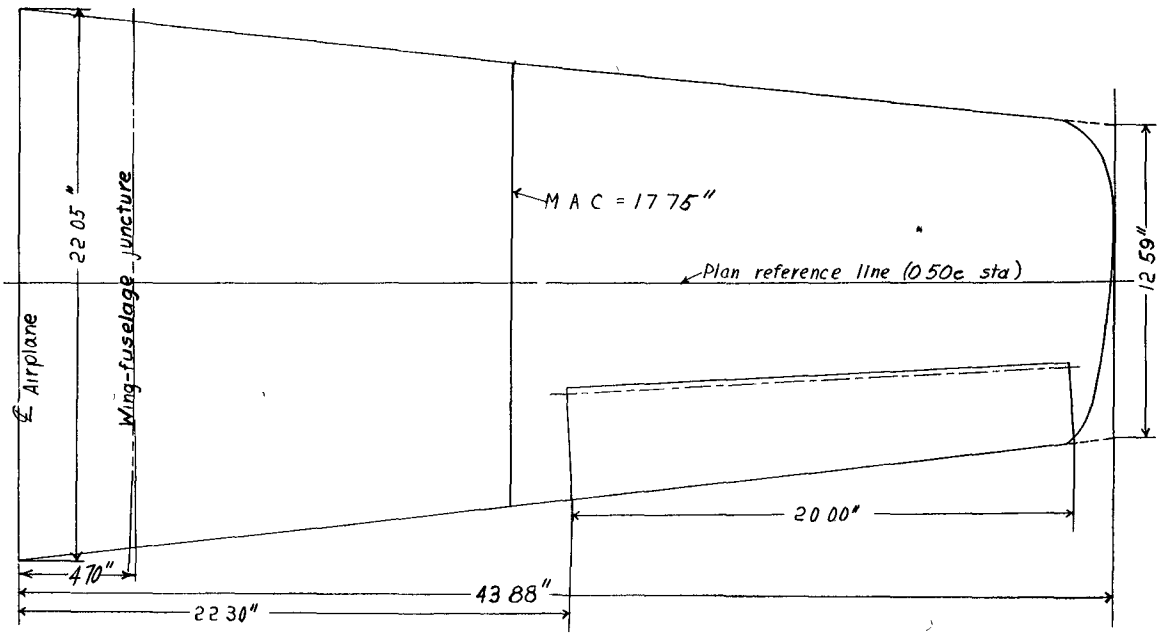

(All dimensions are in chord plane)

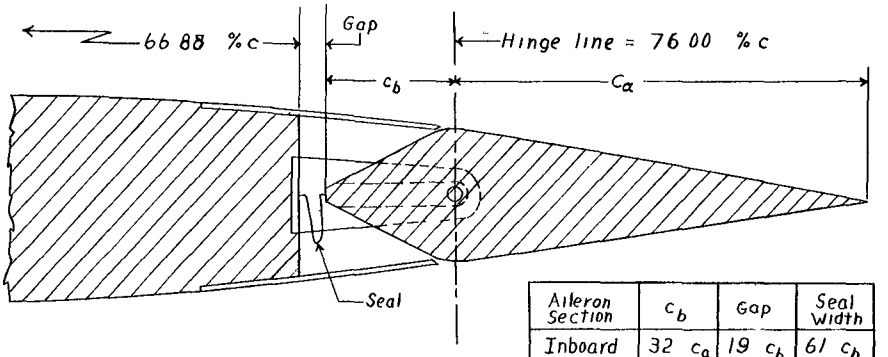

Aileron Section	c_b	Gap	Seal Width
Inboard	32 c_a	19 c_b	61 c_b
Outboard	29 c_a	29 c_b	72 c_b

Section through aileron

NATIONAL ADVISORY
COMMITTEE FOR AERONAUTICS

Figure 6 – Plan form of wing and aileron, and typical aileron section of the 1/5-scale model of the Republic XP-84 airplane.

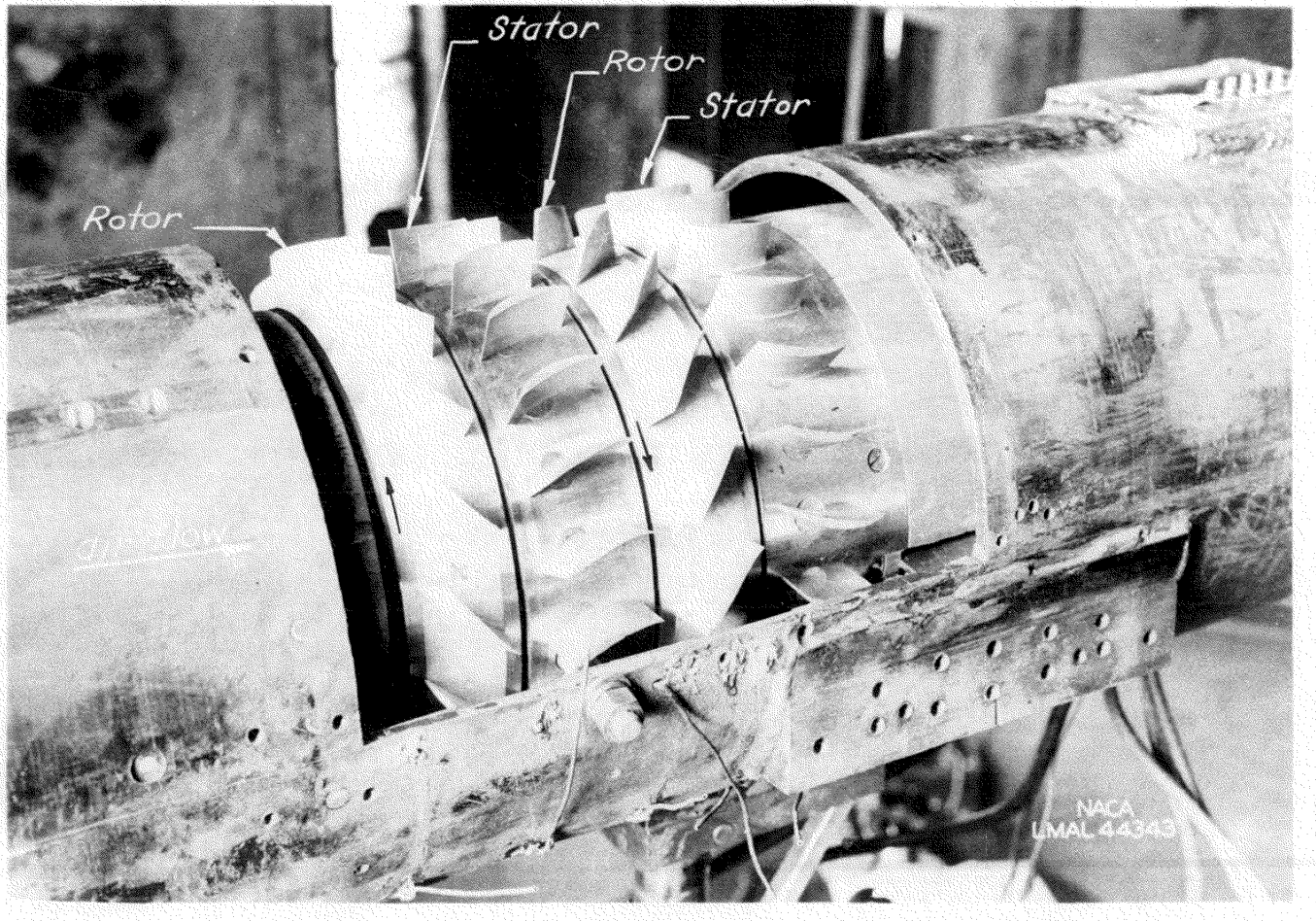

Figure 7.- Axial-flow blower used in the $\frac{1}{5}$-scale model of the Republic XP-84 airplane.

NATIONAL ADVISORY COMMITTEE FOR AERONAUTICS
LANGLEY MEMORIAL AERONAUTICAL LABORATORY - LANGLEY FIELD, VA.

MR No. L6D15

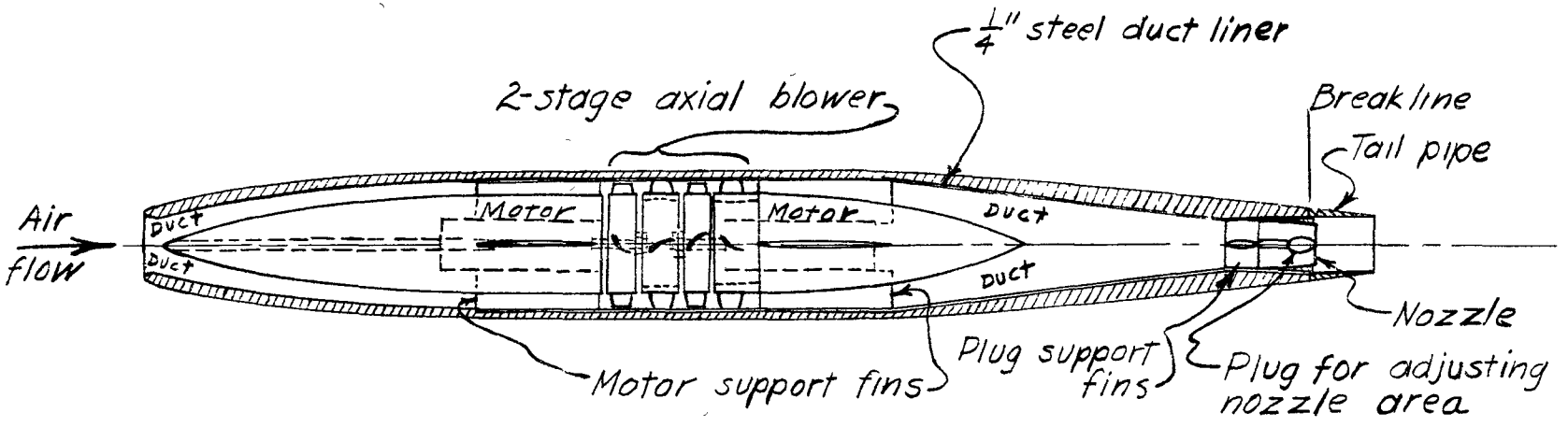

Power: 2 -27 h.p. variable frequency induction motors
Transverse section of duct is circular

NATIONAL ADVISORY
COMMITTEE FOR AERONAUTICS

Figure 8: Schematic longitudinal section of the fuselage of the 1/5 - scale model of the Republic XP-84 airplane.

MR No. L6D15

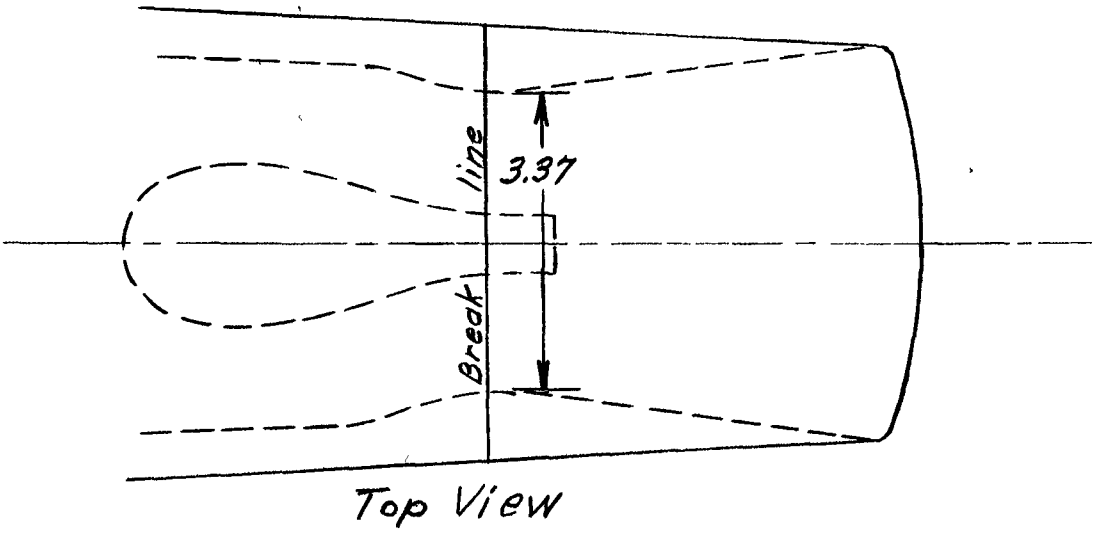

Top View

Note: cross section is elliptical

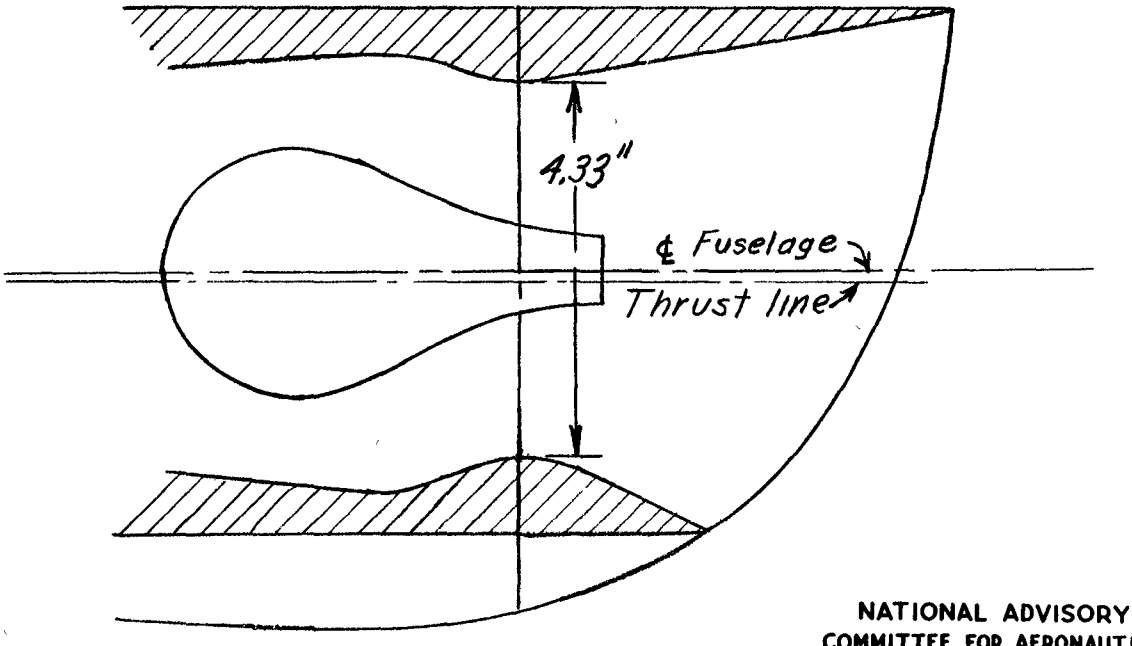

NATIONAL ADVISORY
COMMITTEE FOR AERONAUTICS

Side View

(a) Original nozzle

Figure 9. - Original and modified nozzles for the 1/5-scale model of the Republic XP-84 airplane.

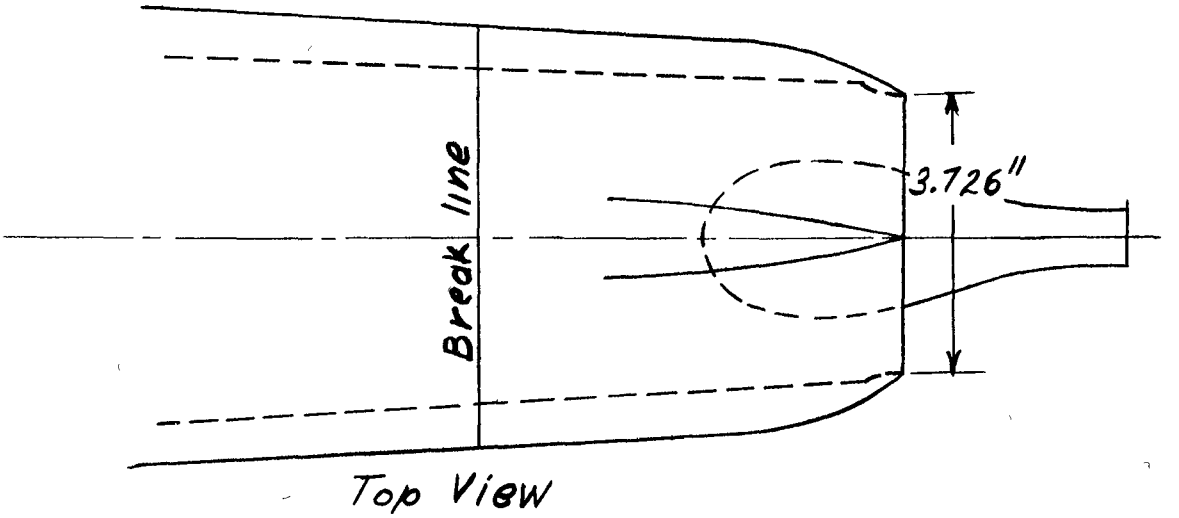

Top View

Note: cross section is elliptical

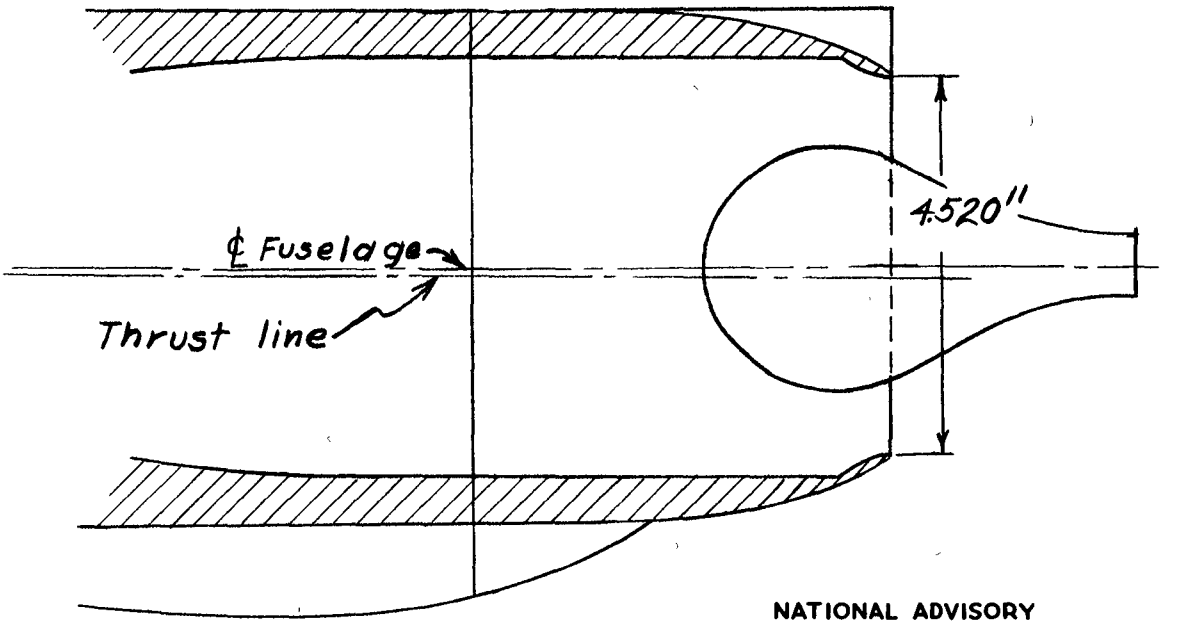

Side View

NATIONAL ADVISORY
COMMITTEE FOR AERONAUTICS

(b)-Revision#1

Figure 9.-(Continued)

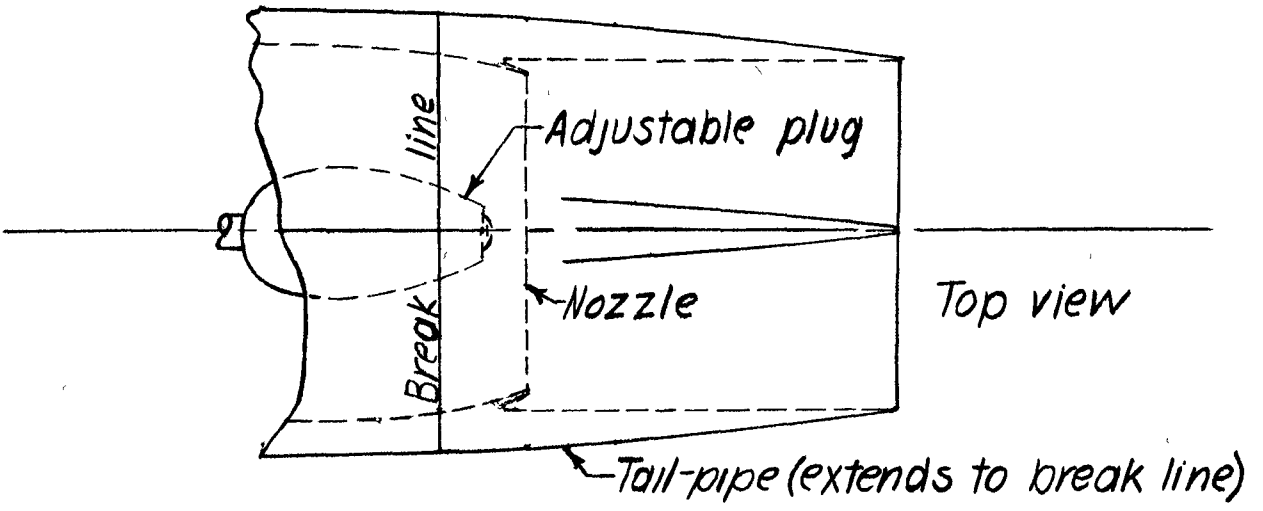

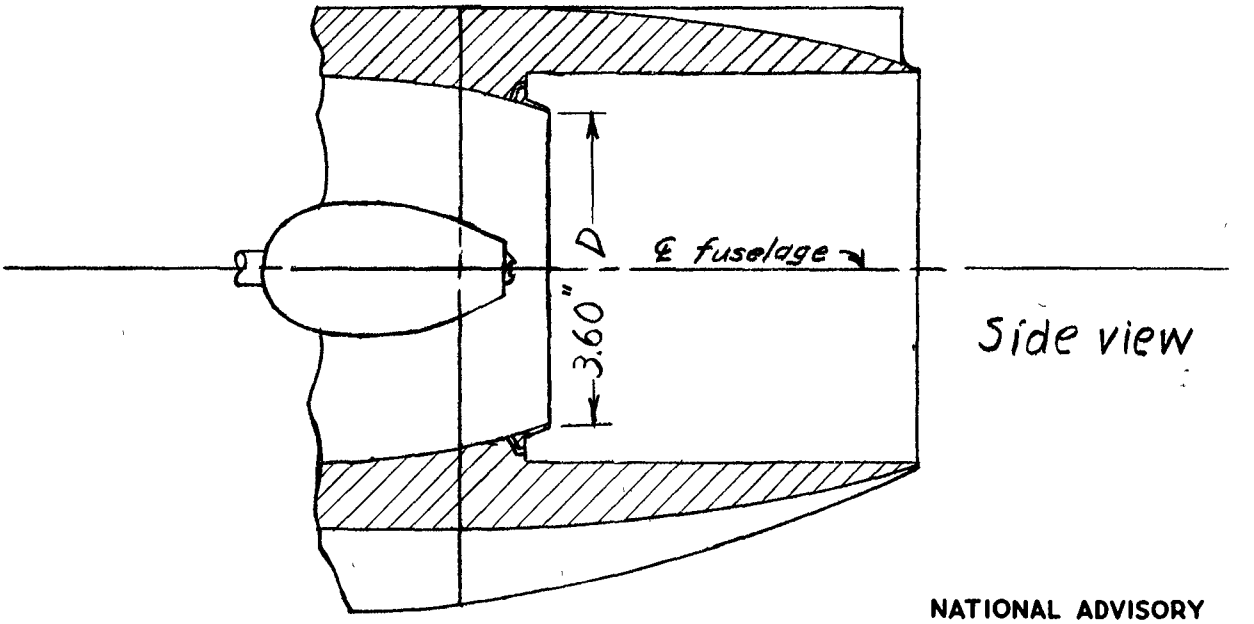

NATIONAL ADVISORY
COMMITTEE FOR AERONAUTICS

(c) Revision #2

Figure 9-(concluded)

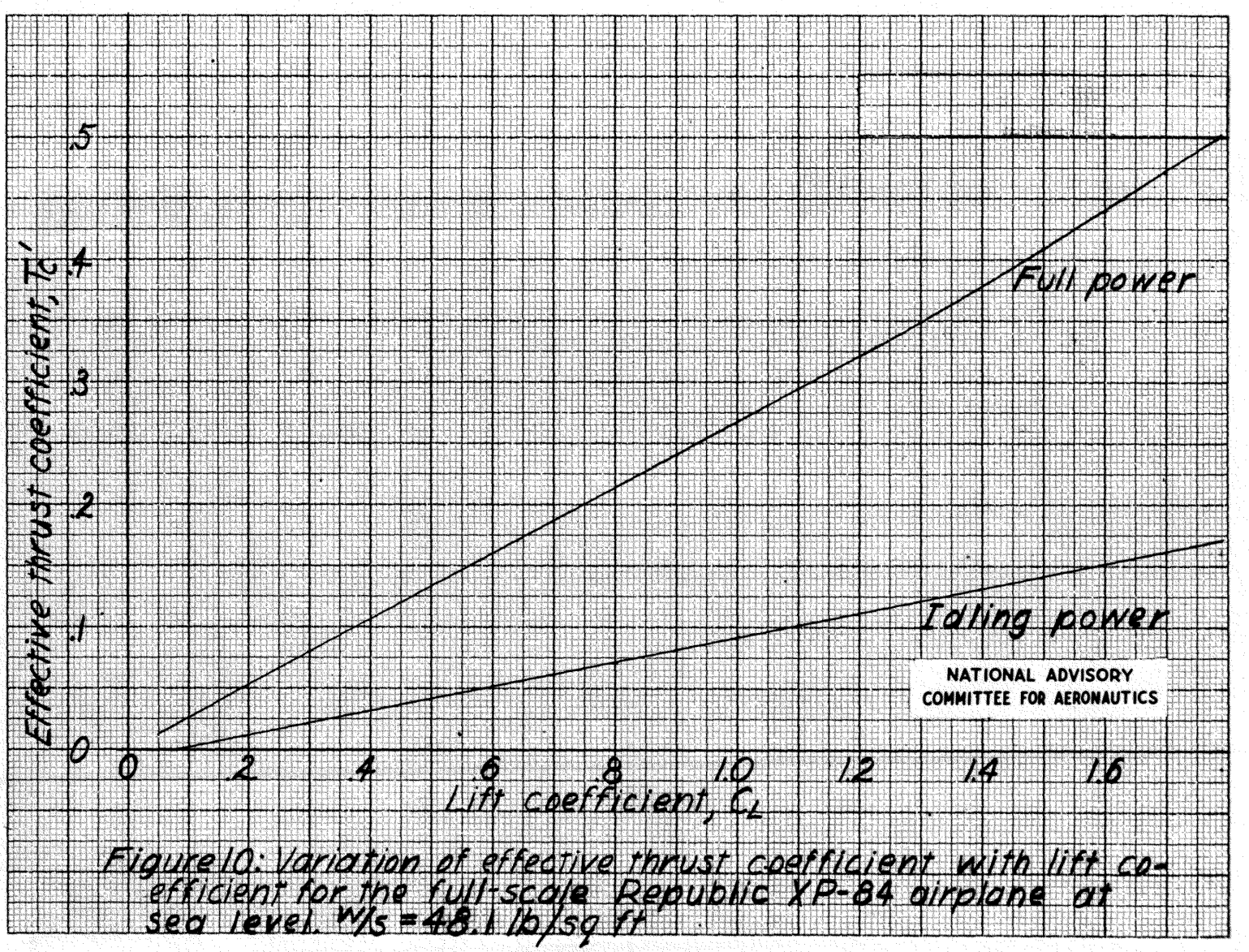

Figure 10: Variation of effective thrust coefficient with lift coefficient for the full-scale Republic XP-84 airplane at sea level. $W/S = 48.1$ lb/sq ft

MR No. L6D15

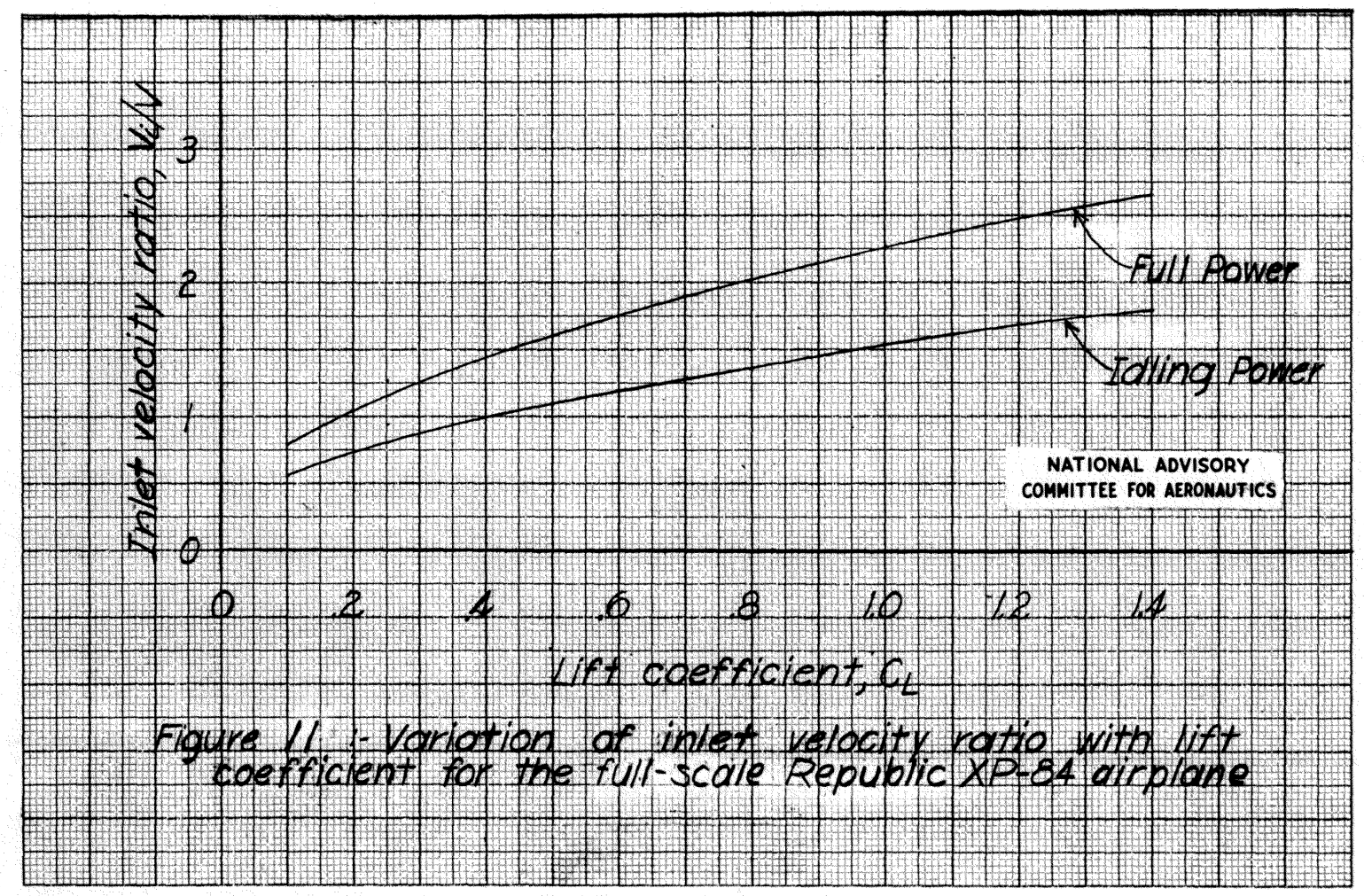

Figure 11.- Variation of inlet velocity ratio with lift coefficient for the full-scale Republic XP-84 airplane

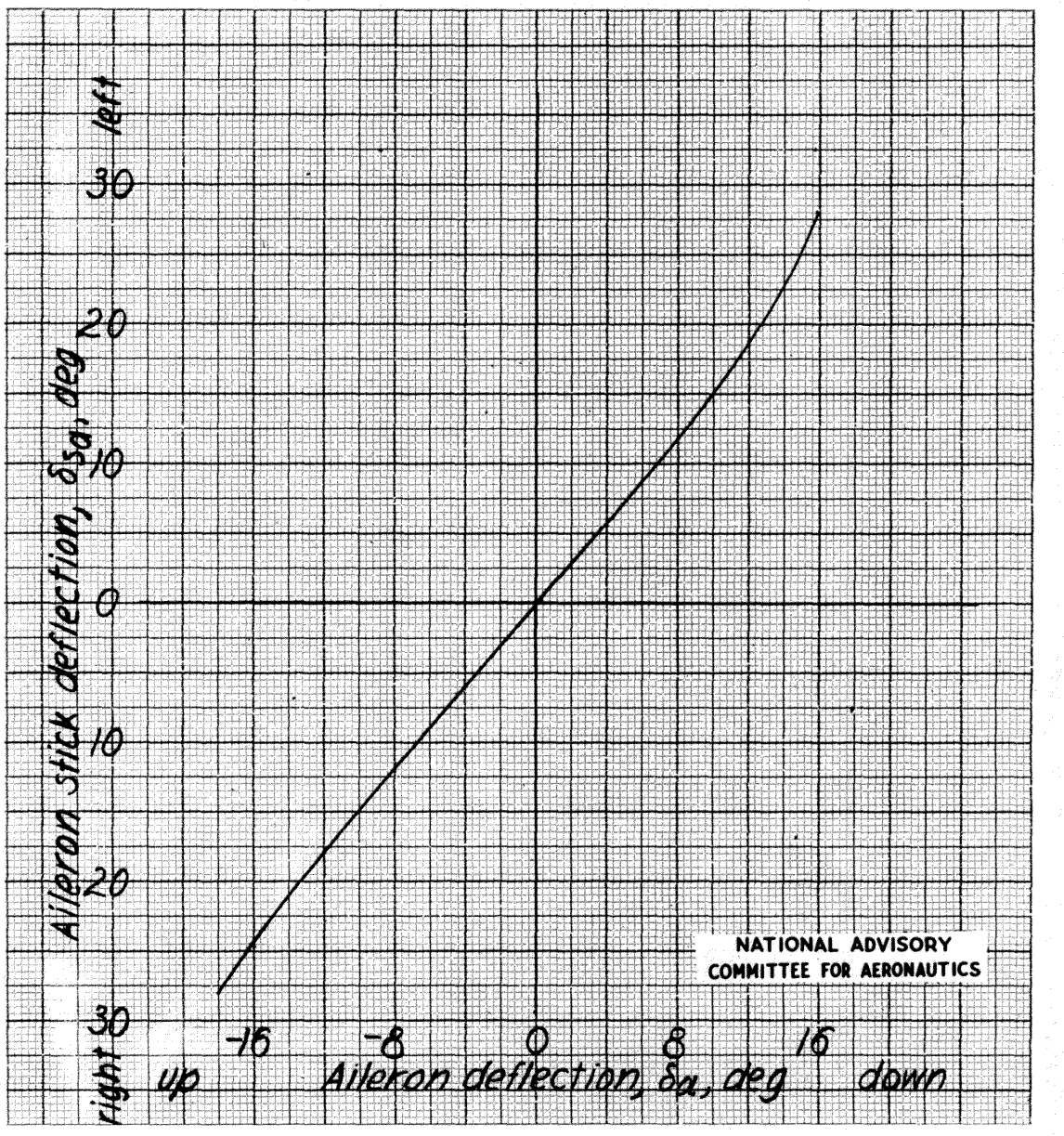

Figure 12 : Aileron and stick geometry for the right aileron of the Republic XP-84 airplane.

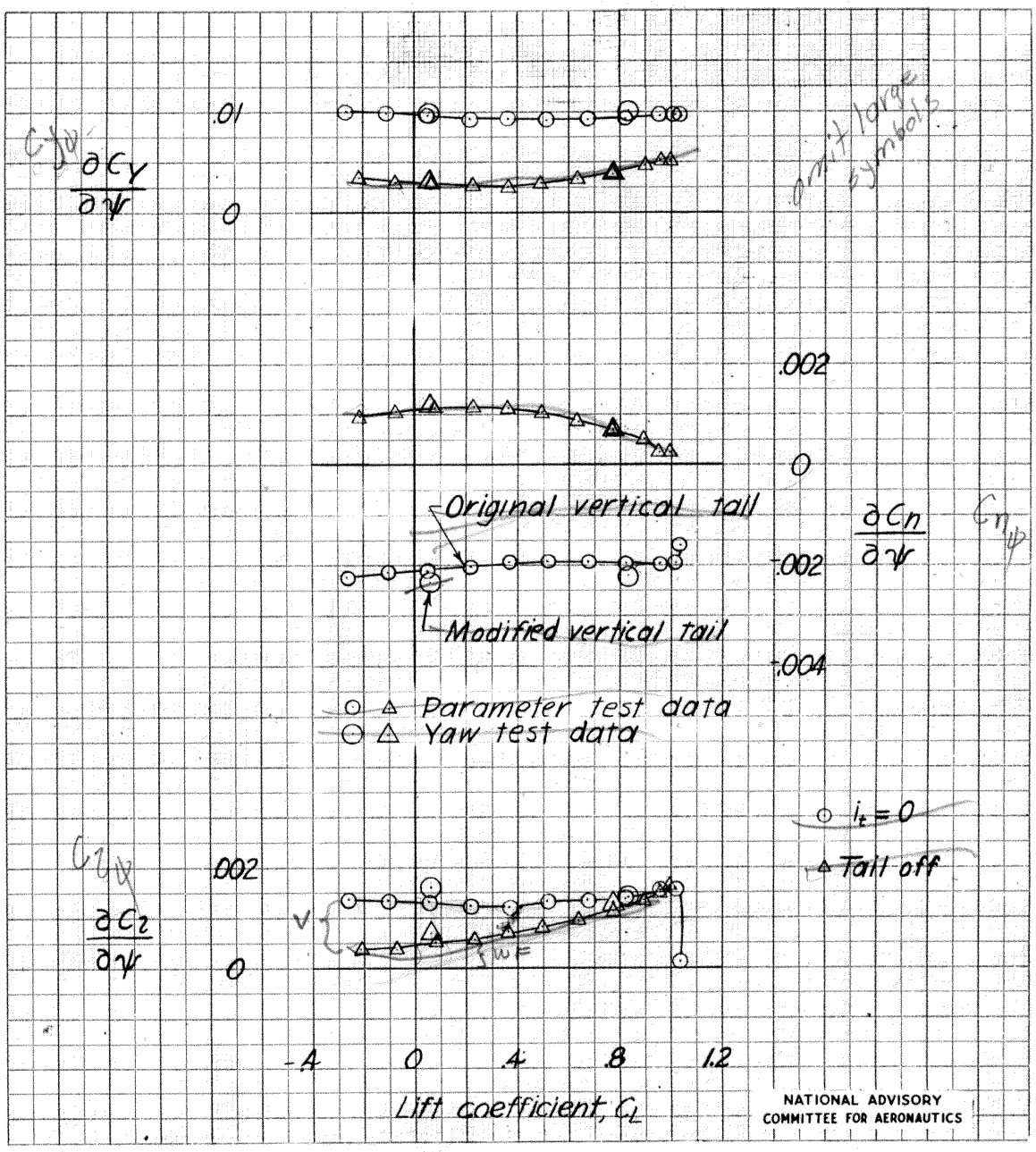

(a) Cruising configuration.

Figure 13: Lateral-stability parameters for the 1/5-scale model of the Republic XP-84 airplane. Power off.

omit large symbols

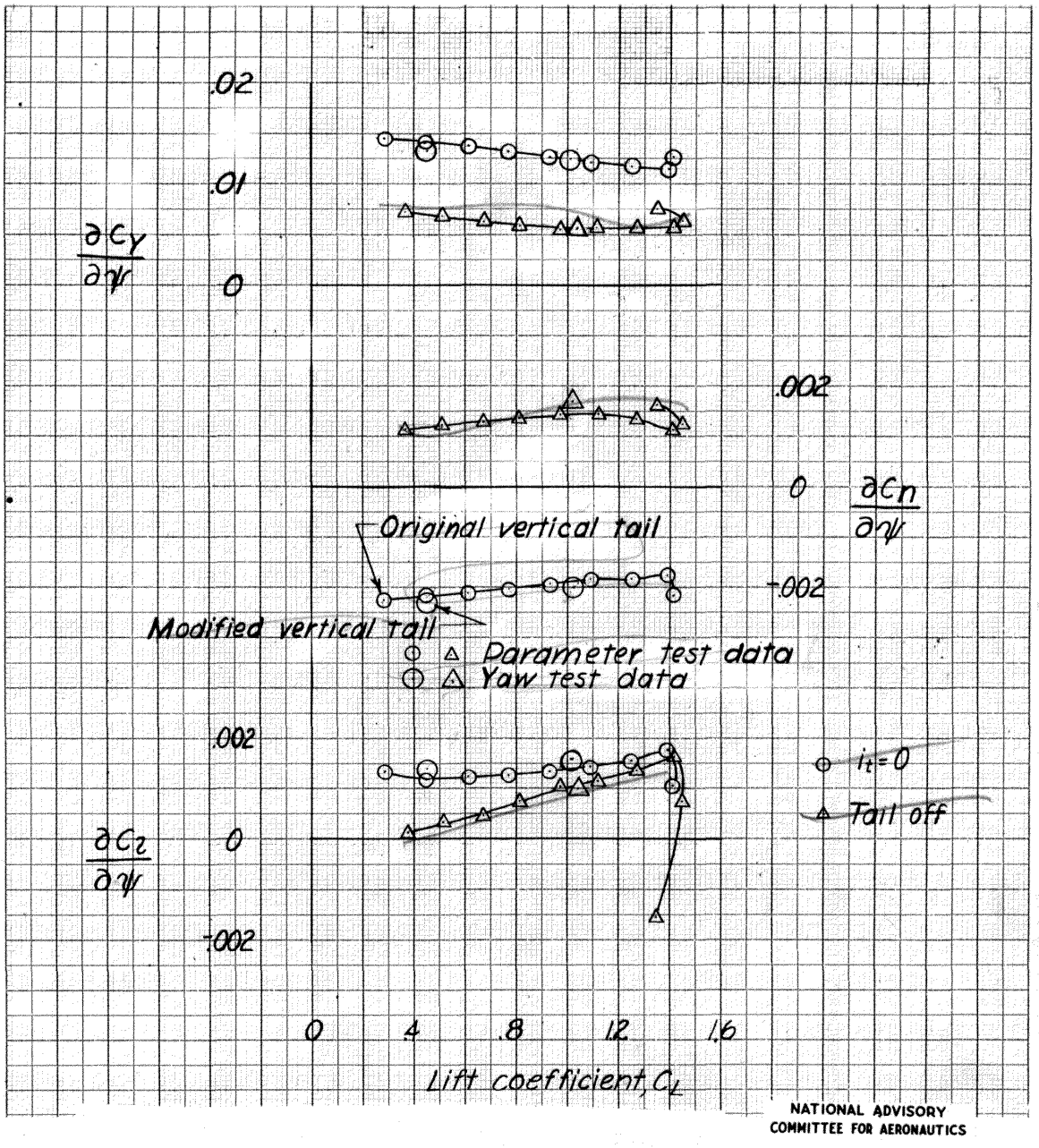

(b) Landing configuration.

Figure 13 :Concluded.

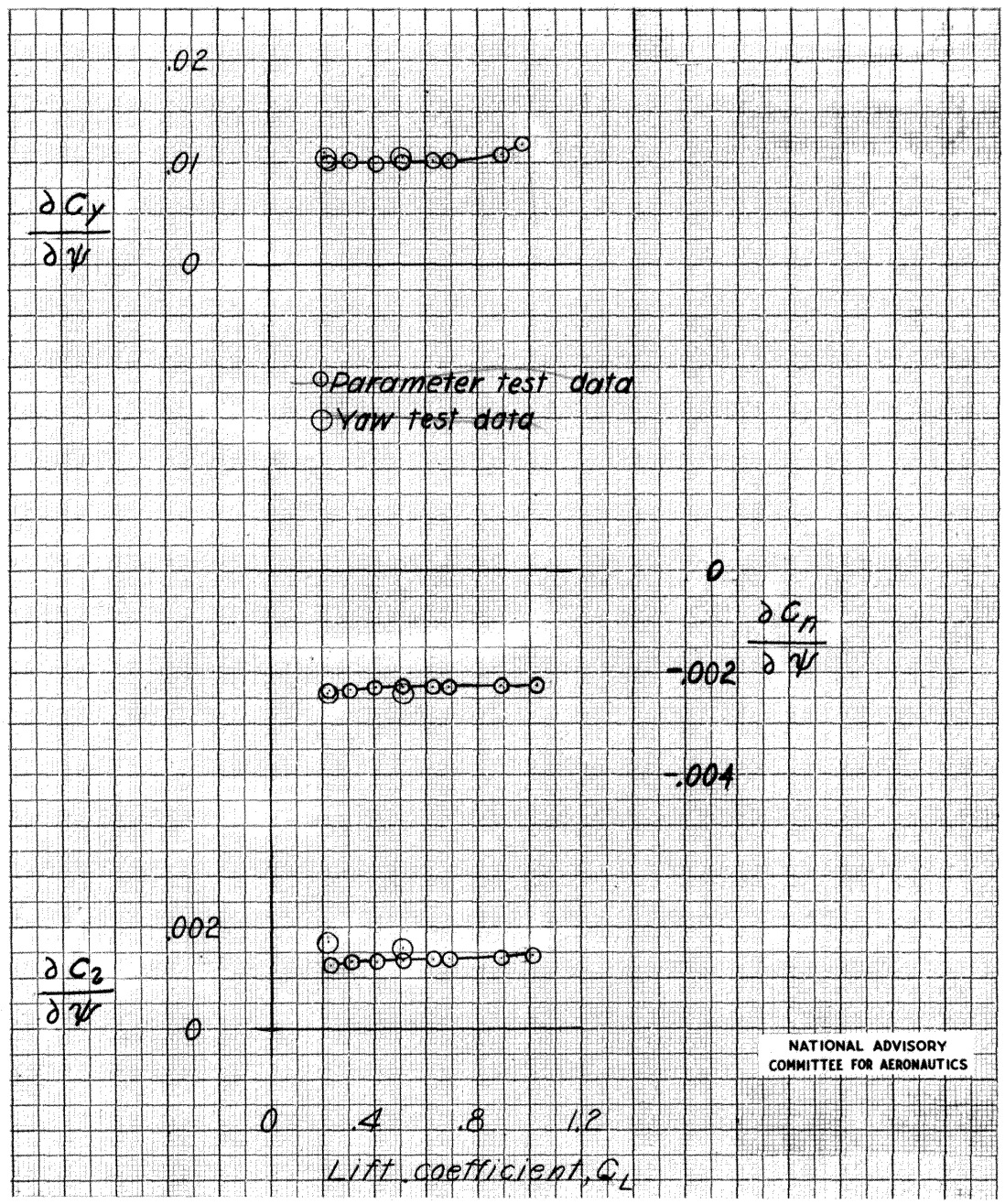

(a) Cruising configuration.

Figure 14 :Lateral-stability parameters for the 1/5-scale model of the Republic XP-84 airplane. Full power; $i_t = 0°$.

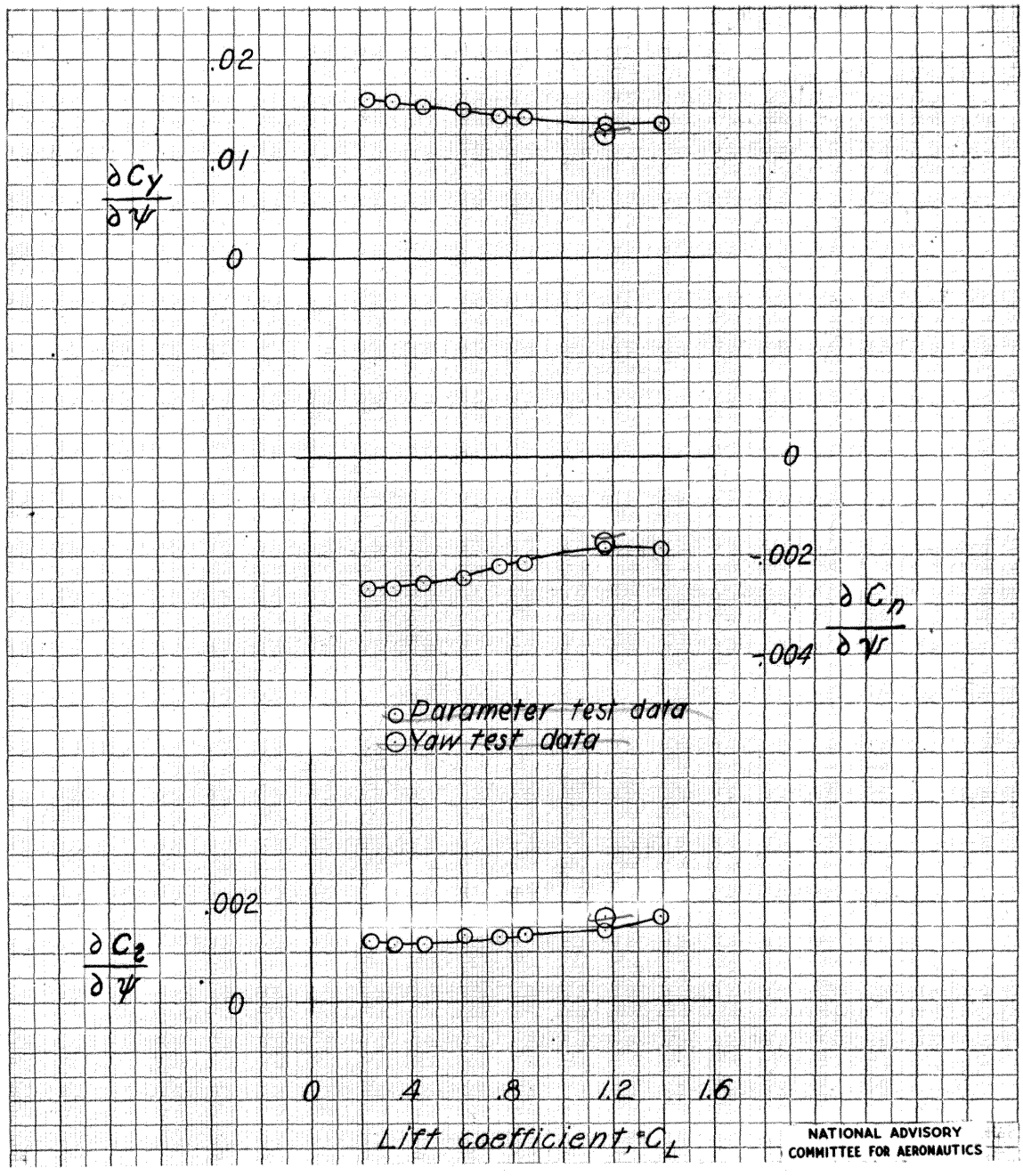

(b) Landing configuration.

Figure 14 : Concluded.

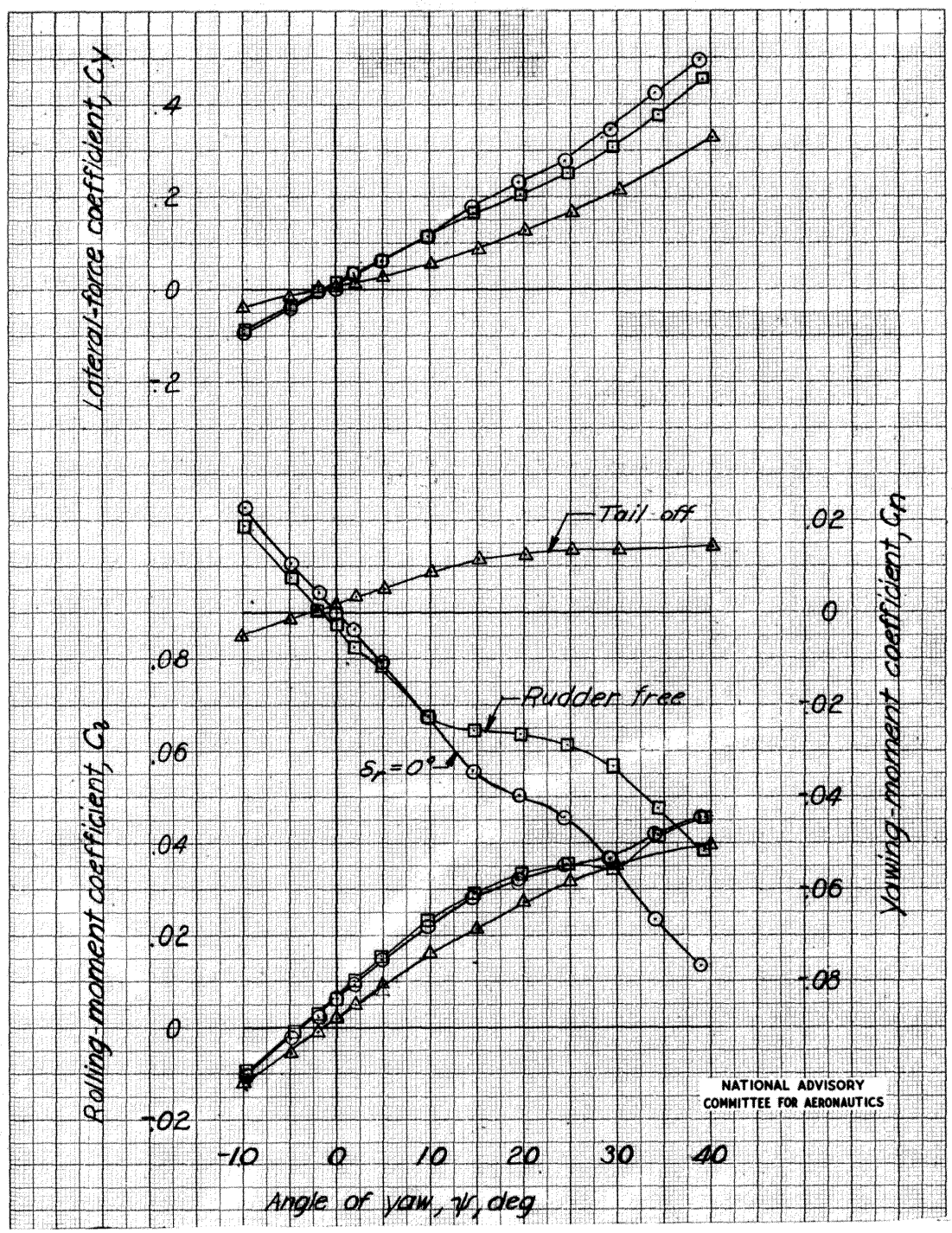

(a) Cruising configuration, $\alpha = 10.8°$

Figure 15 :The aerodynamic characteristics in yaw of the 1/5-scale model of the Republic XP-84 airplane. Power off; $i_t = 0°$.

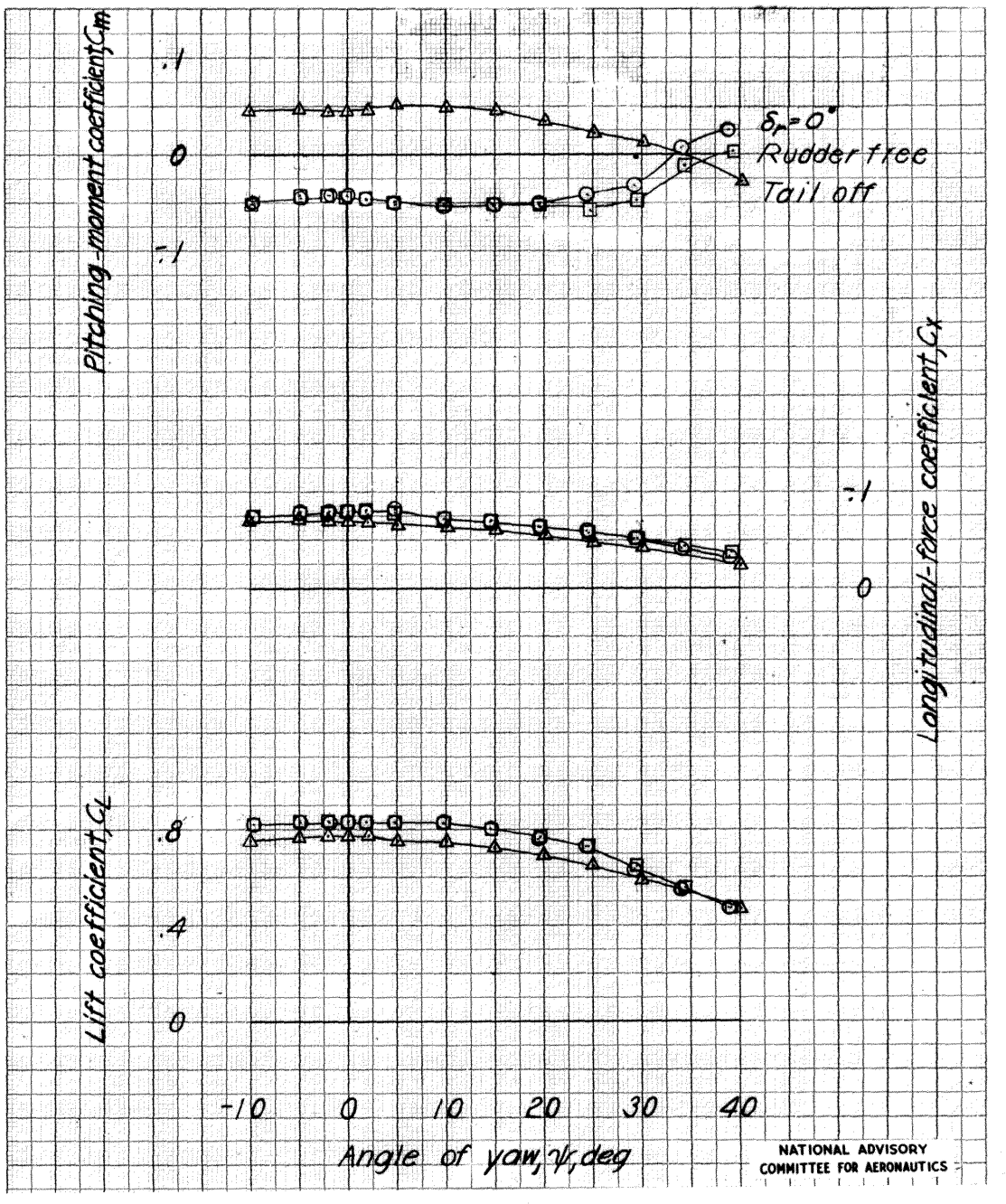

(d) Concluded.

Figure 15 : Continued.

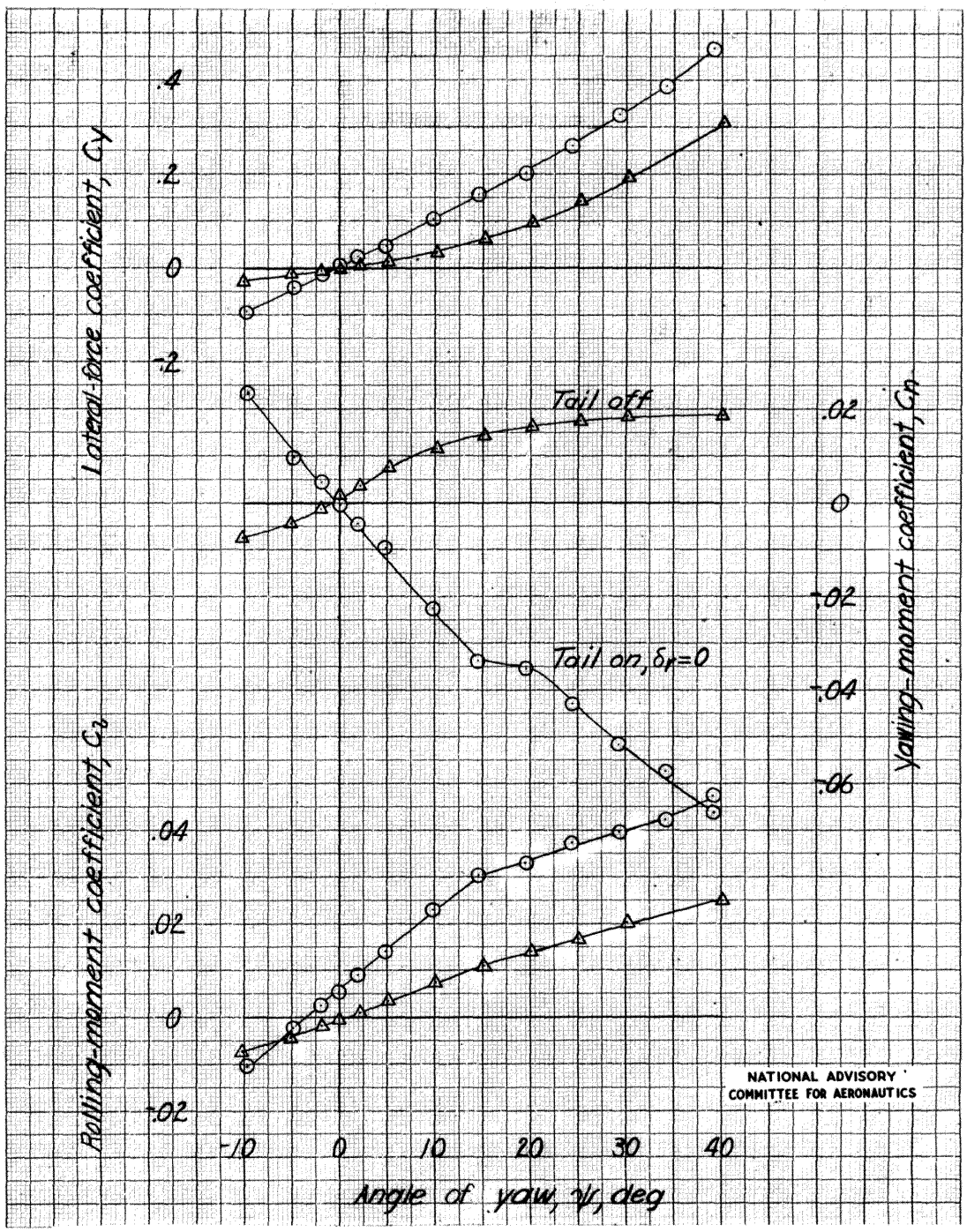

(b) Cruising configuration, $\alpha = 0.1°$

Figure 15 : Continued.

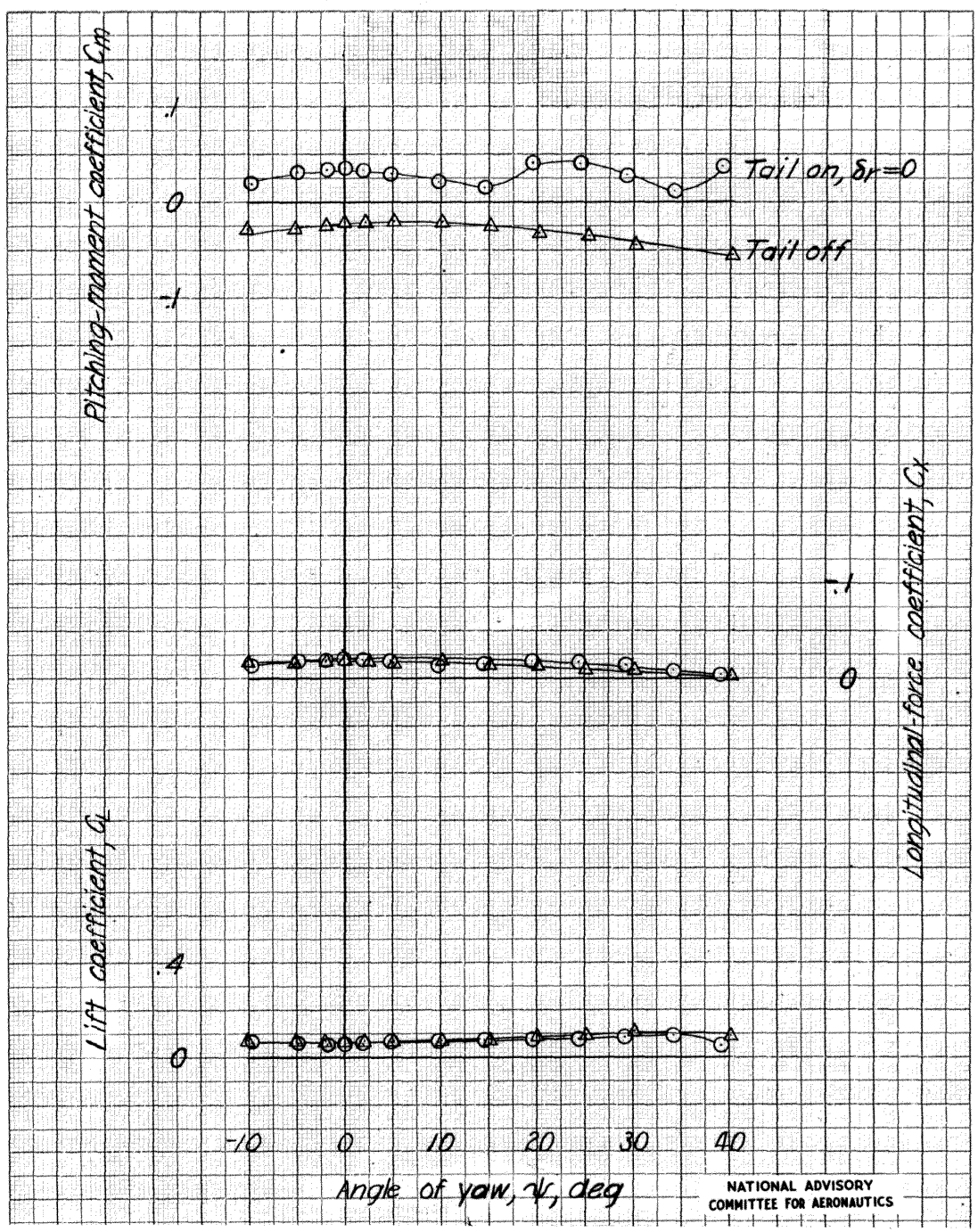

(b) Concluded.

Figure 15 : Continued.

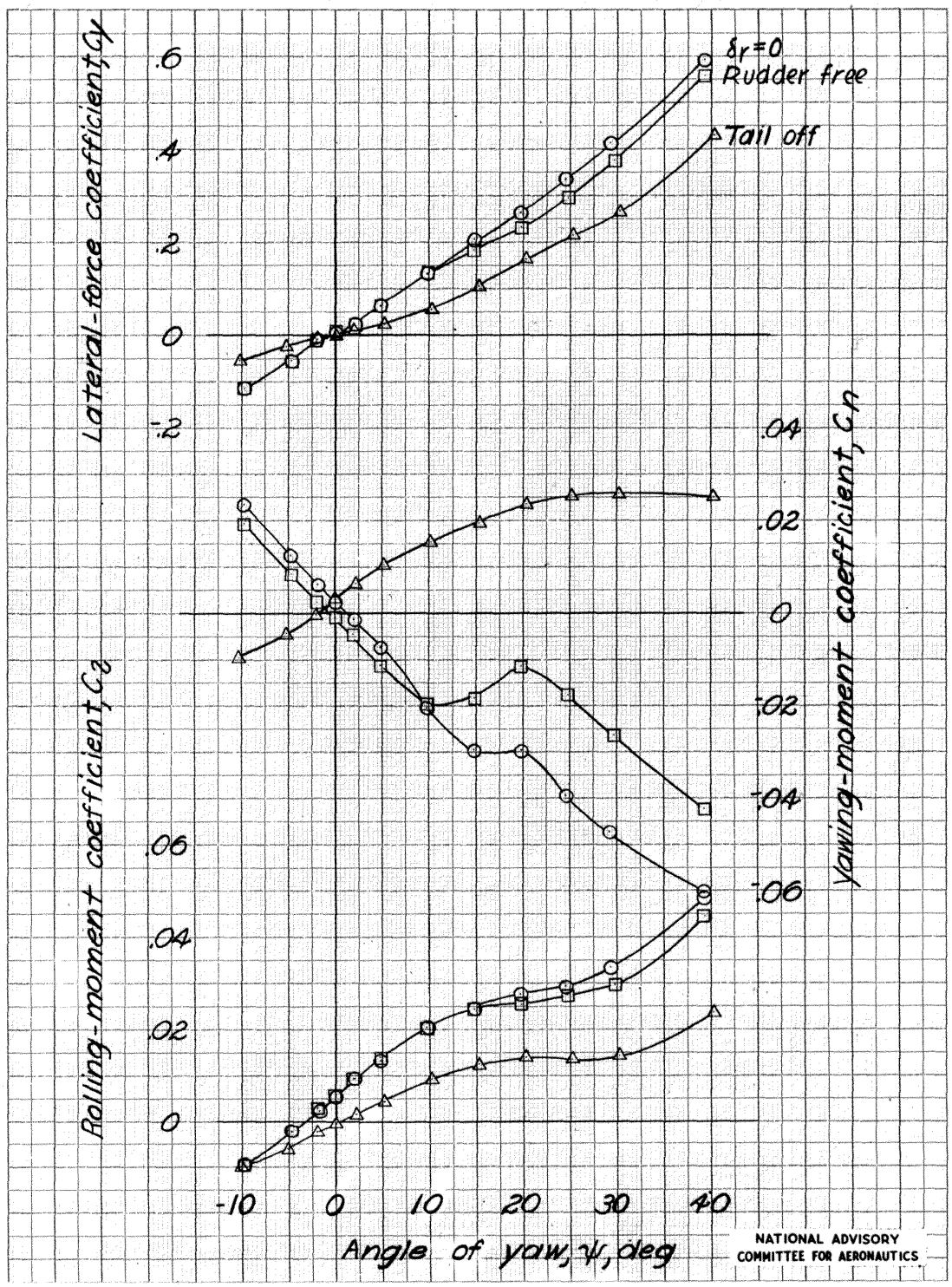

(c) Landing configuration, $\alpha = 6.0°$.

Figure 15 : Continued.

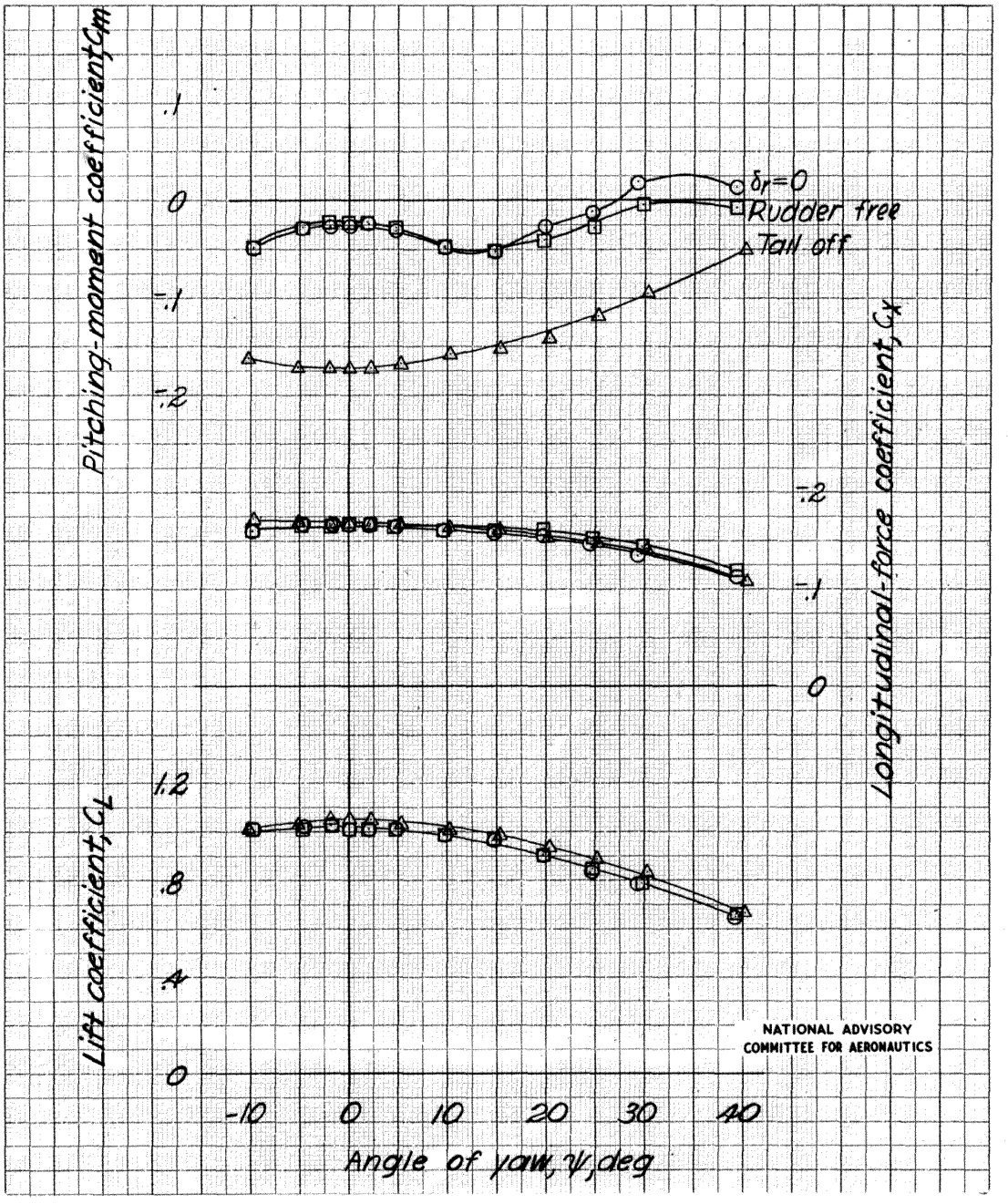

(c) Concluded.

Figure 15 :Continued.

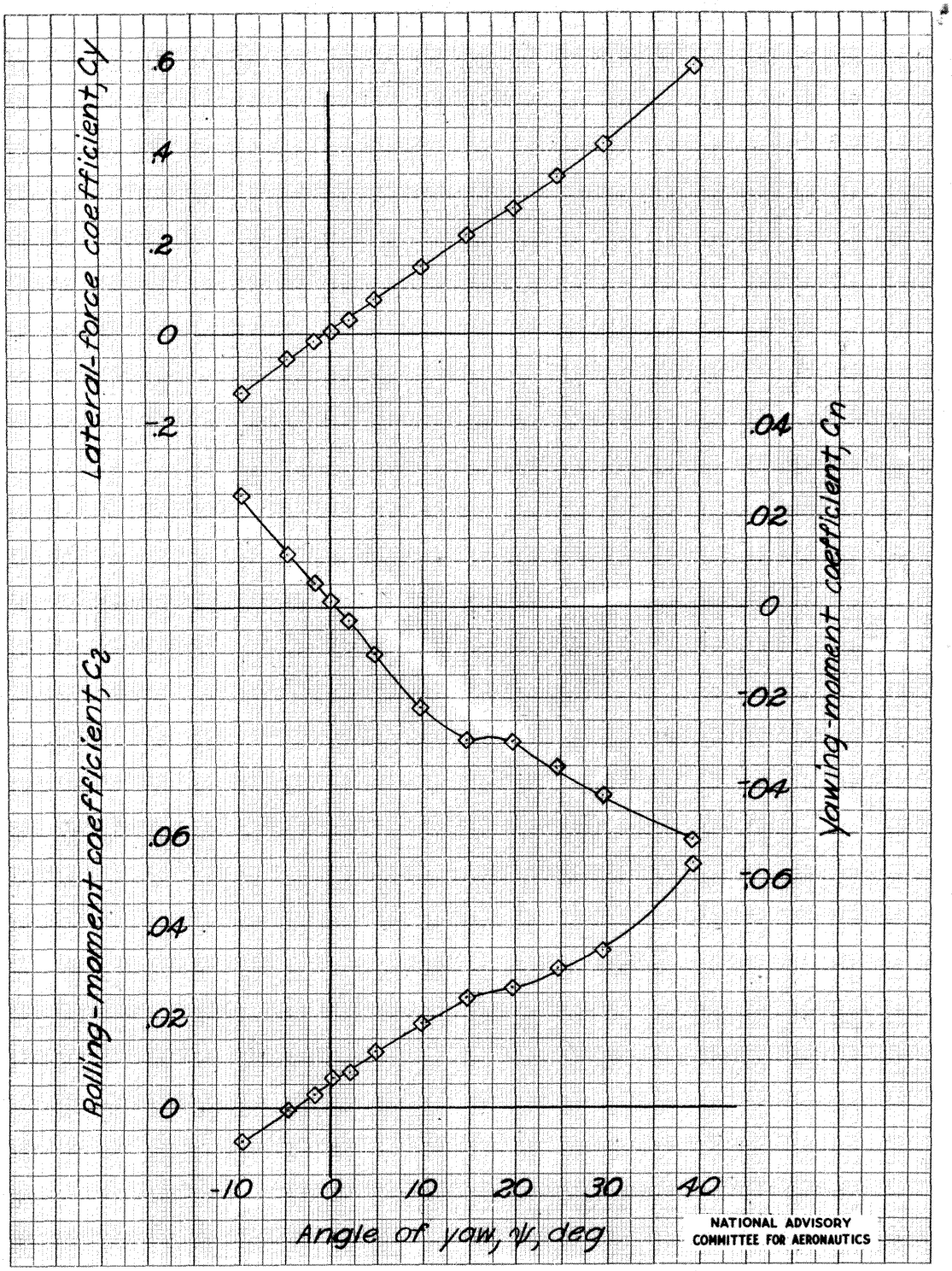

(d) Landing configuration; $\alpha = 11.5°$; $\delta_r = 0°$.

Figure 15 : Continued.

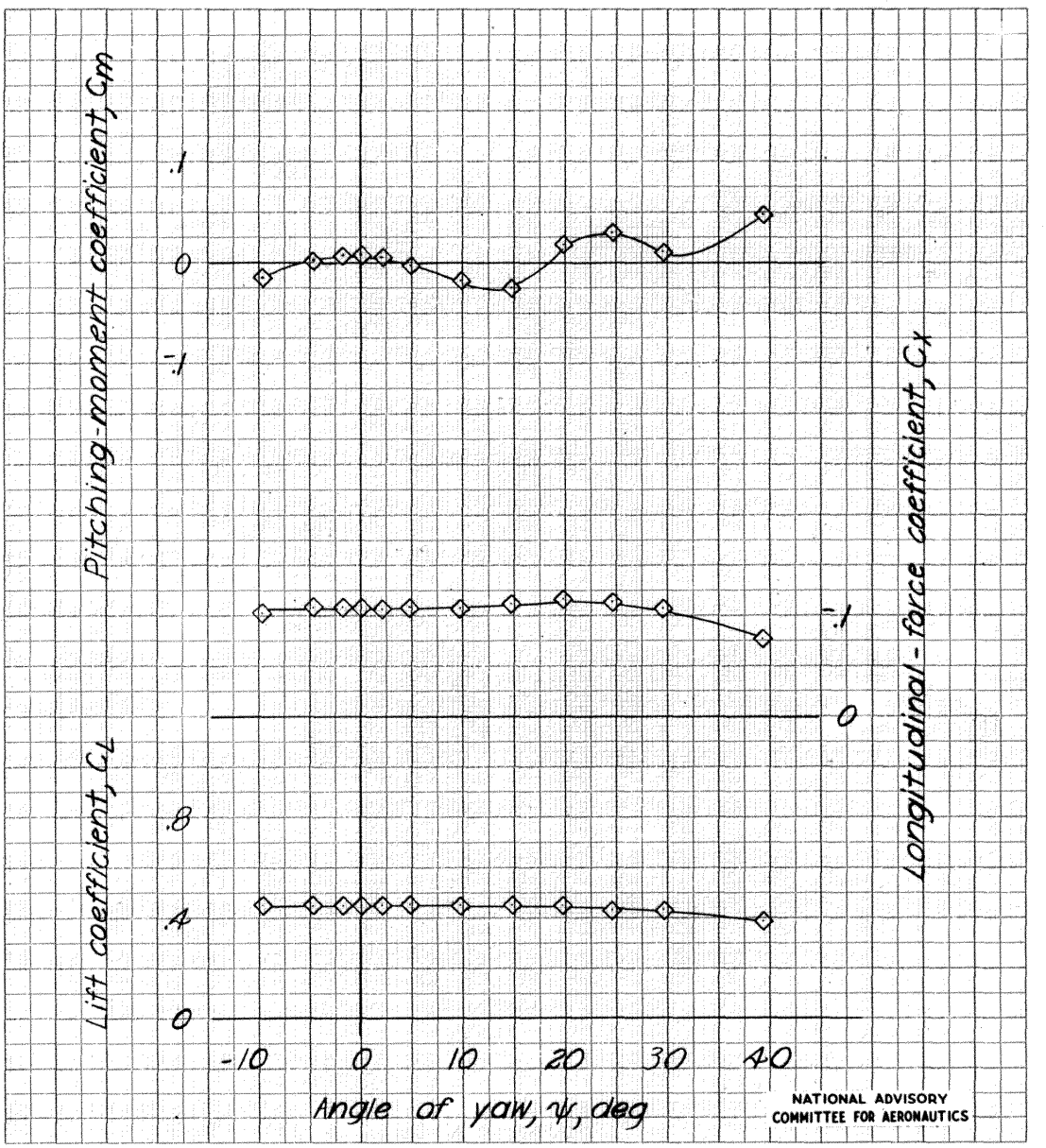

(d) Concluded.

Figure 15 : Concluded.

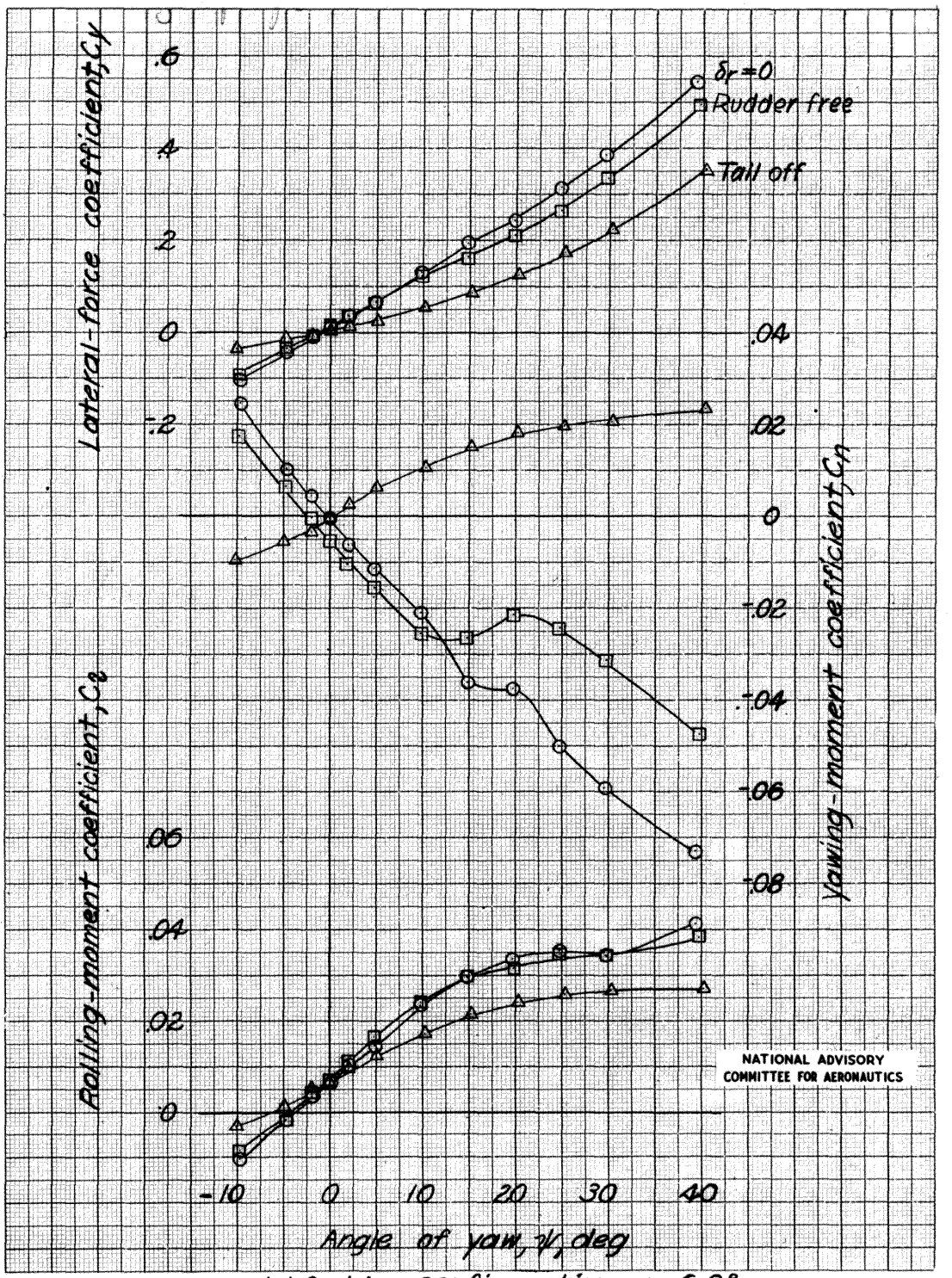

(a) Cruising configuration; $\alpha = 6.0°$

Figure 16: The aerodynamic characteristics in yaw of the 1/5-scale model of the Republic XP-84 airplane. Full power; $i_t = 0°$.

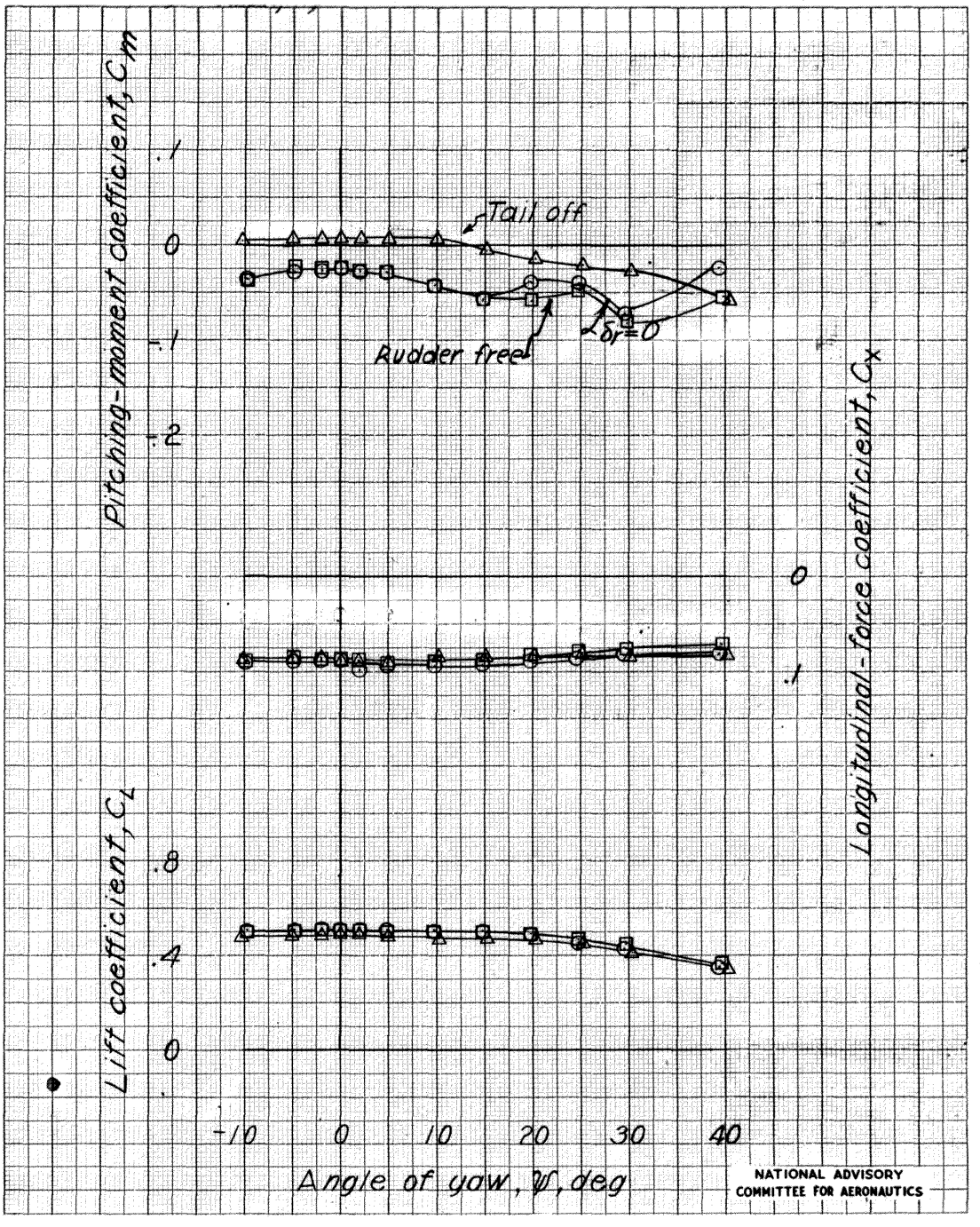

(a) Concluded.

Figure 16 : Continued.

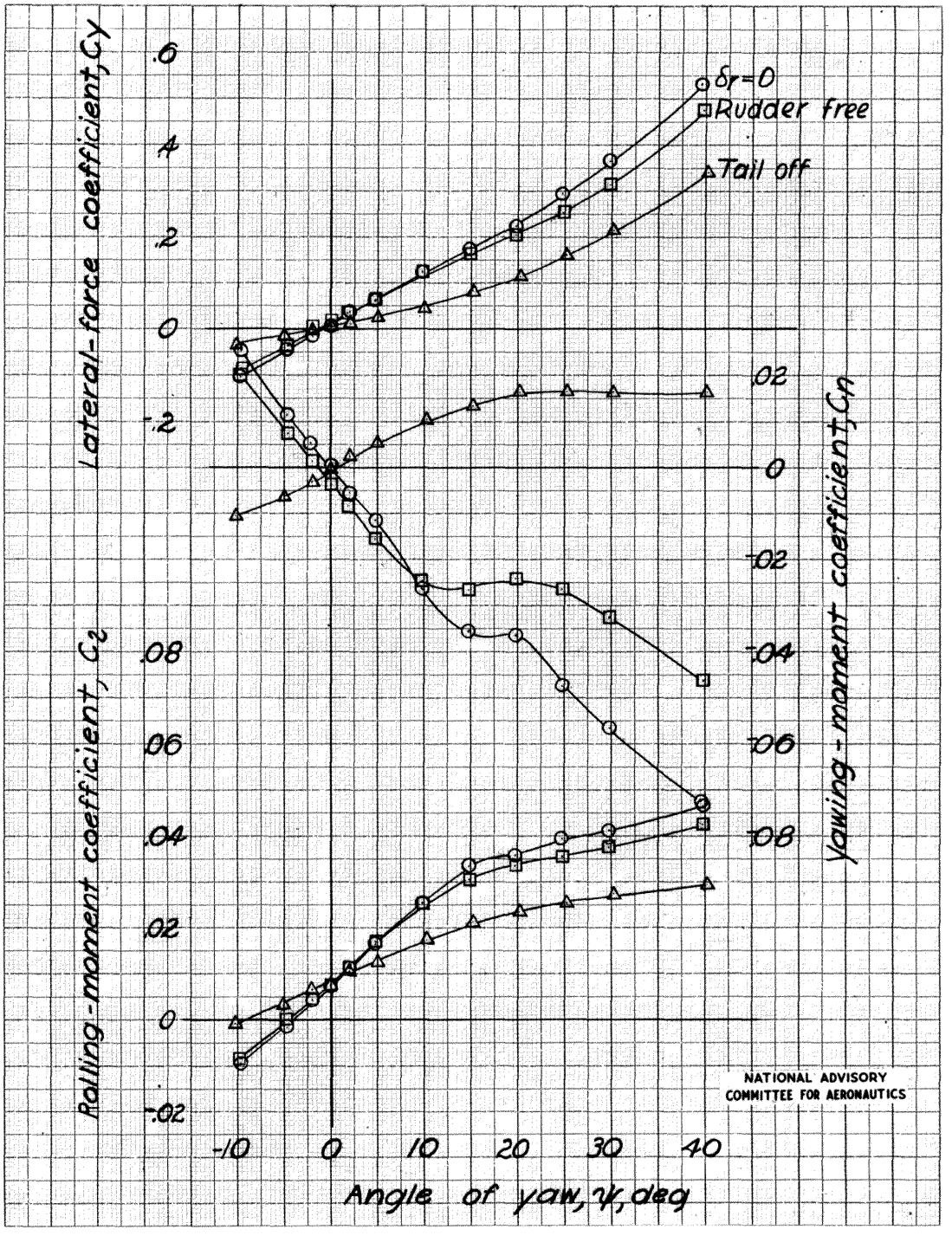

(b) Cruising configuration, $\alpha = 2.0°$

Figure 16 : Continued.

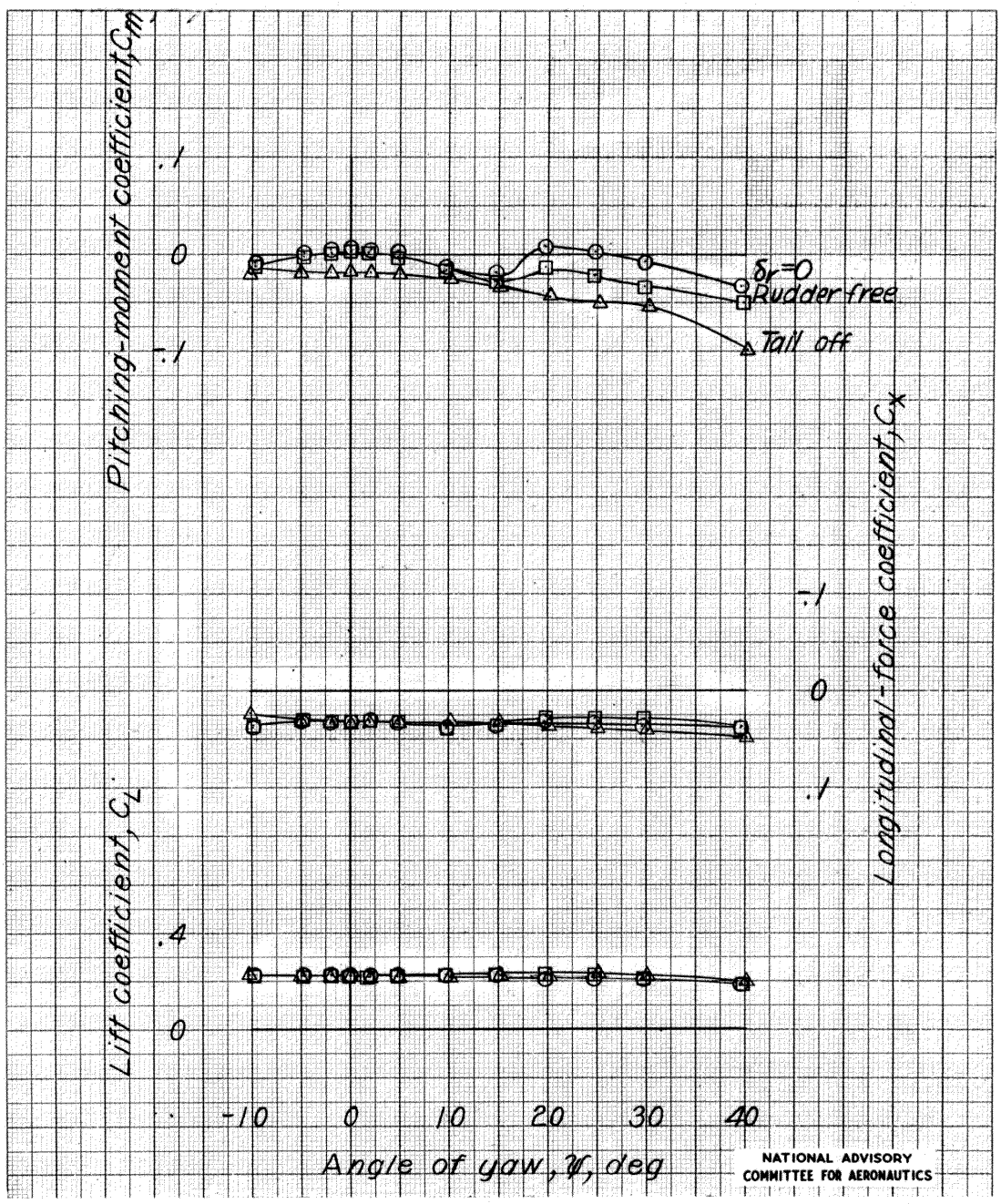

(b) Concluded.

Figure 16 : Continued.

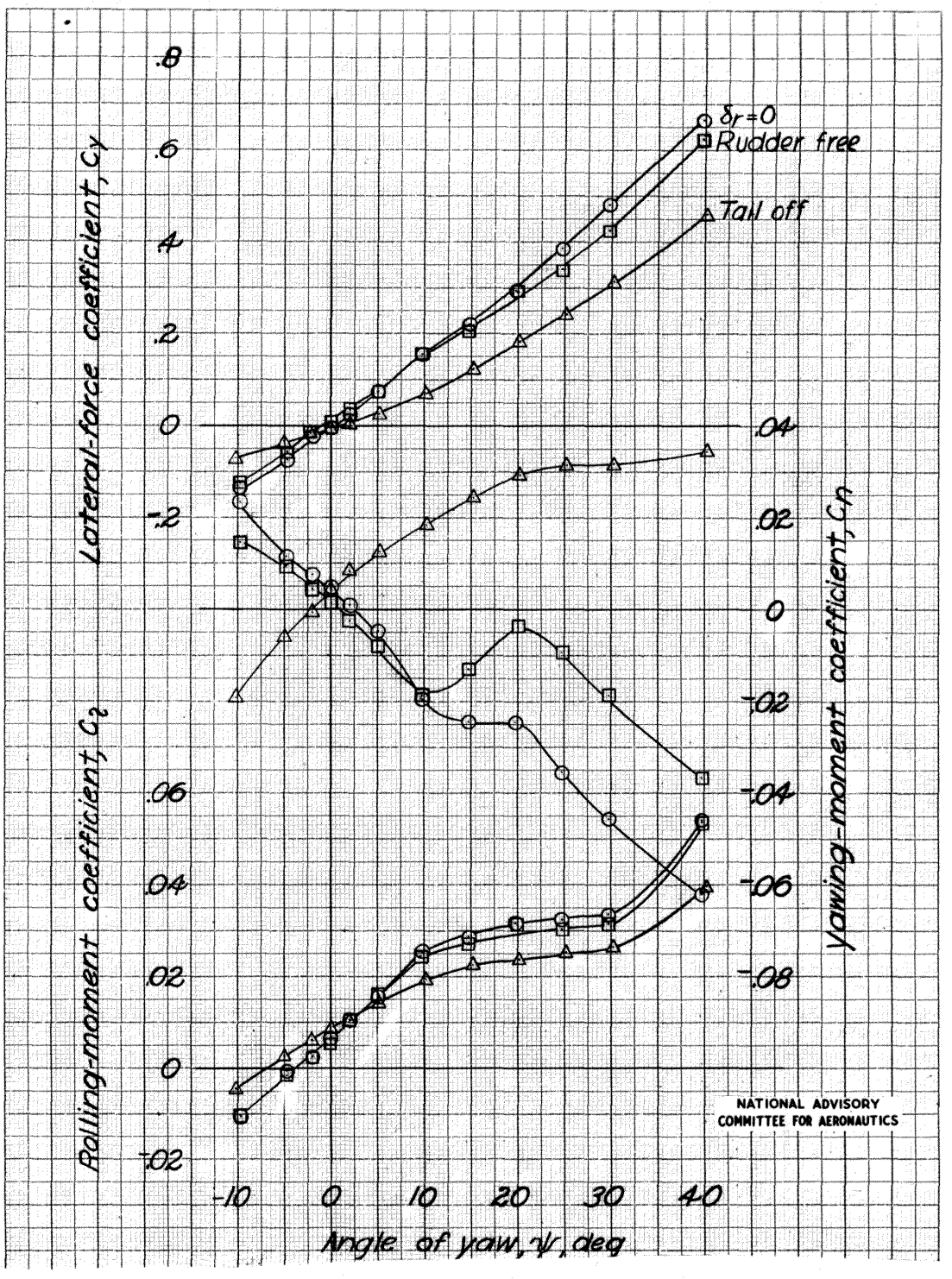

(c) Landing configuration, $\alpha = 7.6°$

Figure 16 : Continued.

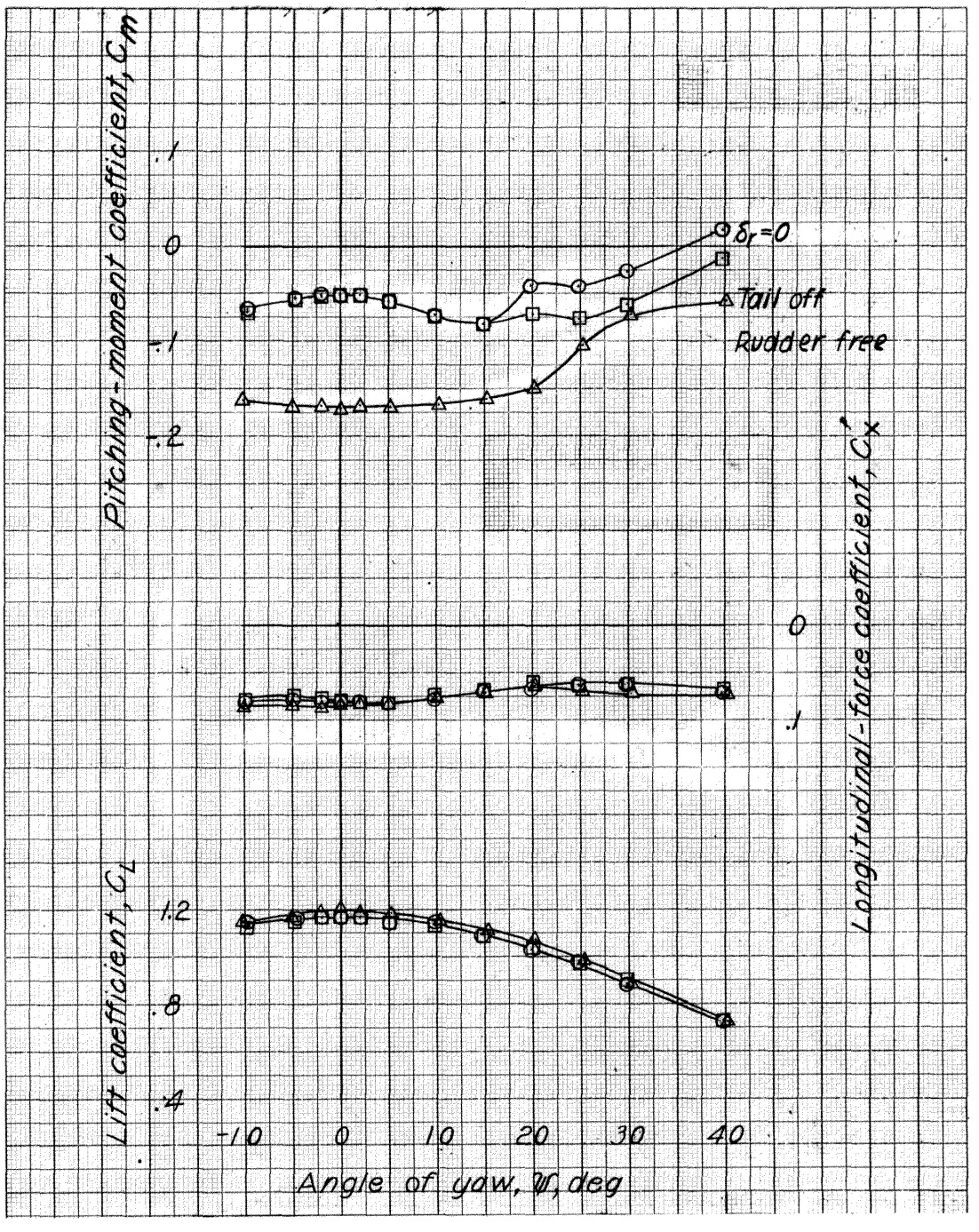

(C) Concluded.

Figure 16 : Concluded.

National Advisory
Committee For Aeronautics

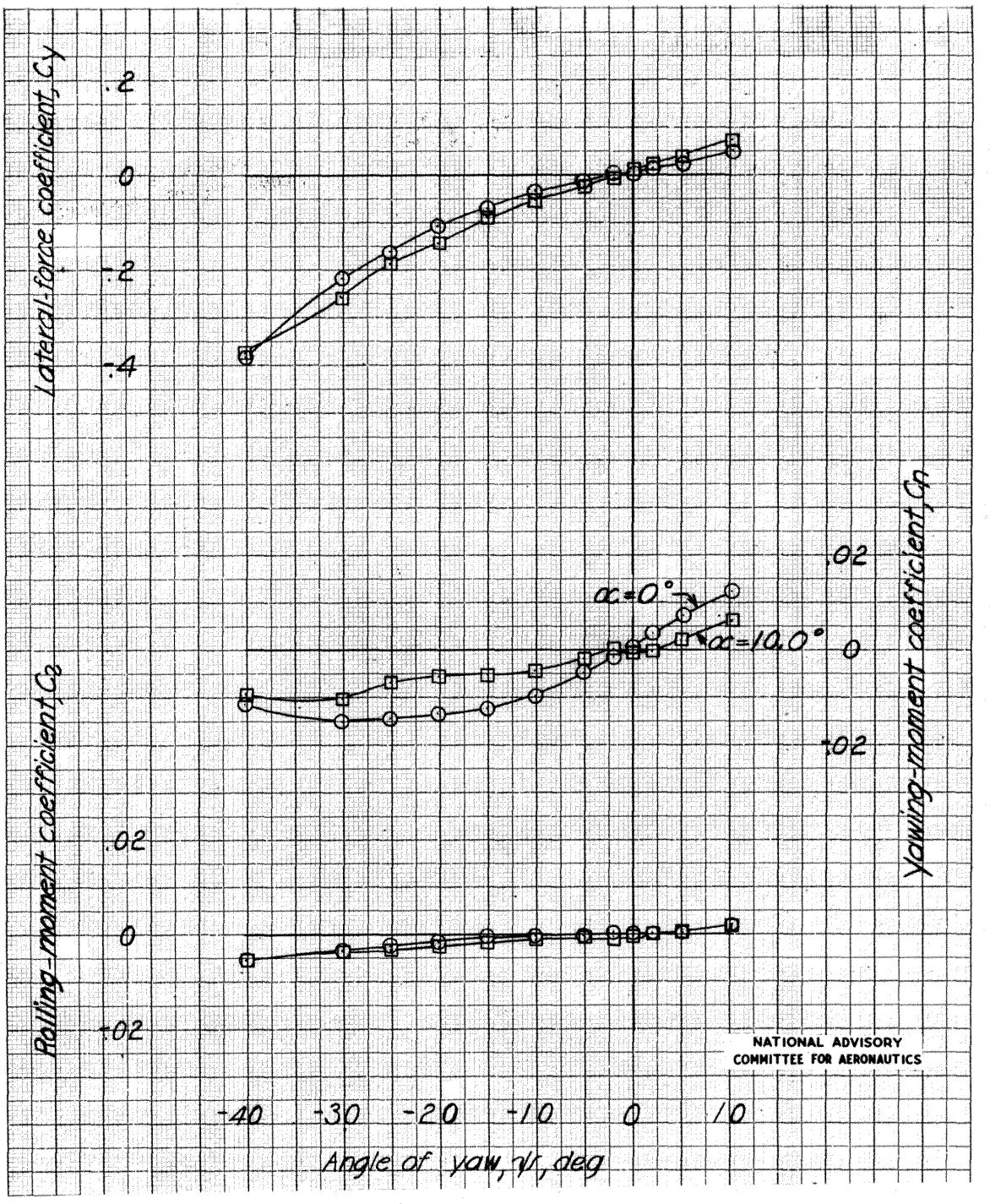

Figure 17: The aerodynamic characteristics in yaw of the fuselage of the 1/5-scale model of the Republic XP-84 airplane. Power off.

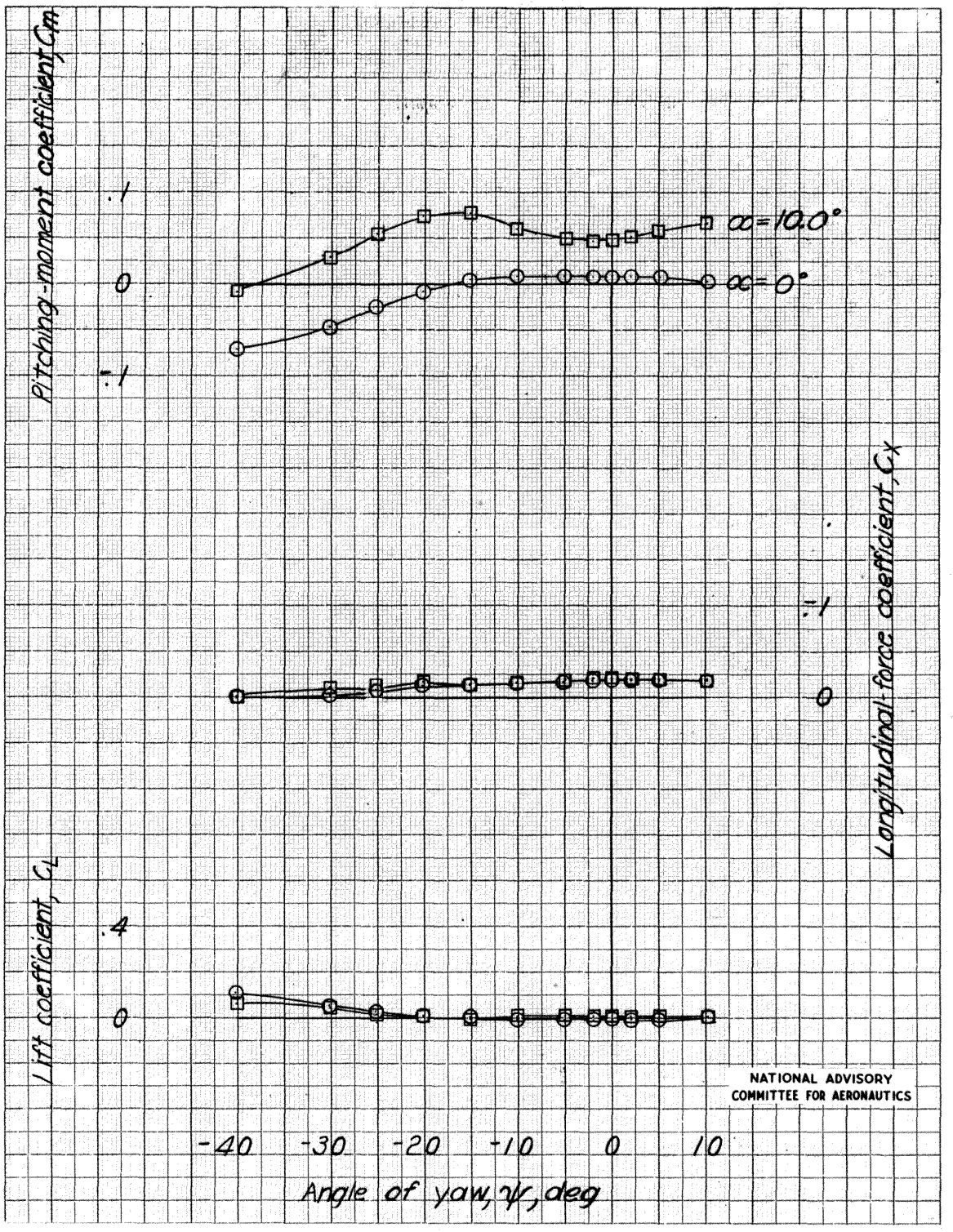

Figure 17: Concluded.

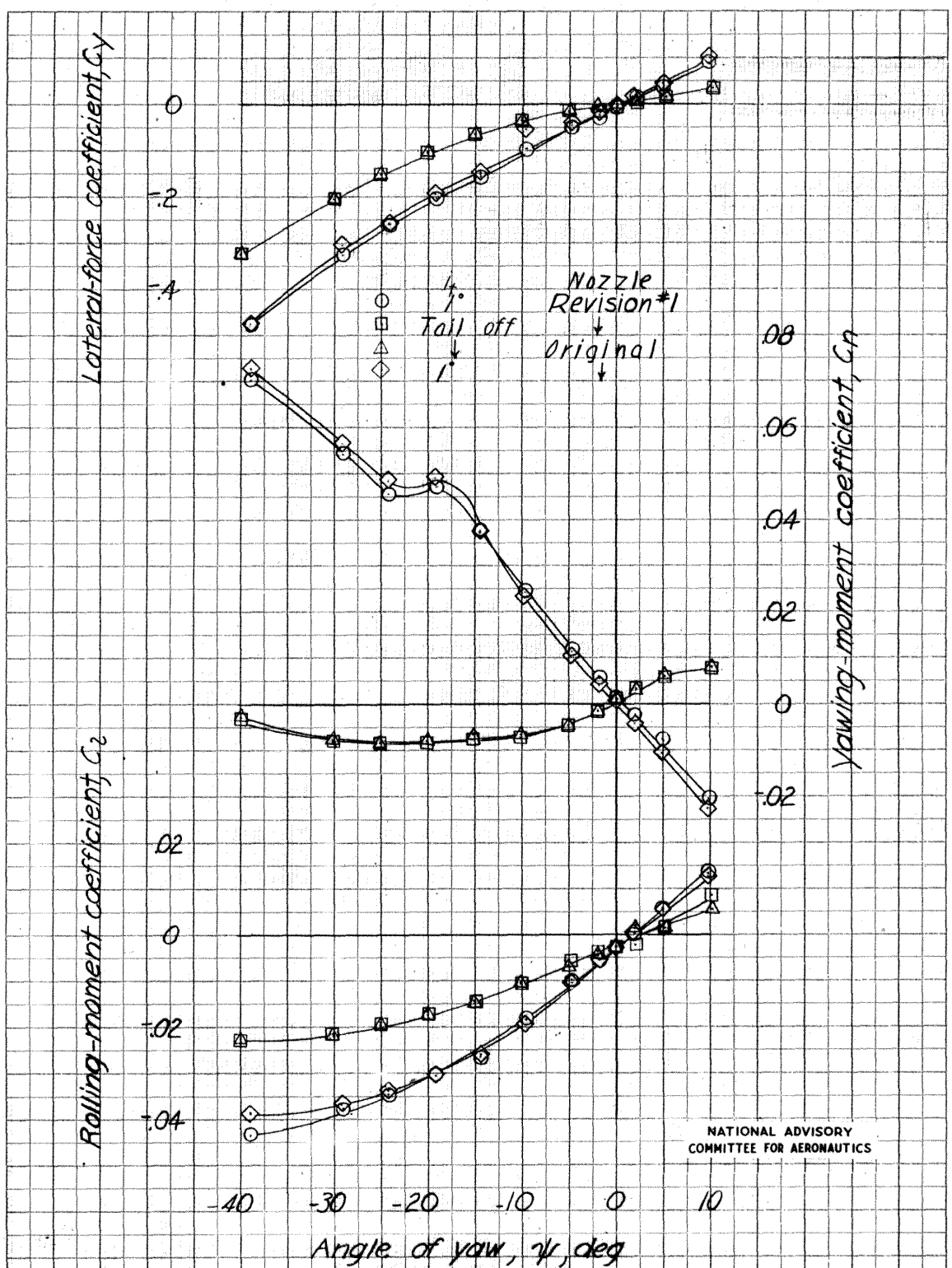

Figure 18: The effect of nozzle shape on the aerodynamic characteristics in yaw of the 1/5-scale model of the Republic XP-84 airplane. Cruising configuration. Power off. $\alpha = 1.2°$.

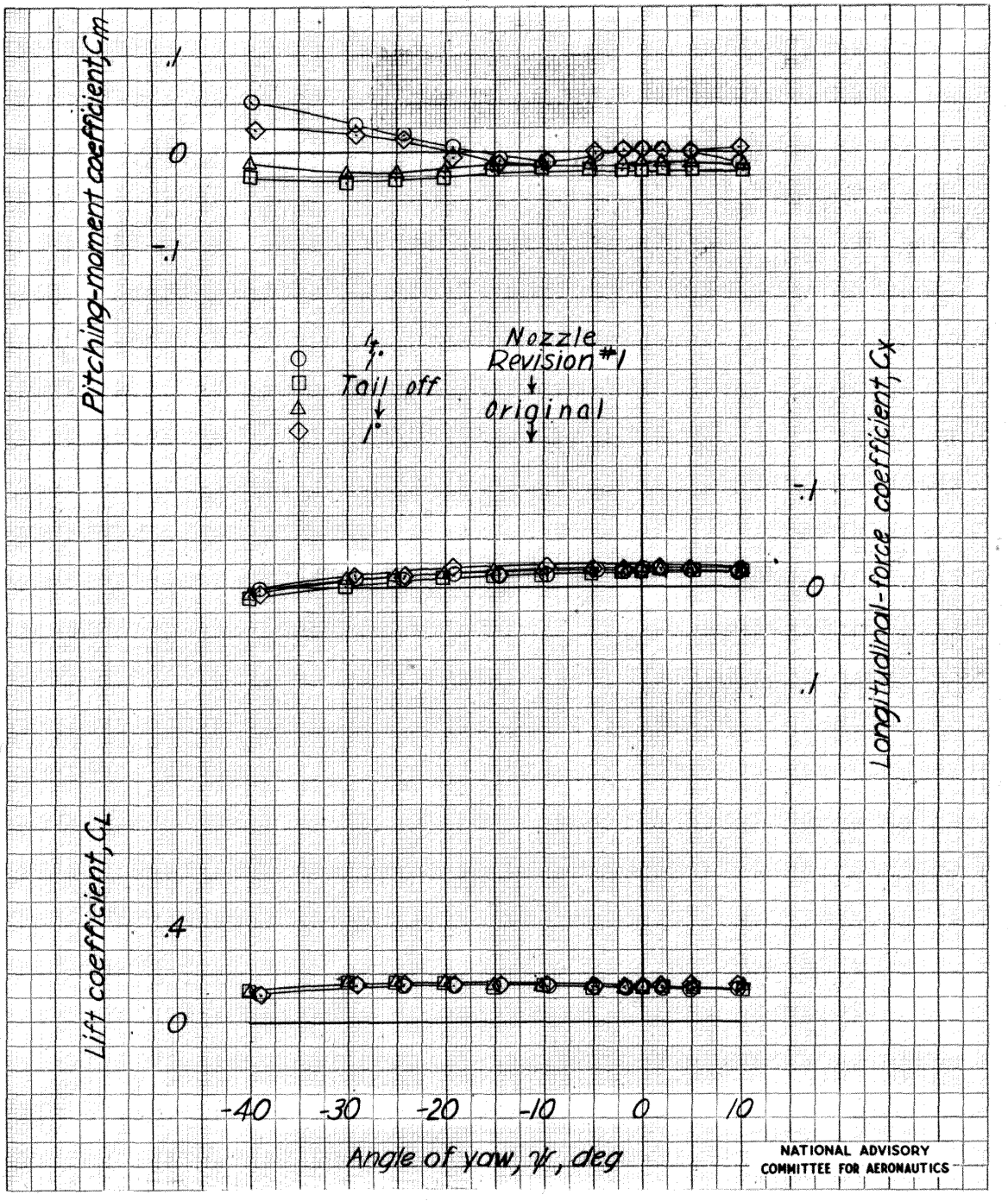

Figure 18: Concluded.

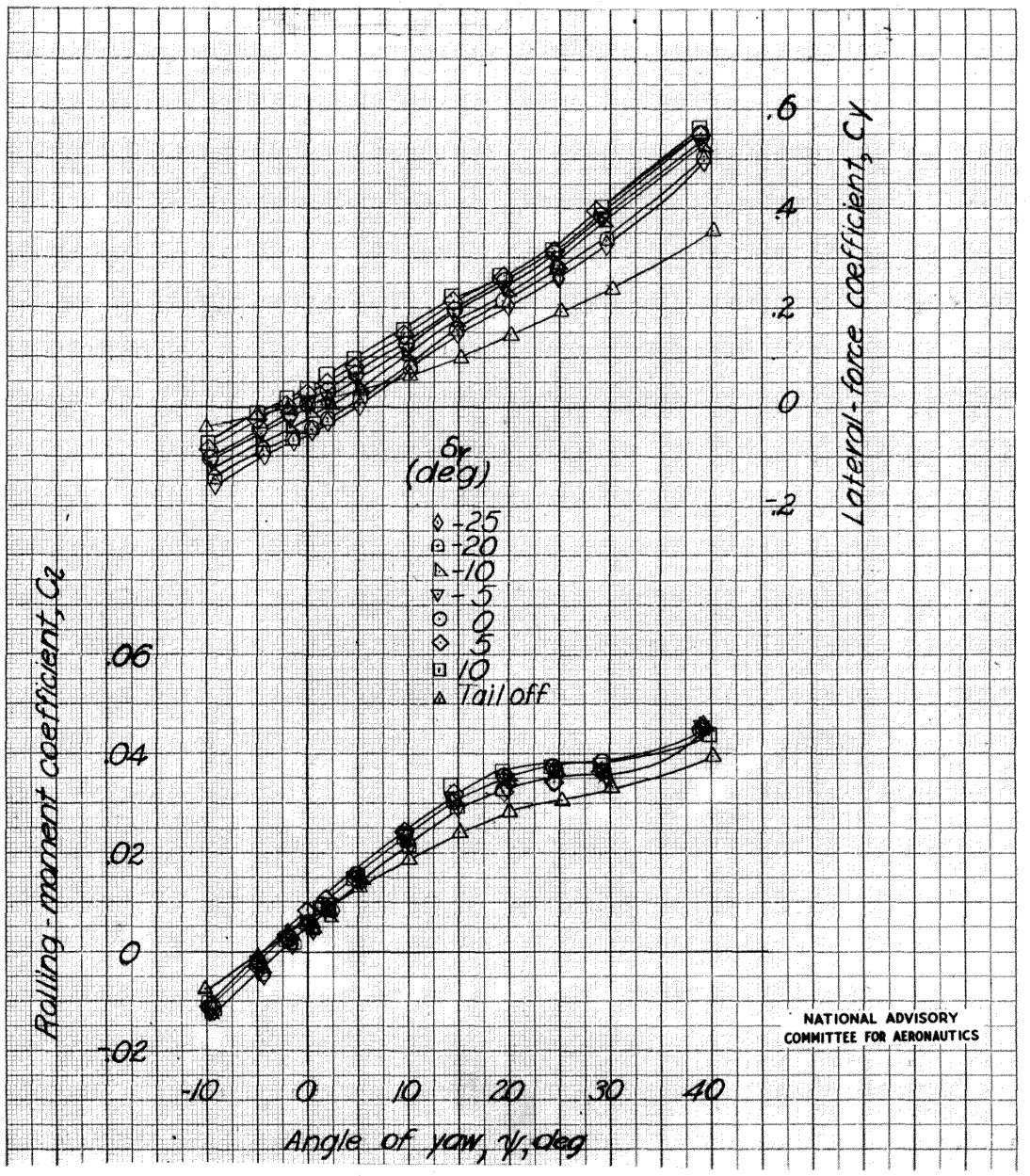

(a) Cruising configuration, $\alpha = 10.1°$.

Figure 19.: Effect of rudder deflection on the aerodynamic characteristics in yaw of the 1/5-scale model of the Republic XP-84 airplane. Idling power; $i_t = 1°$.

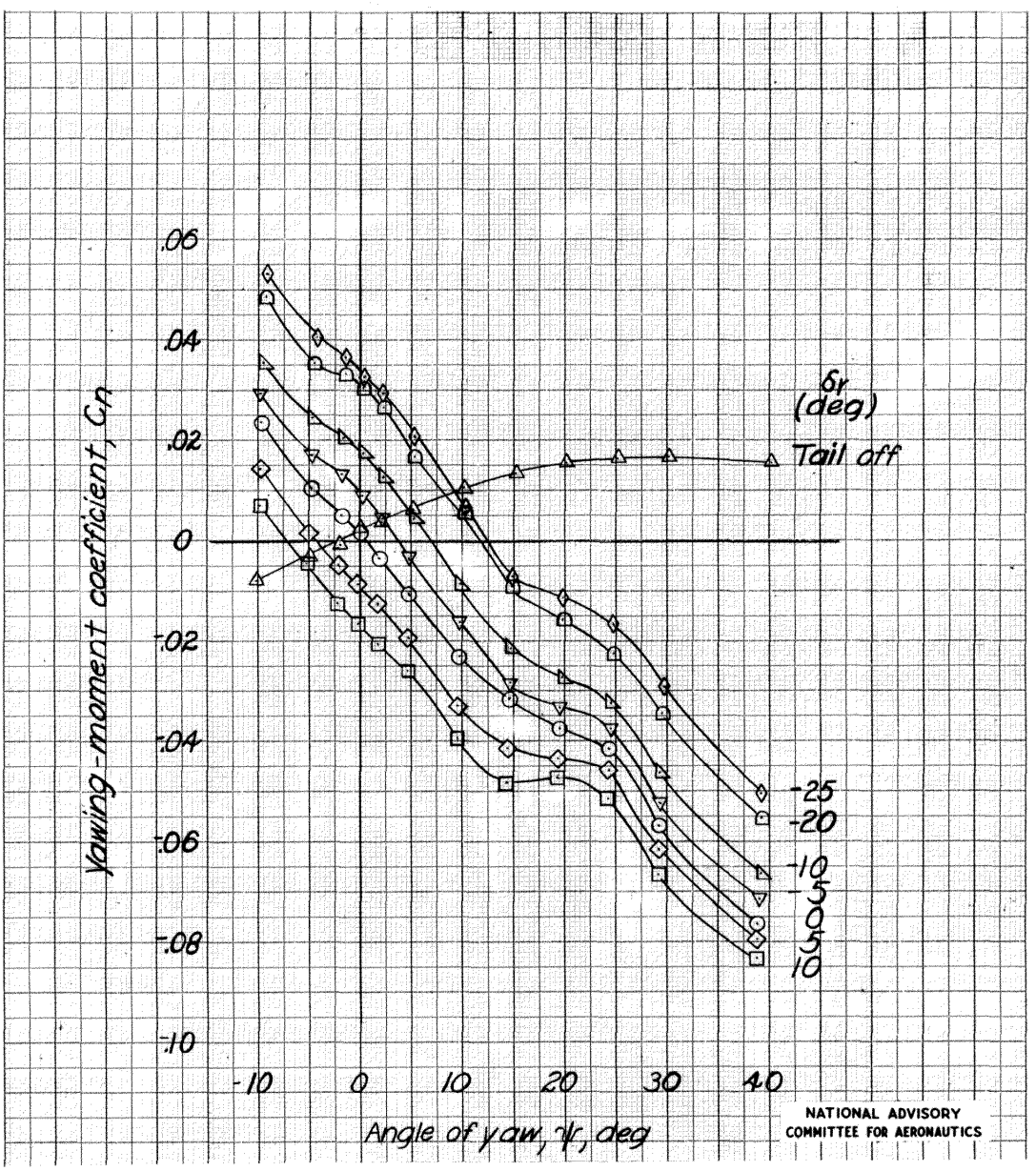

(a) Continued.

Figure 19 : Continued.

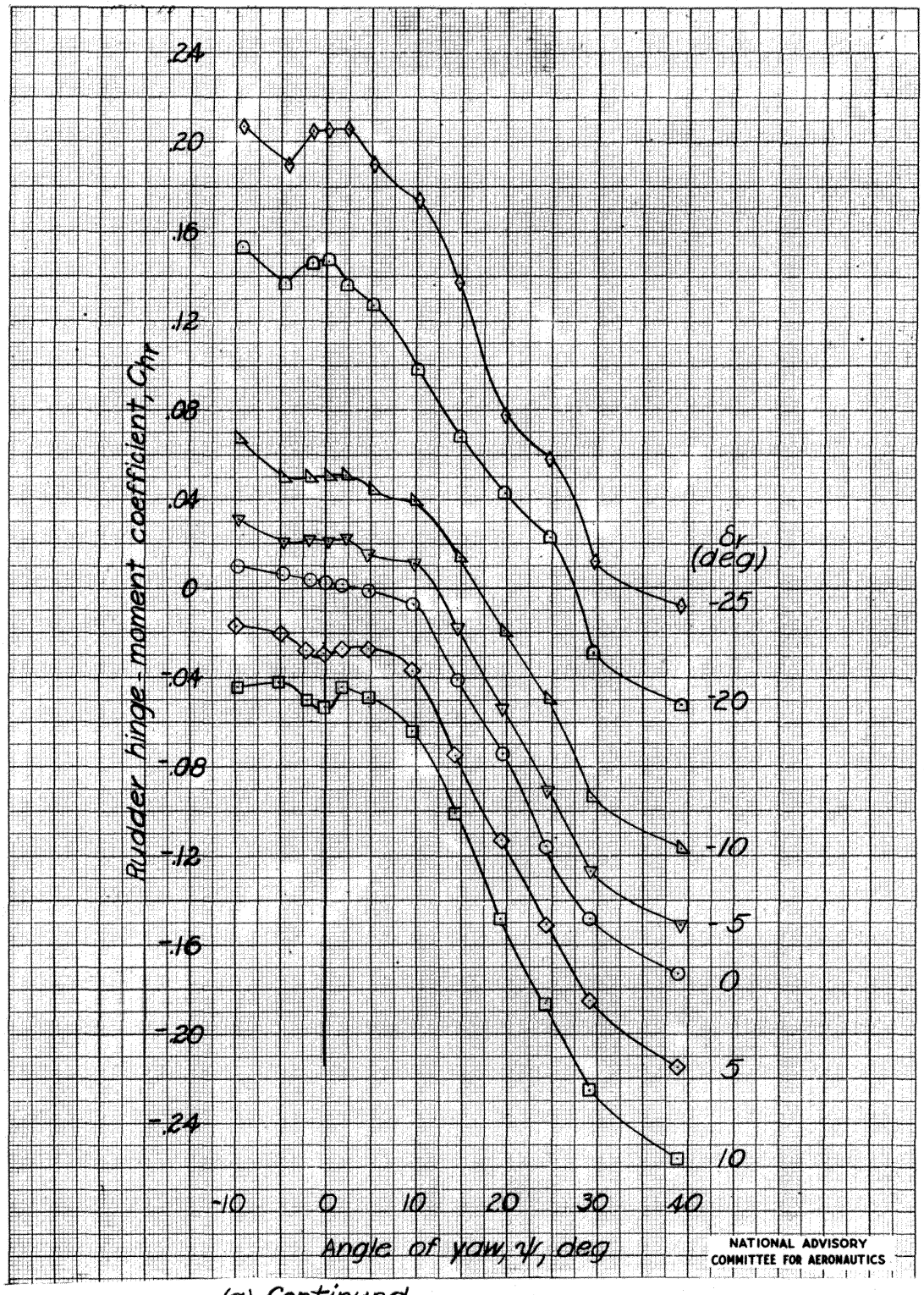

(a) Continued.

Figure 19 :Continued.

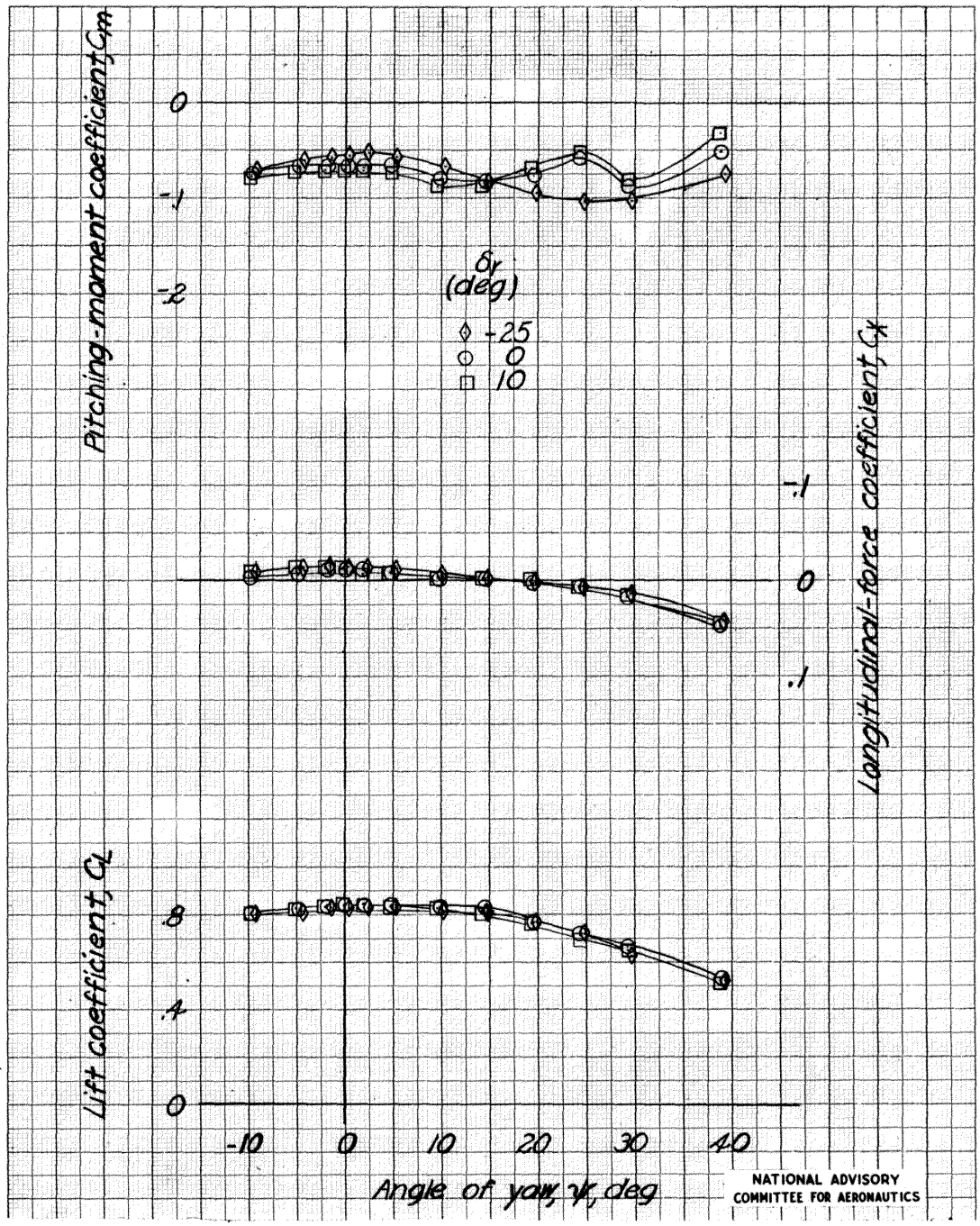

(a) Concluded.

Figure 19 : Continued.

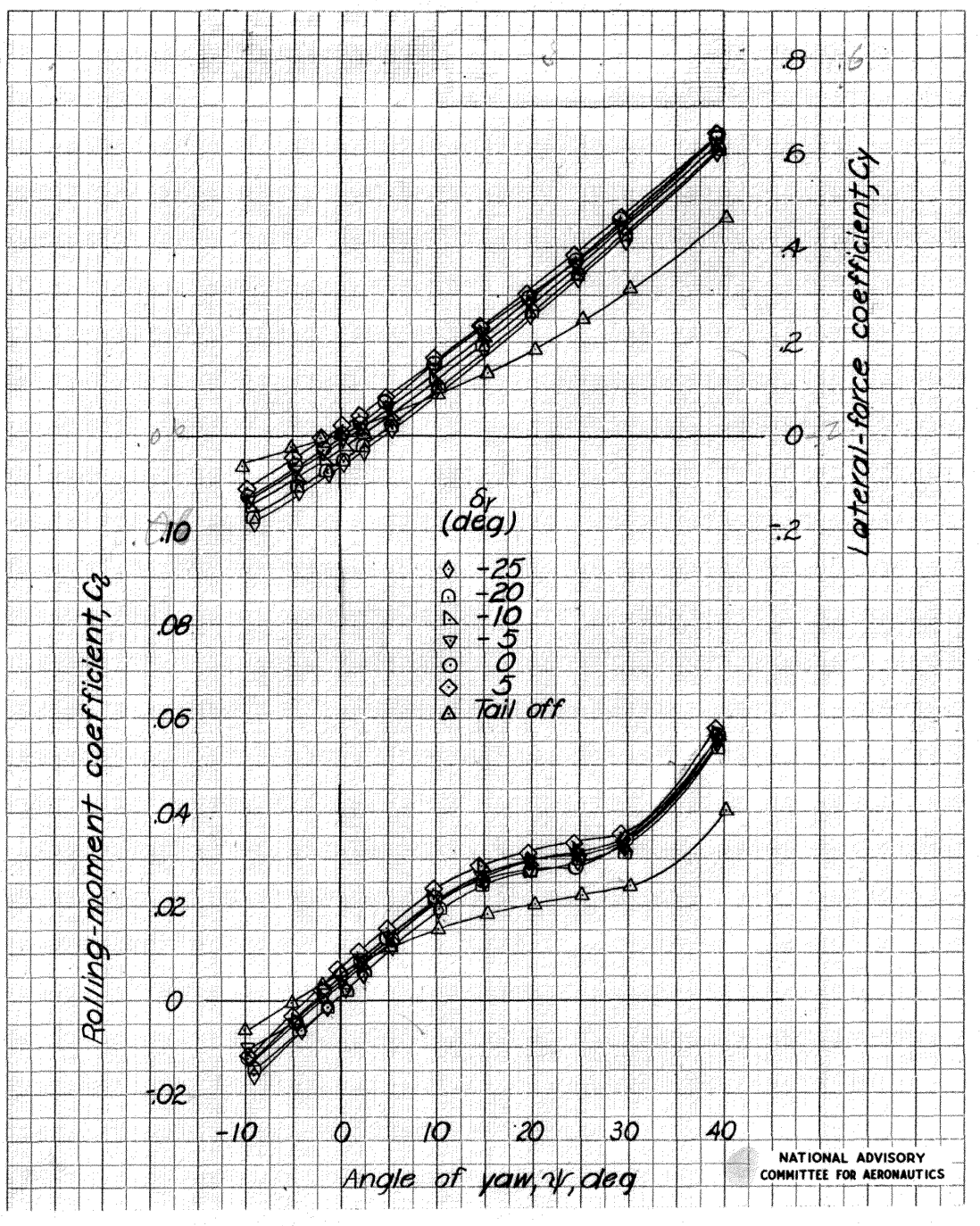

(b) Landing configuration, $\alpha = 6.1°$.

Figure 19 .- Continued.

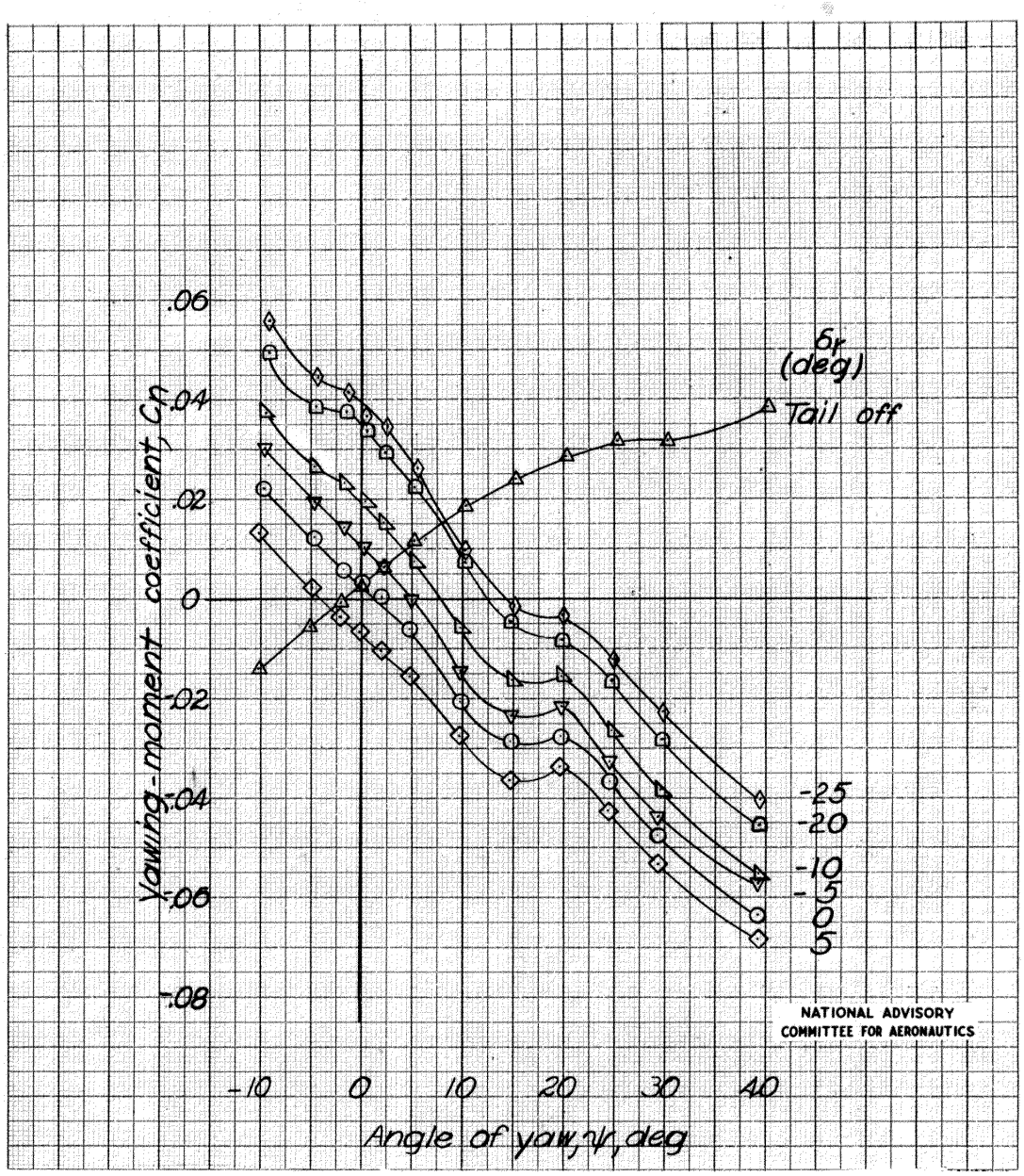

(b) Continued.

Figure 19 : Continued.

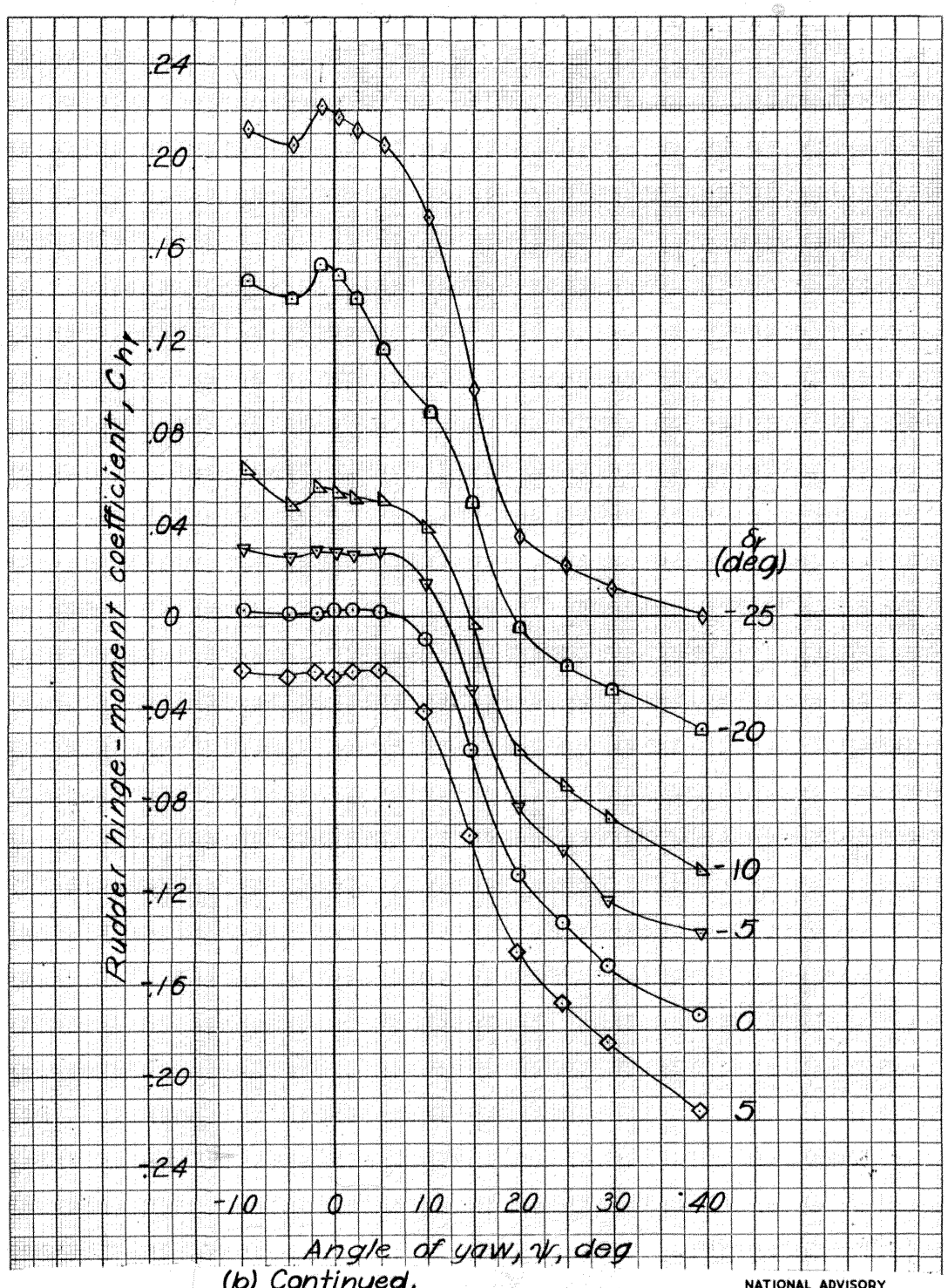

(b) Continued.

NATIONAL ADVISORY COMMITTEE FOR AERONAUTICS

Figure 19 Continued

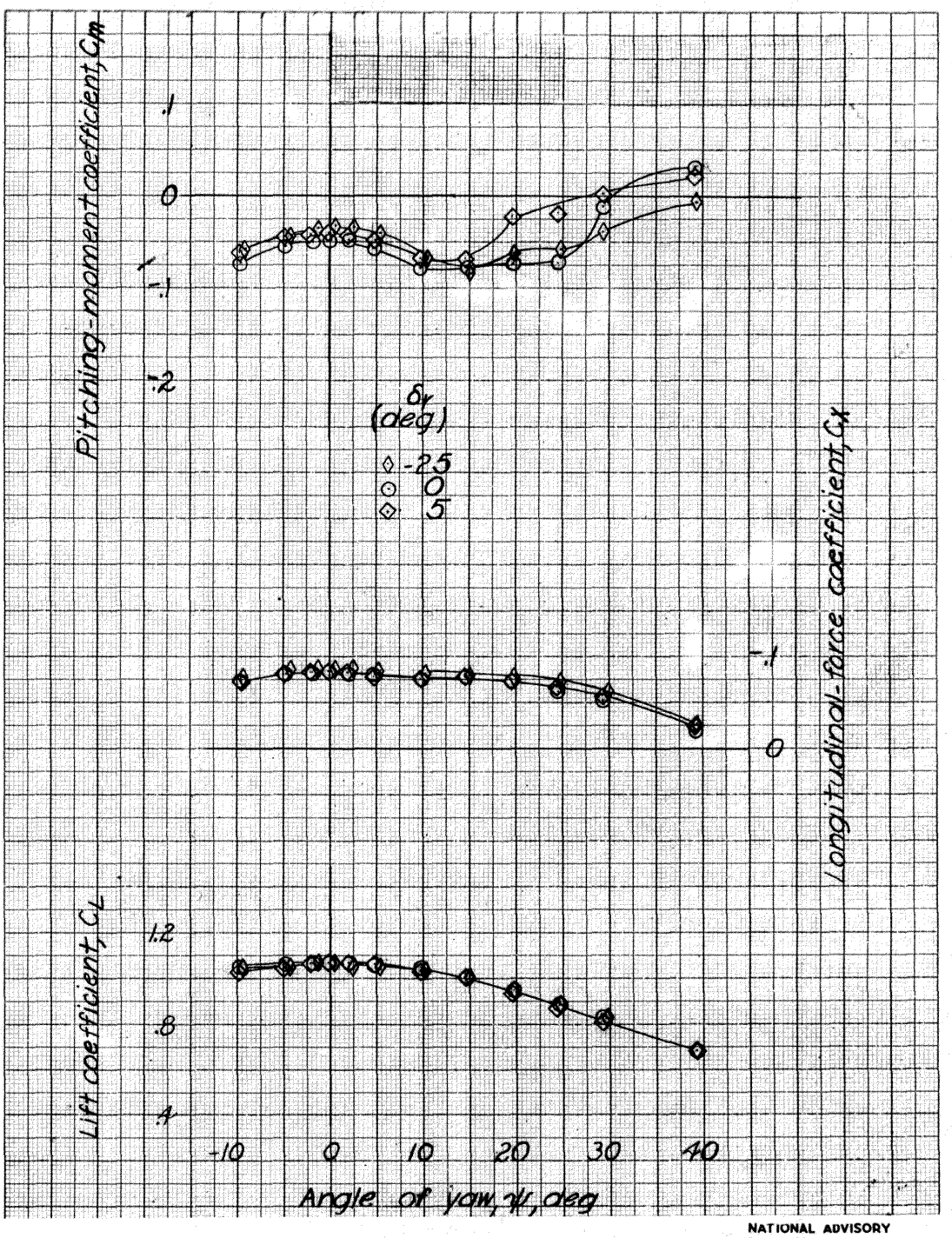

(b) Concluded.

Figure 19 : Concluded.

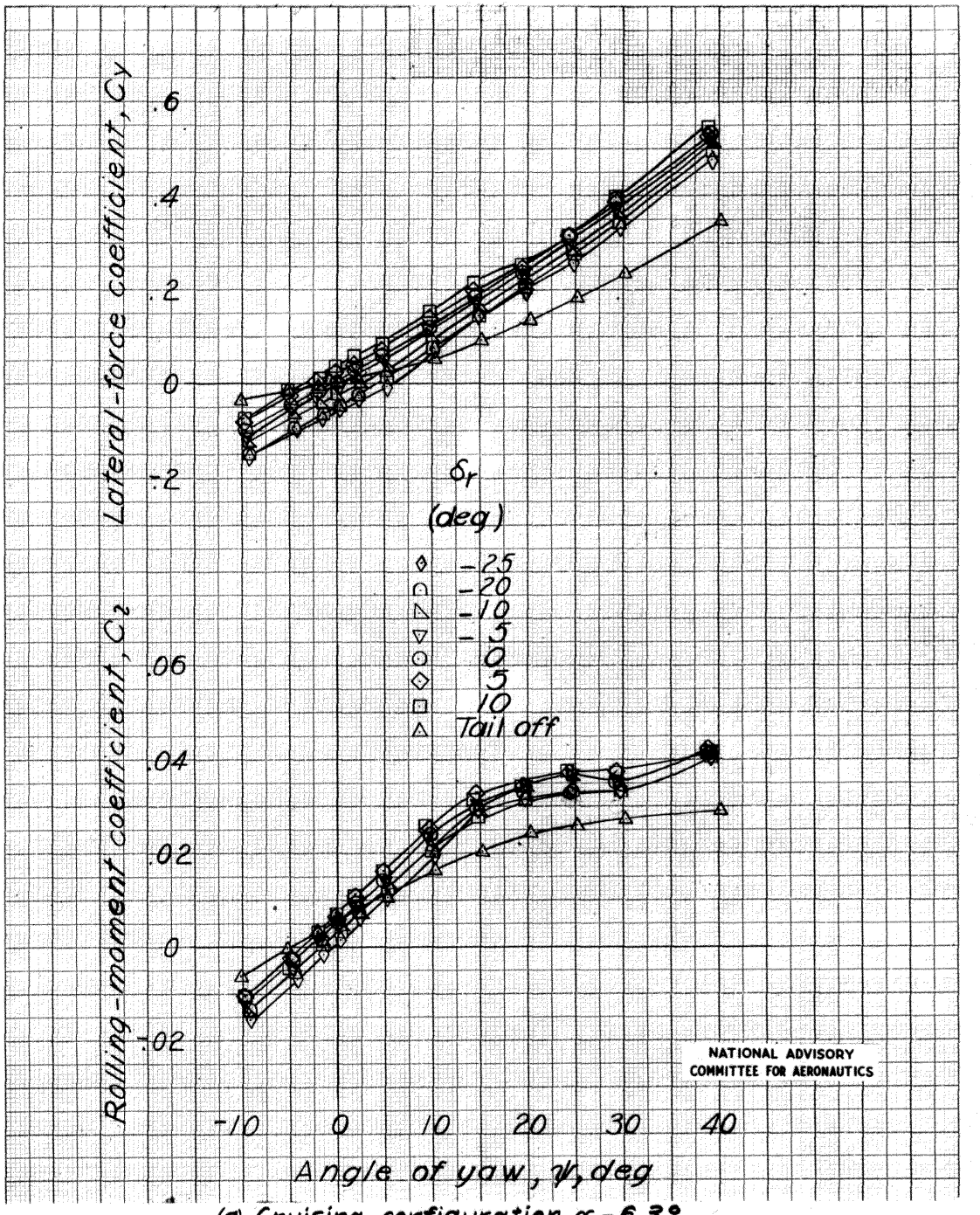

(a) Cruising configuration, $\alpha = 6.3°$

Figure 20: The effect of rudder deflection on the aerodynamic characteristics in yaw of the 1/5-scale model of the Republic XP-84 airplane. Full power, $i_t = 1°$

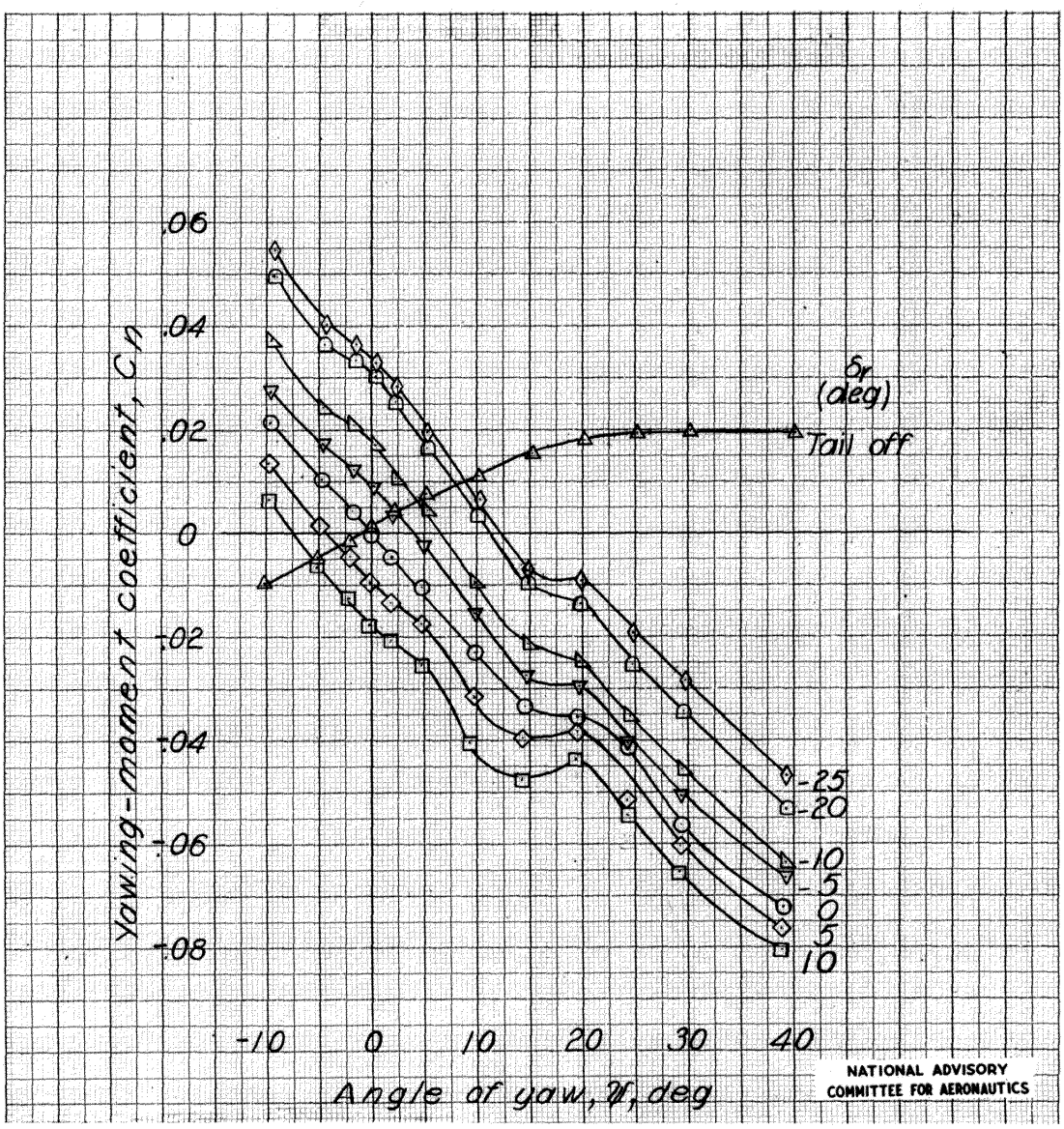

(a) Continued.

Figure 20 : Continued.

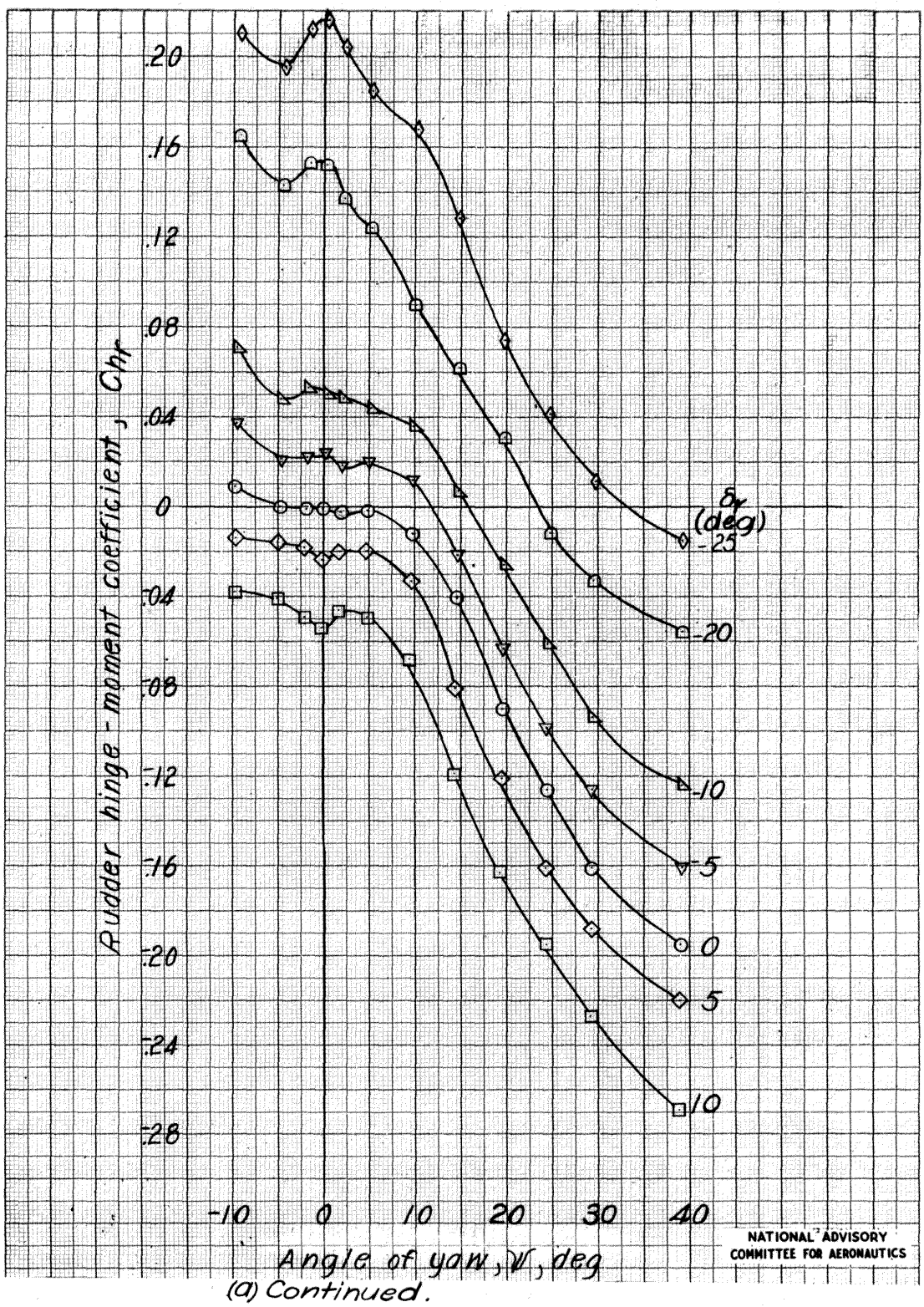

(a) Continued.

Figure 20 : Continued.

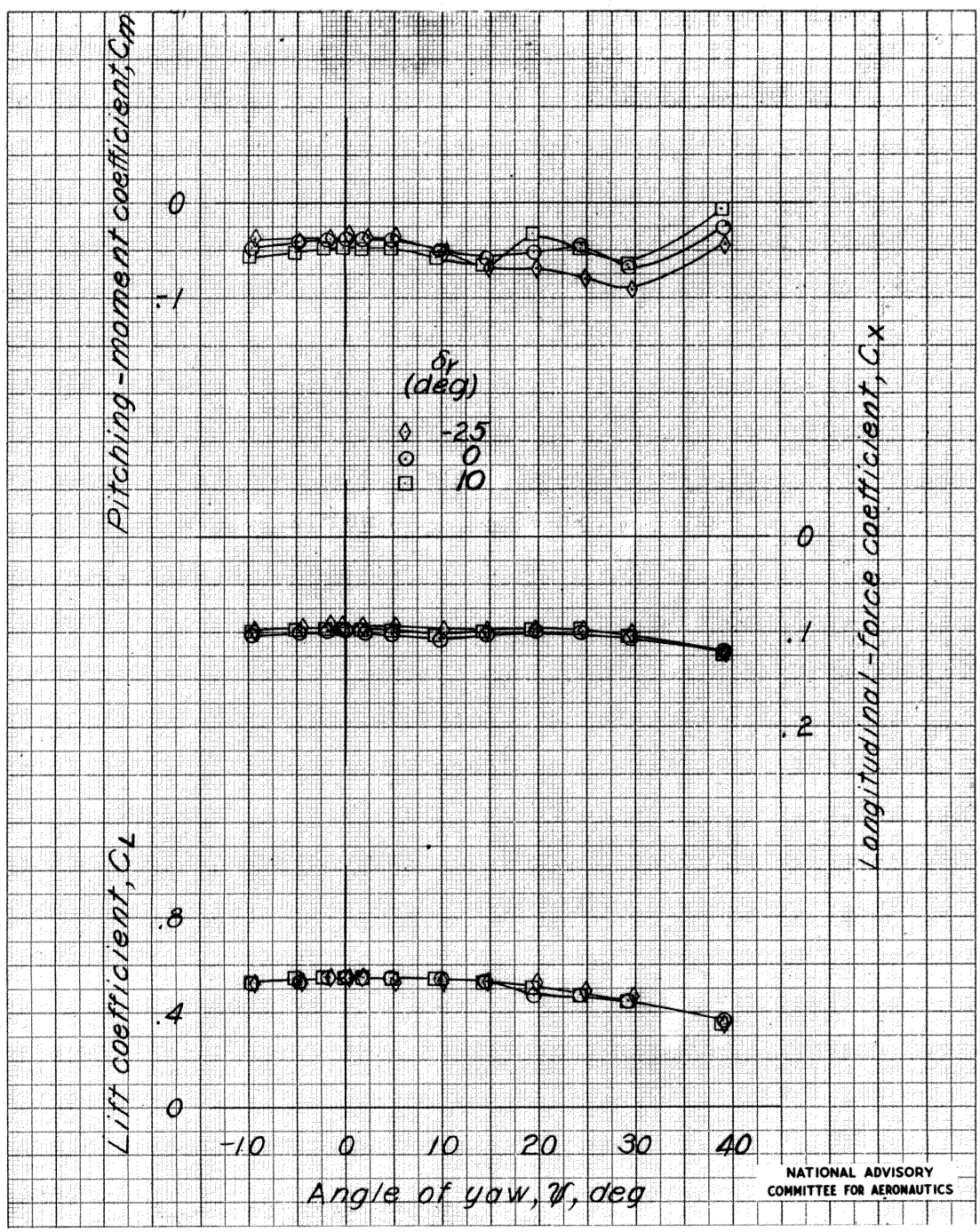

(a) Concluded.

Figure 20 : Continued.

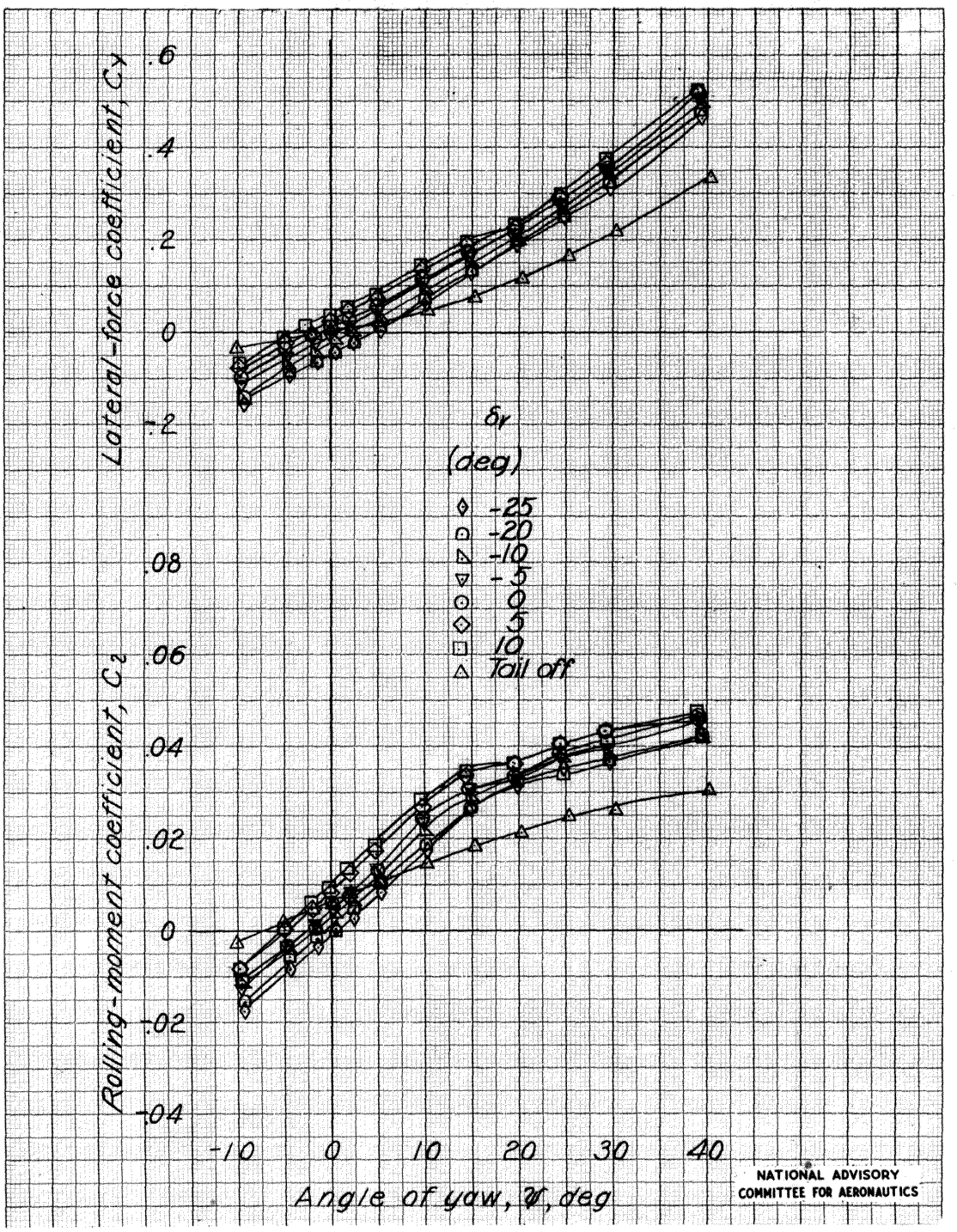

(b) Cruising configuration, $\alpha = 1.4°$.

Figure 20: Continued.

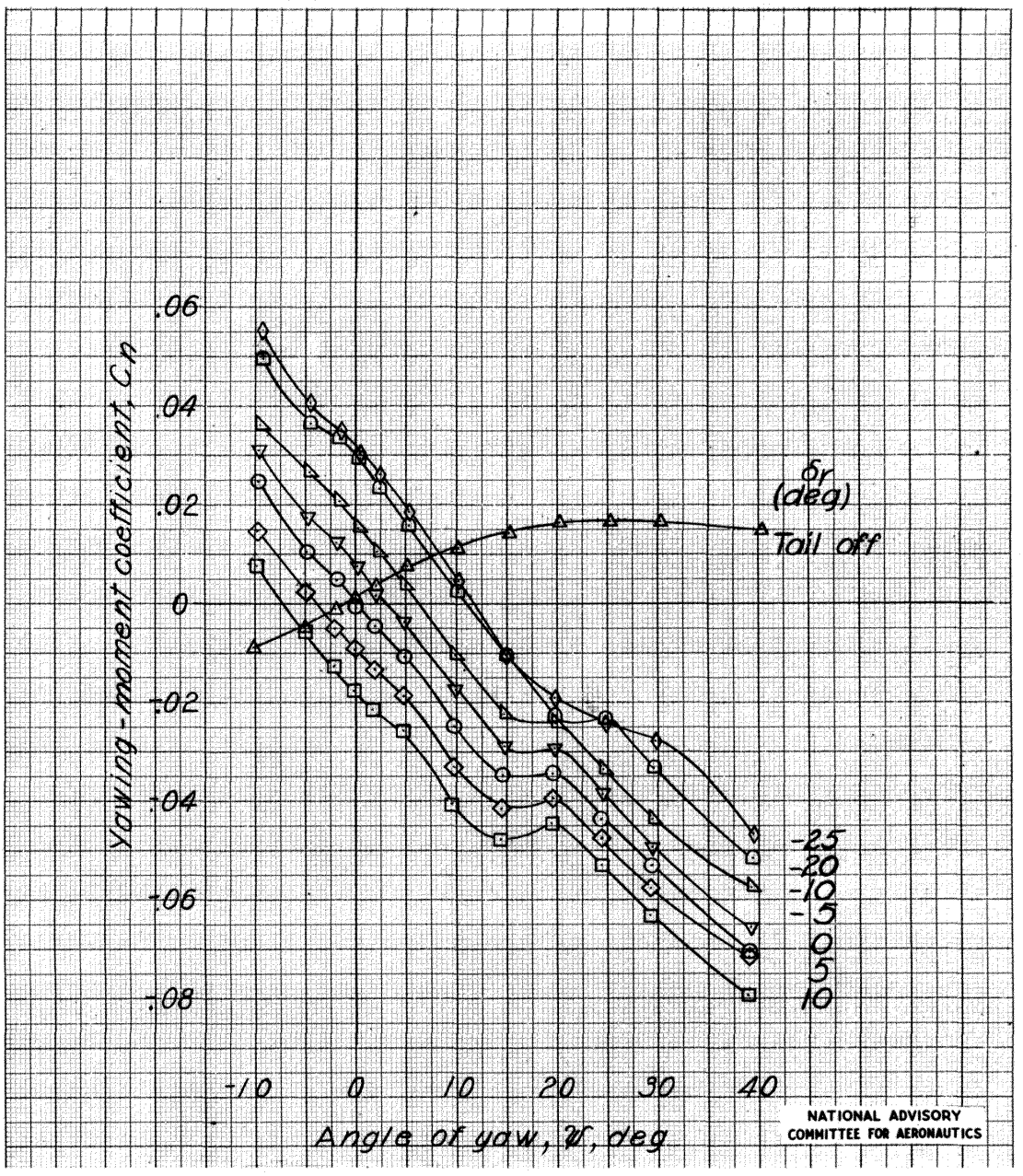

(b) Continued.

Figure 20 : Continued.

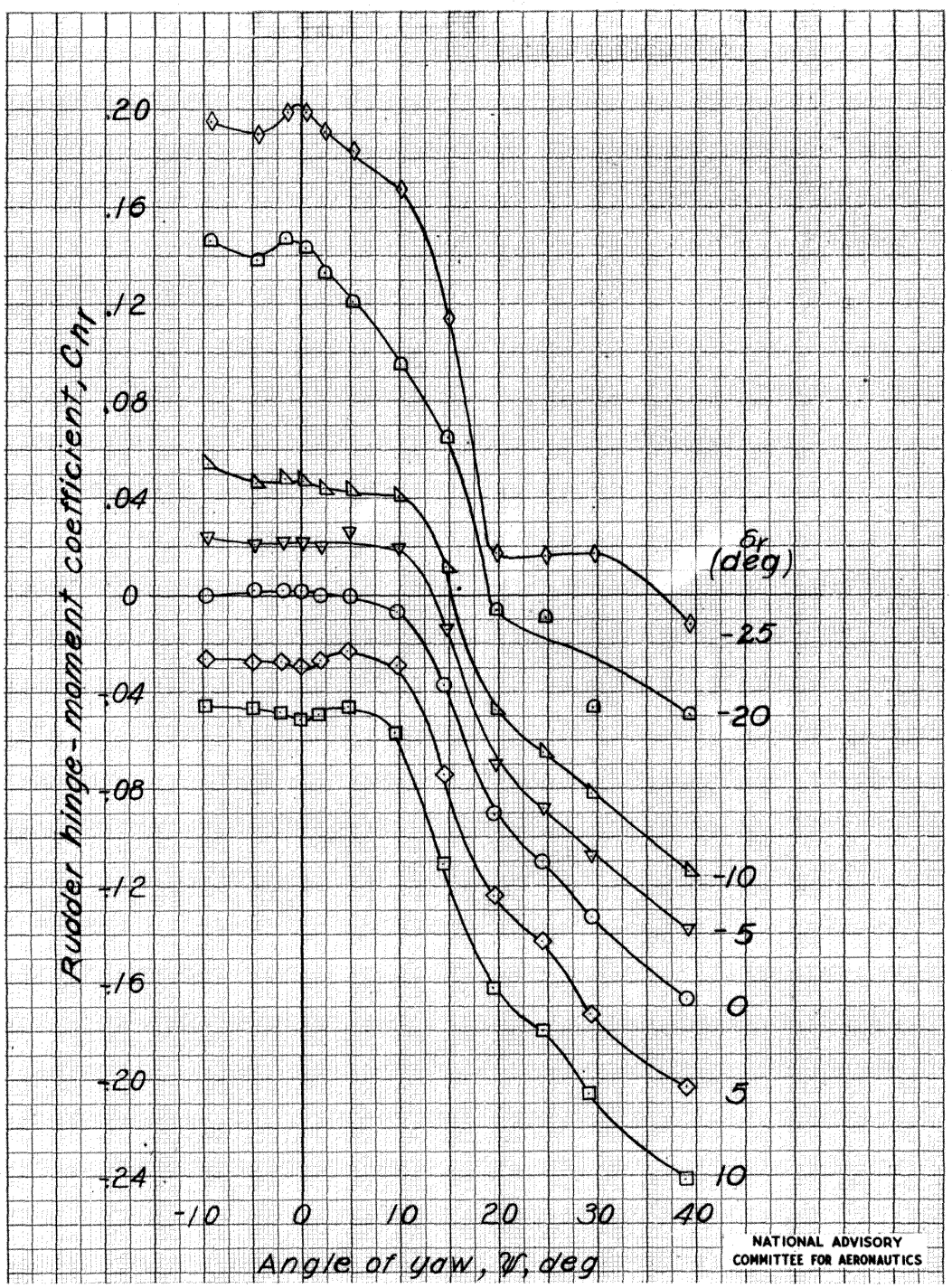

(b) Continued.

Figure 20 : Continued.

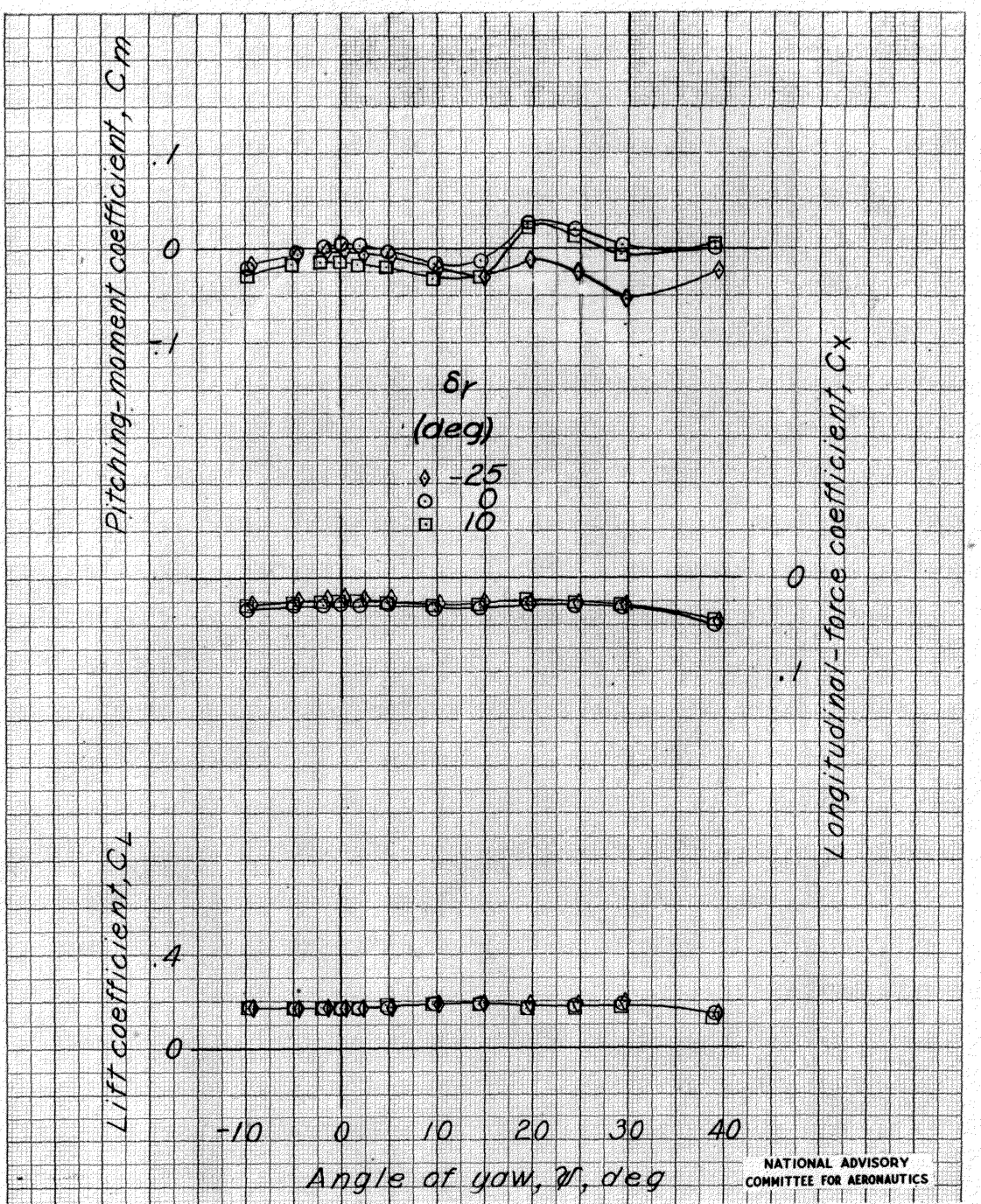

(b) Concluded.

Figure 20 : Continued.

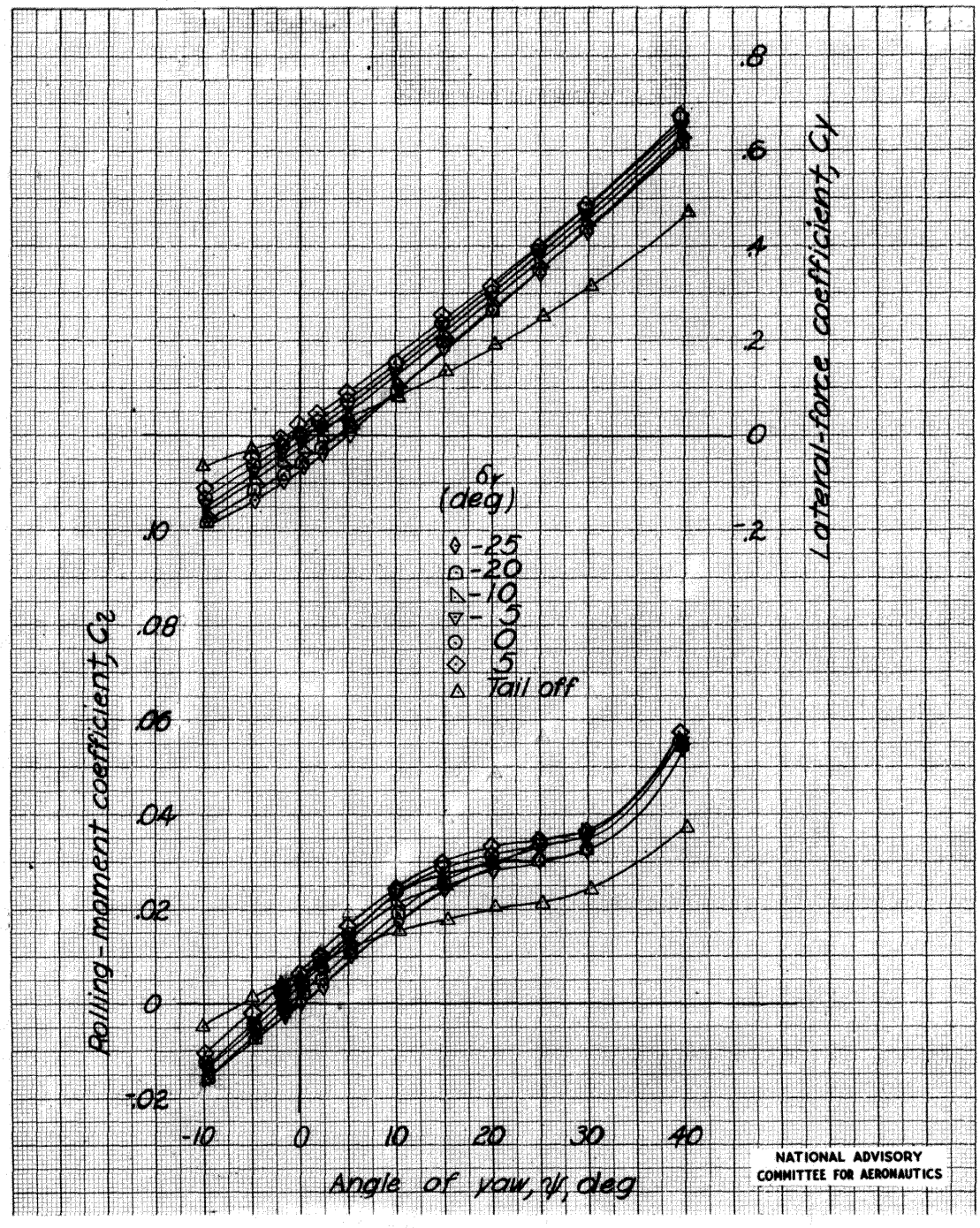

(c) Landing configuration, $\alpha = 5.6°$.

Figure 20: Continued.

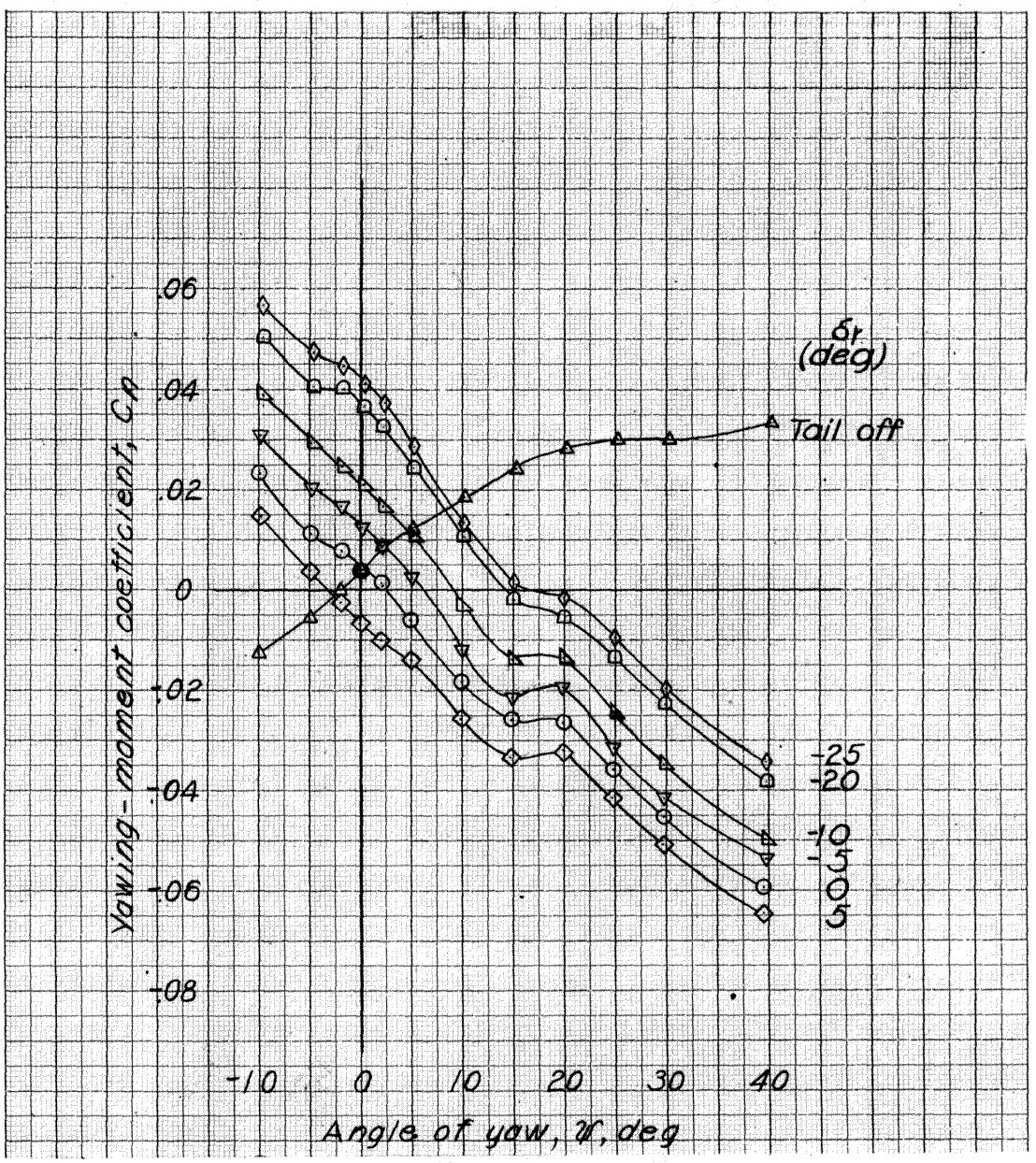

(c) Continued.

Figure 20: Continued.

National Advisory
Committee For Aeronautics

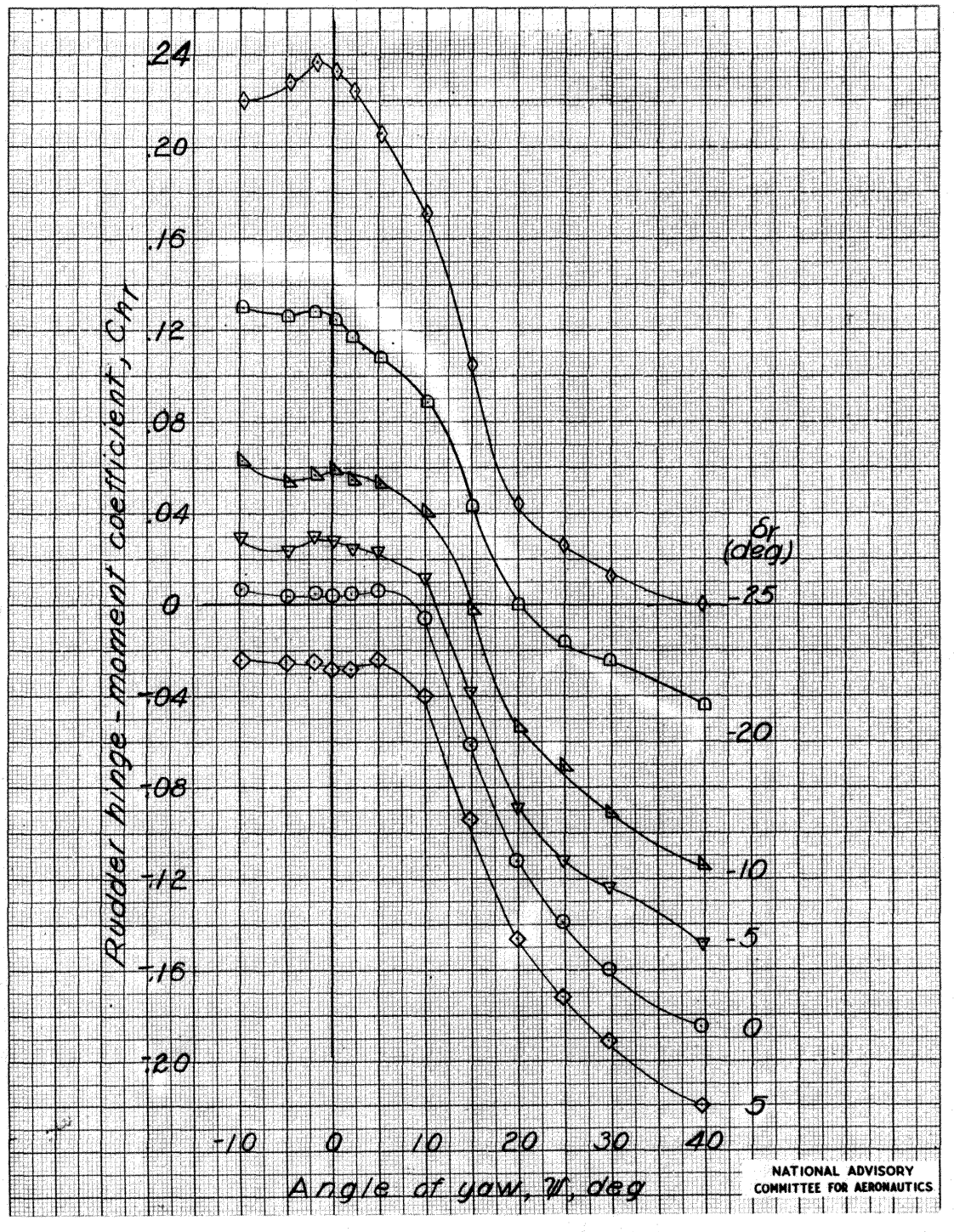

(C) Continued.

Figure 20 : Continued.

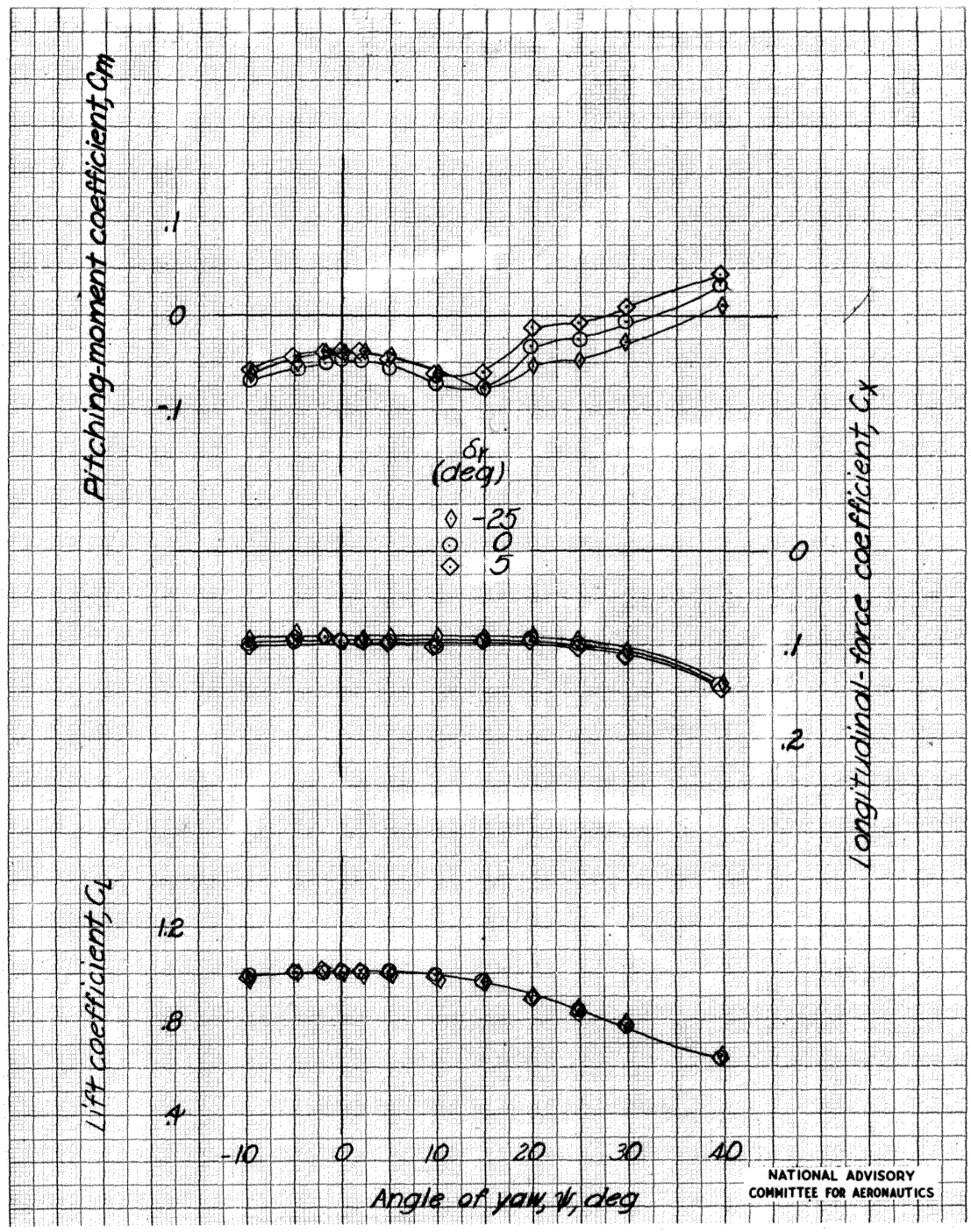

(c) Concluded.

Figure 20 : Concluded.

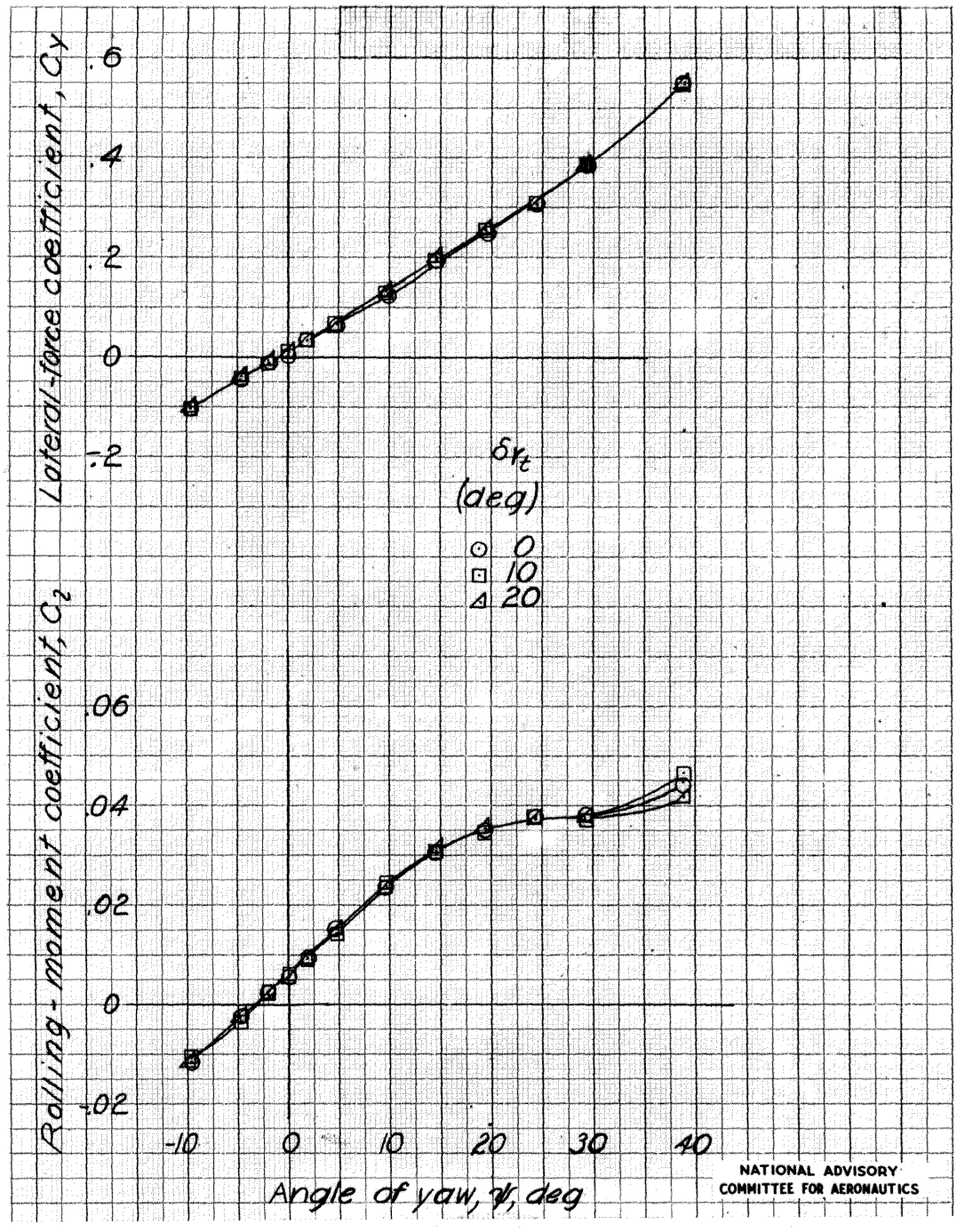

Figure 21 : Effect of rudder tab deflection on the aerodynamic characteristics in yaw of the 1/5-scale model of the Republic XP-84 airplane. Cruising configuration; Idling power; $\delta_r = 0$; $\alpha = 10.1°$; $i_t = 1°$.

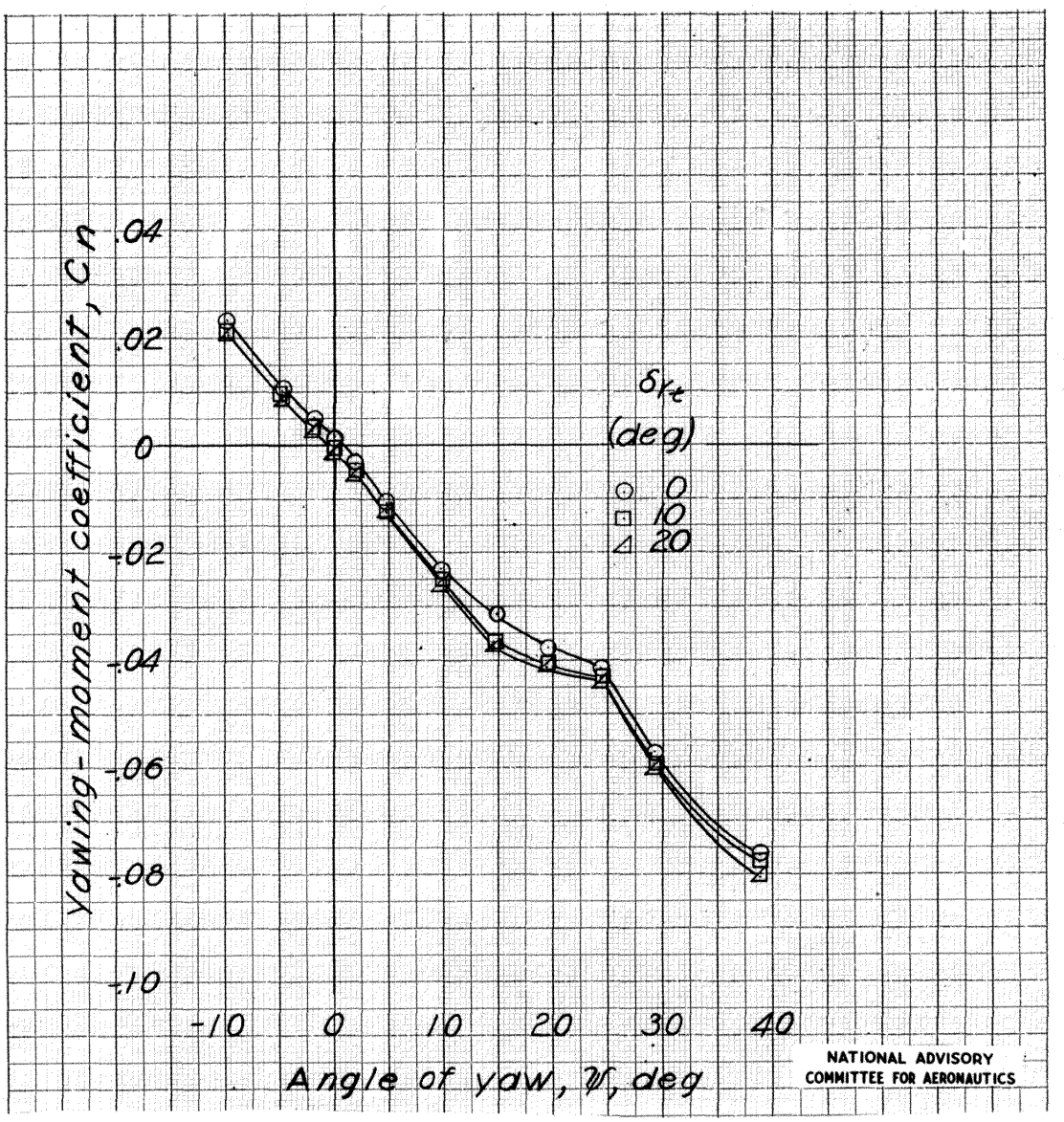

Figure 21 : Continued.

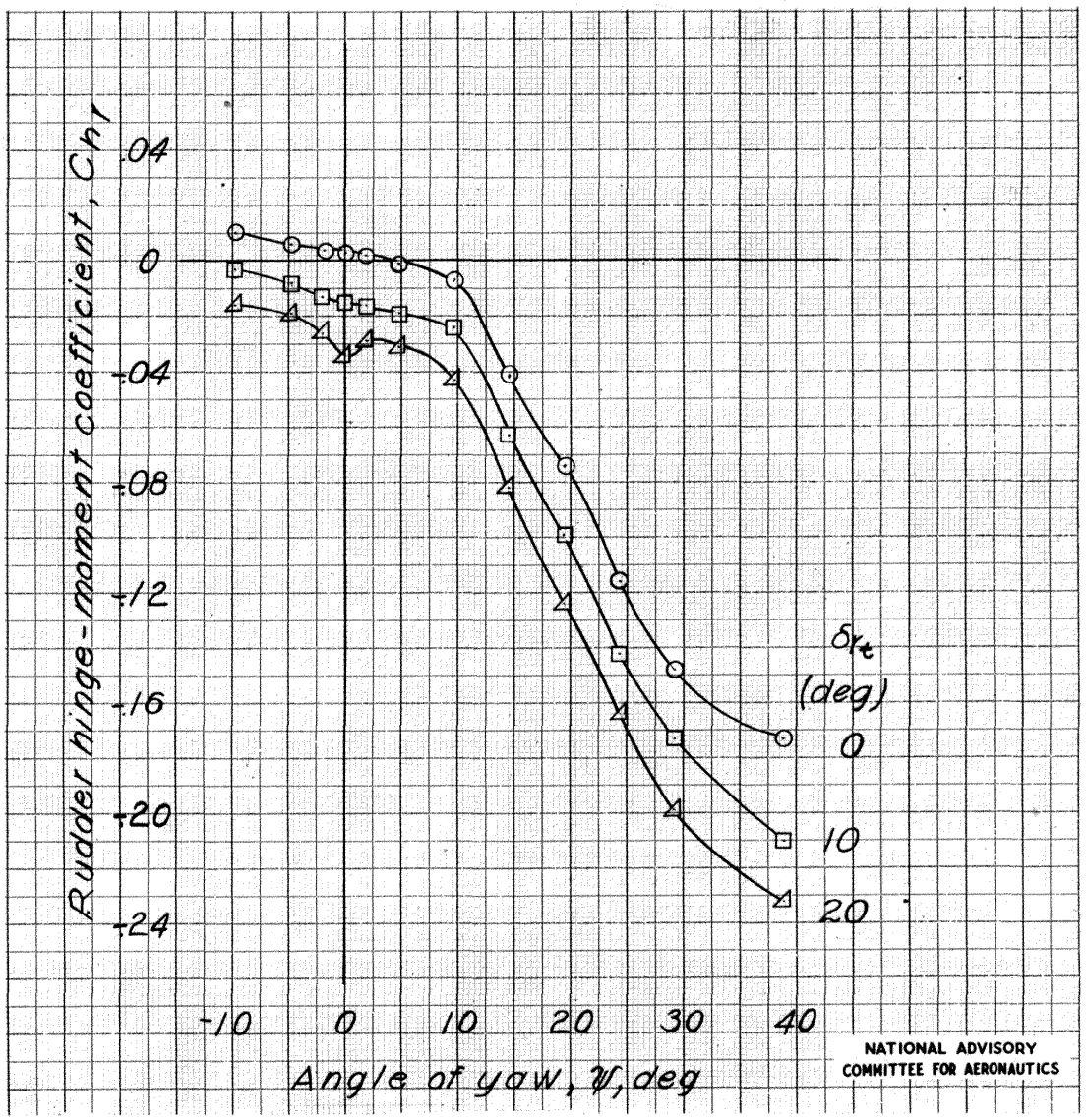

Figure 21 : Concluded.

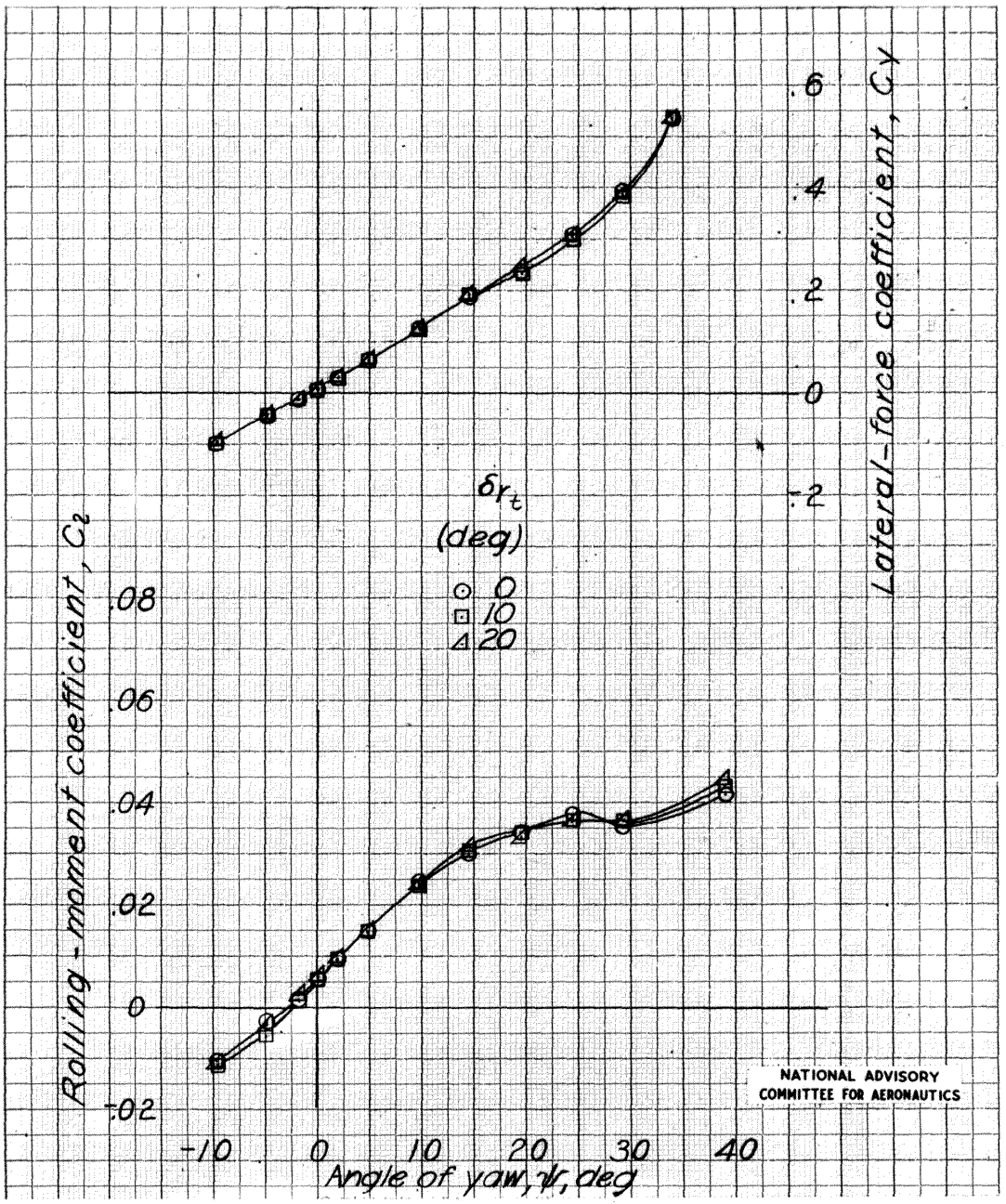

(a) $\alpha = 6.3°$.

Figure 22 : Effect of rudder tab deflection on the aerodynamic characteristics in yaw of the 1/5-scale model of the XP-84 airplane. Full power; $\delta_r = 0$; $i_t = 1°$. Cruising configuration.

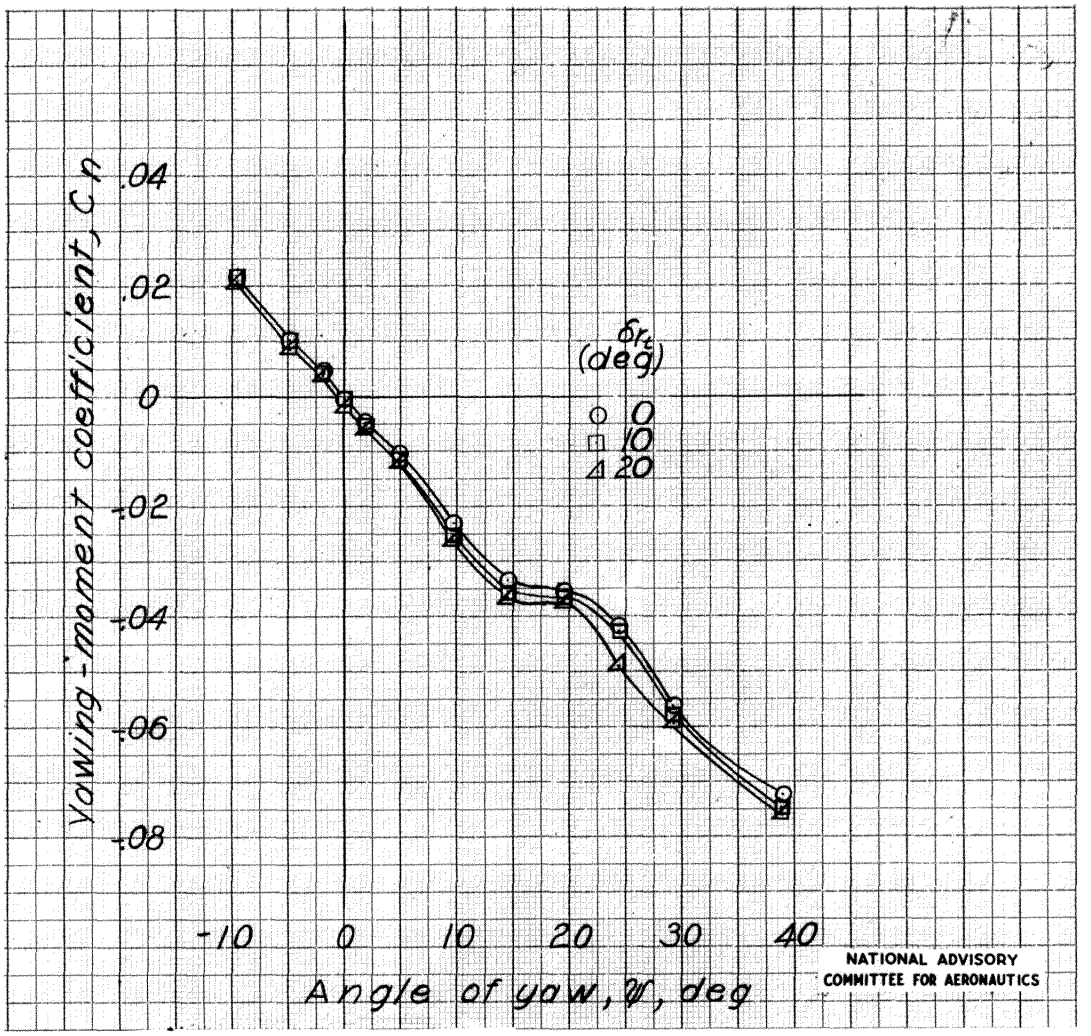

(a) Continued.

Figure 22 :Continued.

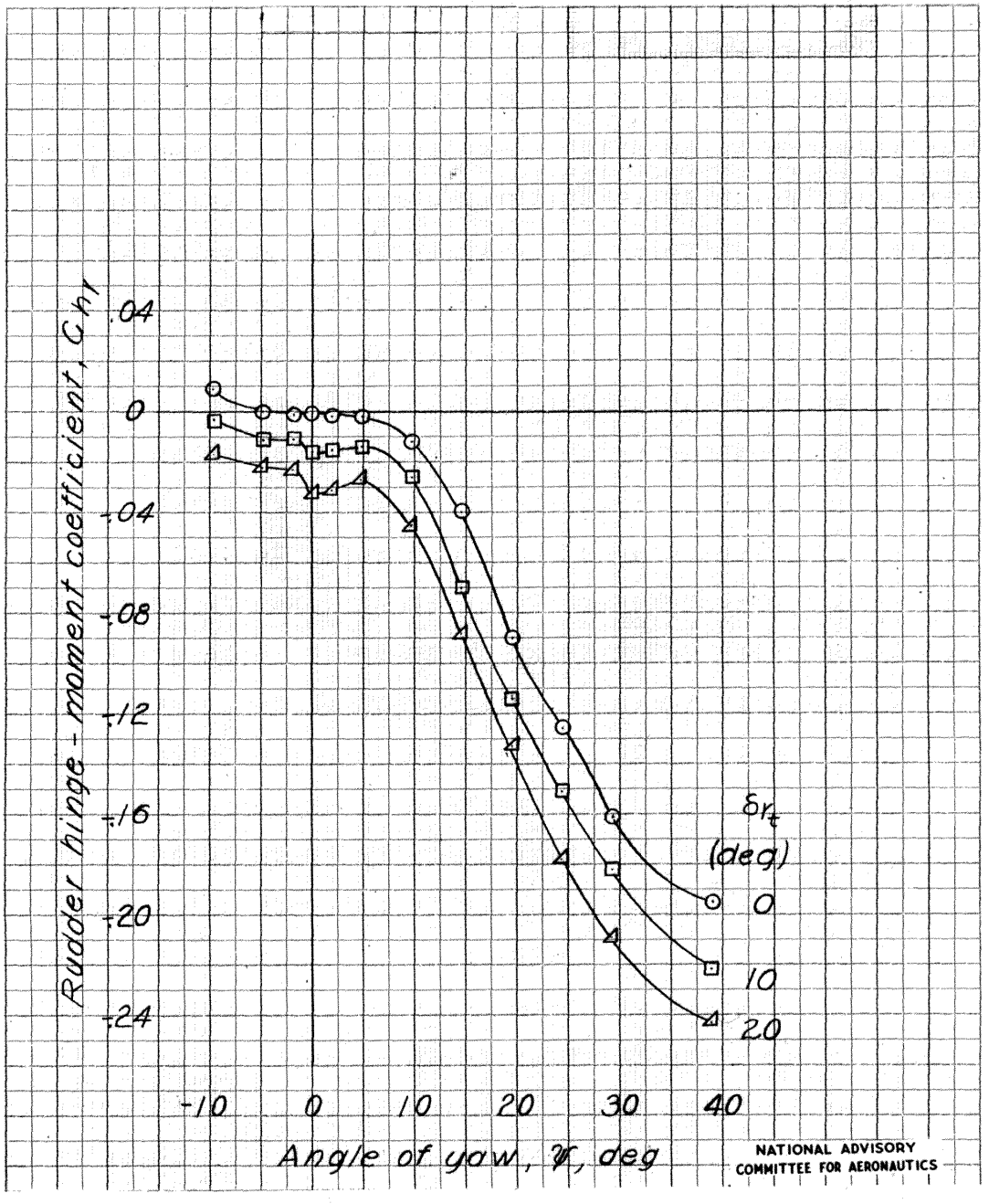

(a) Concluded.

Figure 22 : Continued.

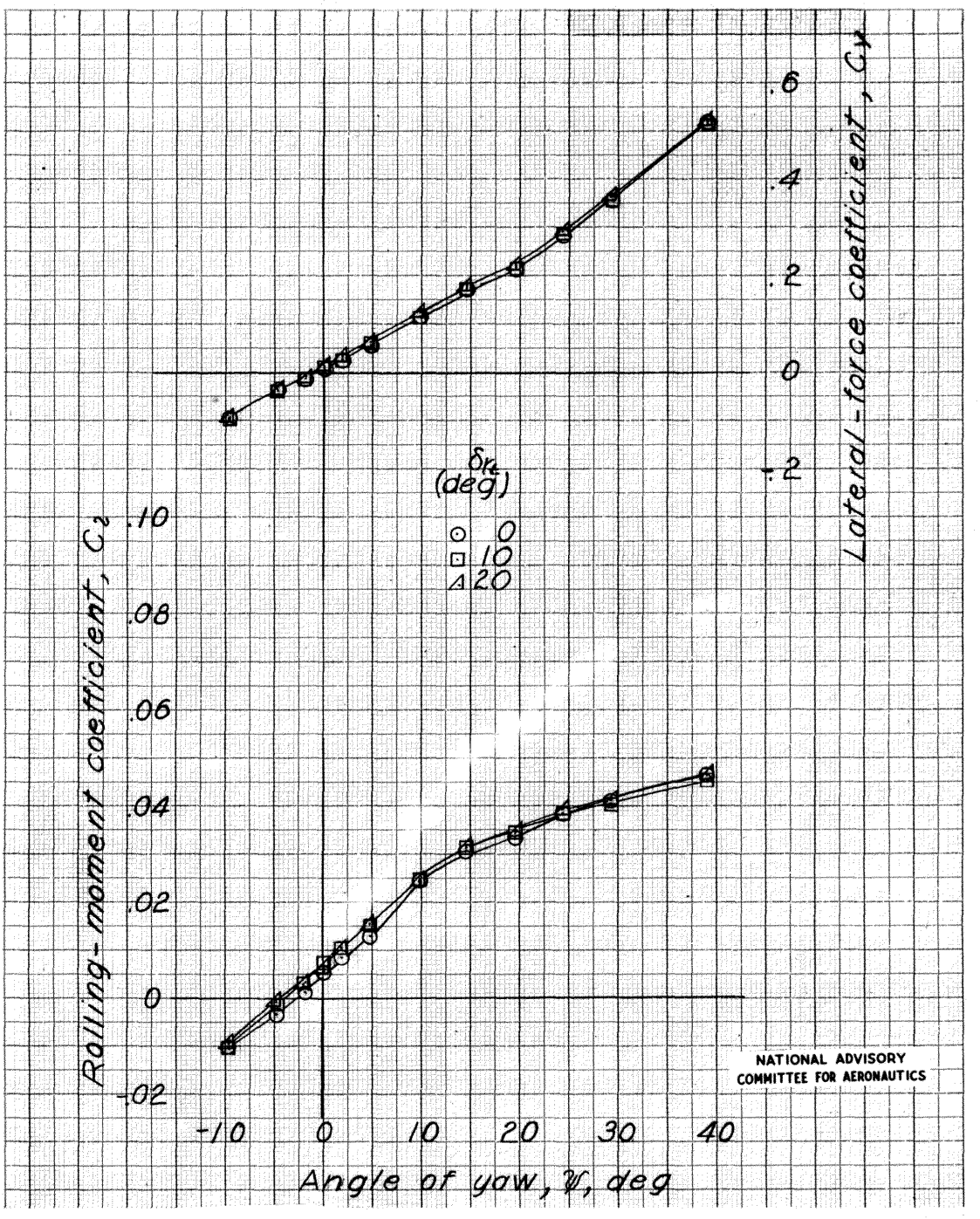

(b) $\alpha = 1.4°$

Figure 22 : Continued.

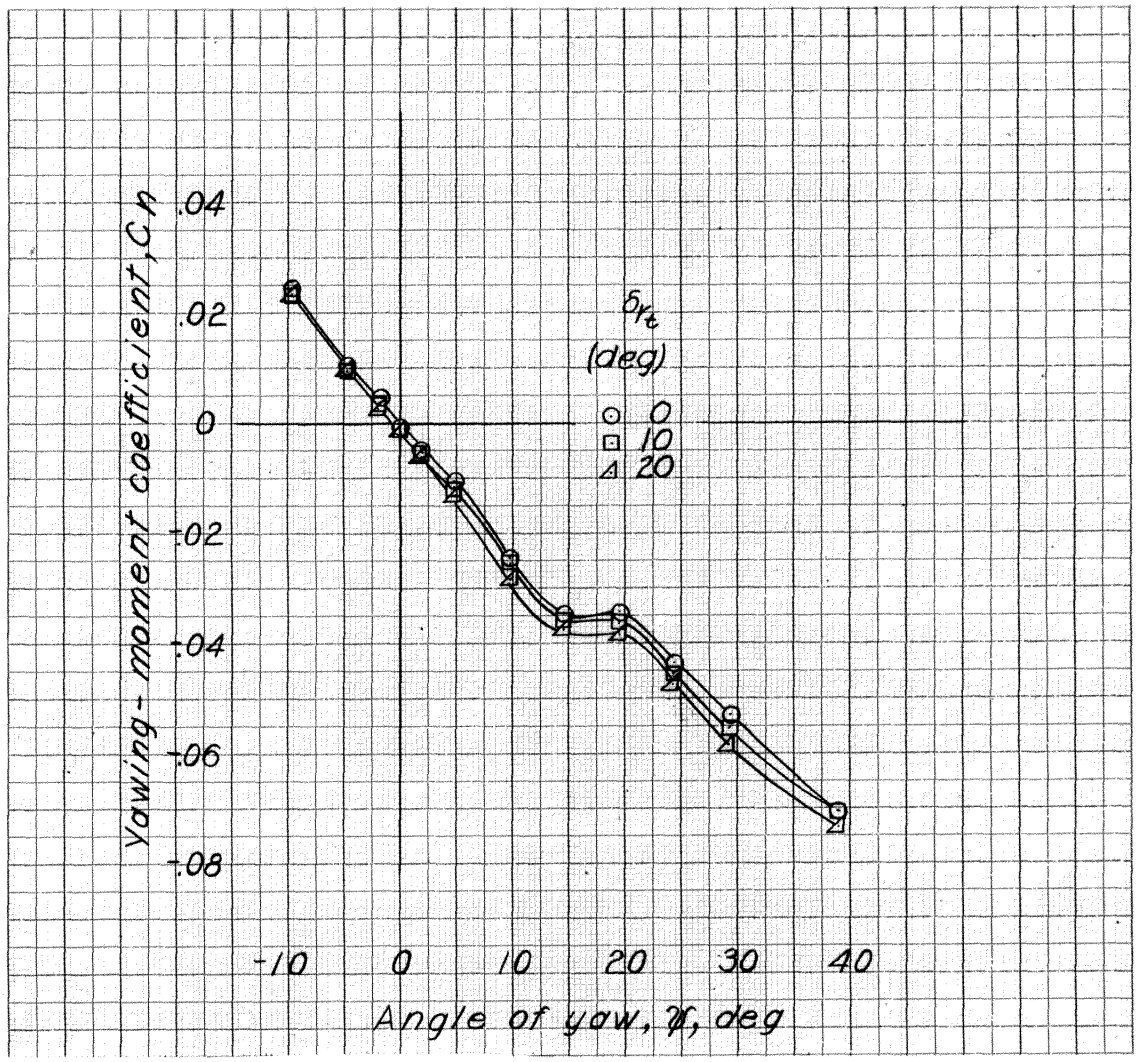

(b) Continued.

National Advisory Committee For Aeronautics

Figure 22 : Continued.

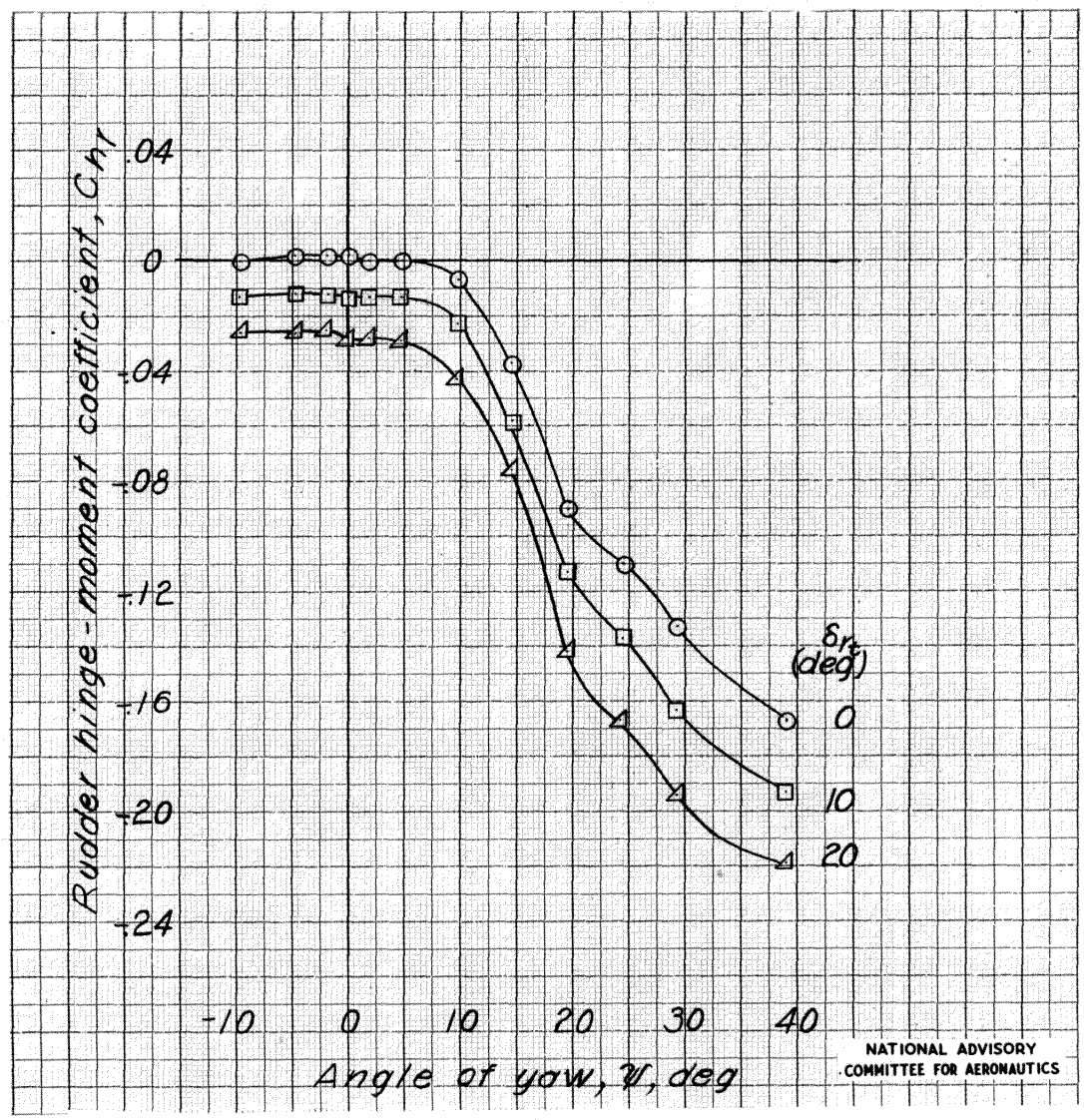

(b) Concluded.

Figure 22: Concluded.

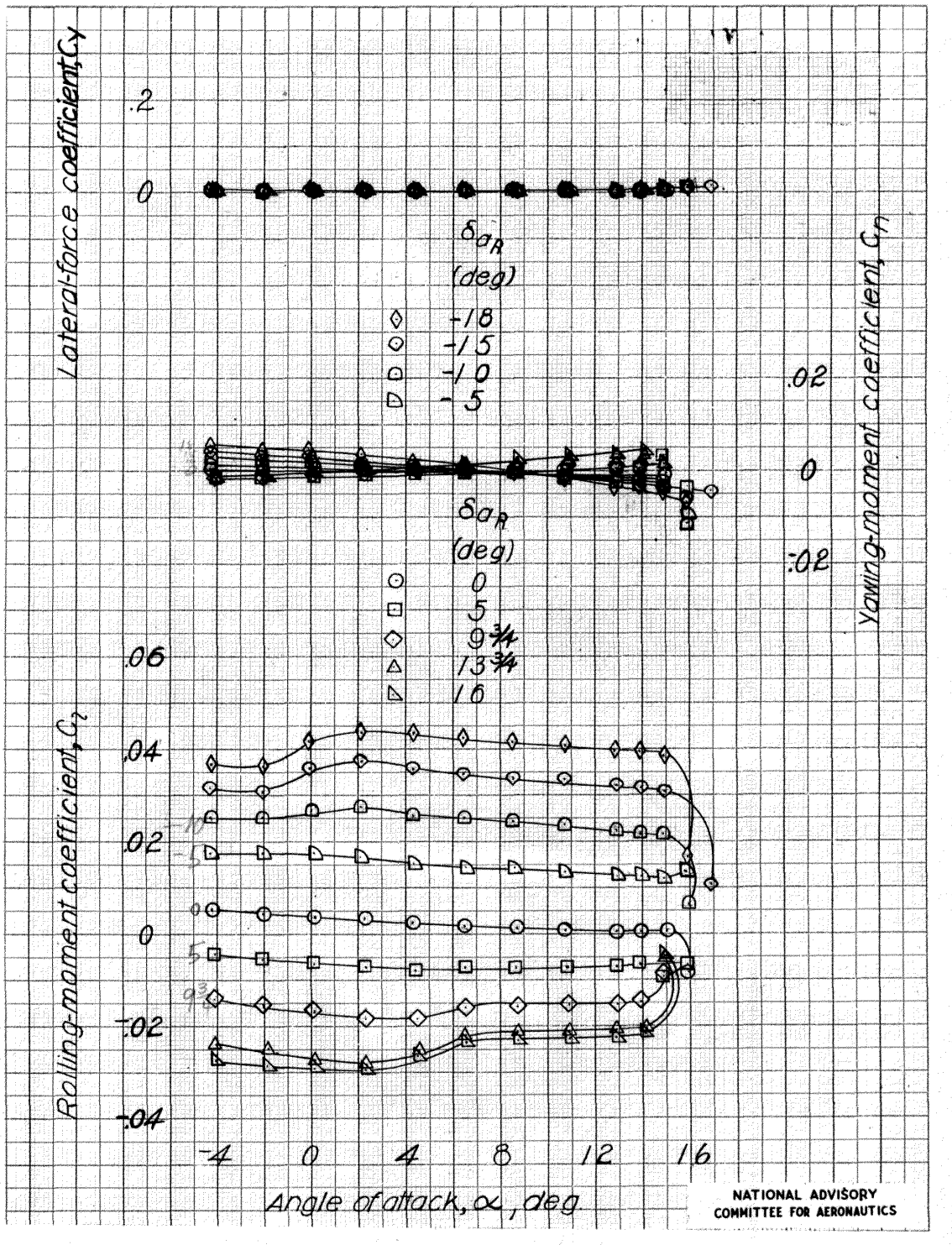

(a) Cruising configuration.

Figure 23 : Aileron characteristics of the 1/5-scale model of the Republic XP-84 airplane. Power off; $i_t = 0°$.

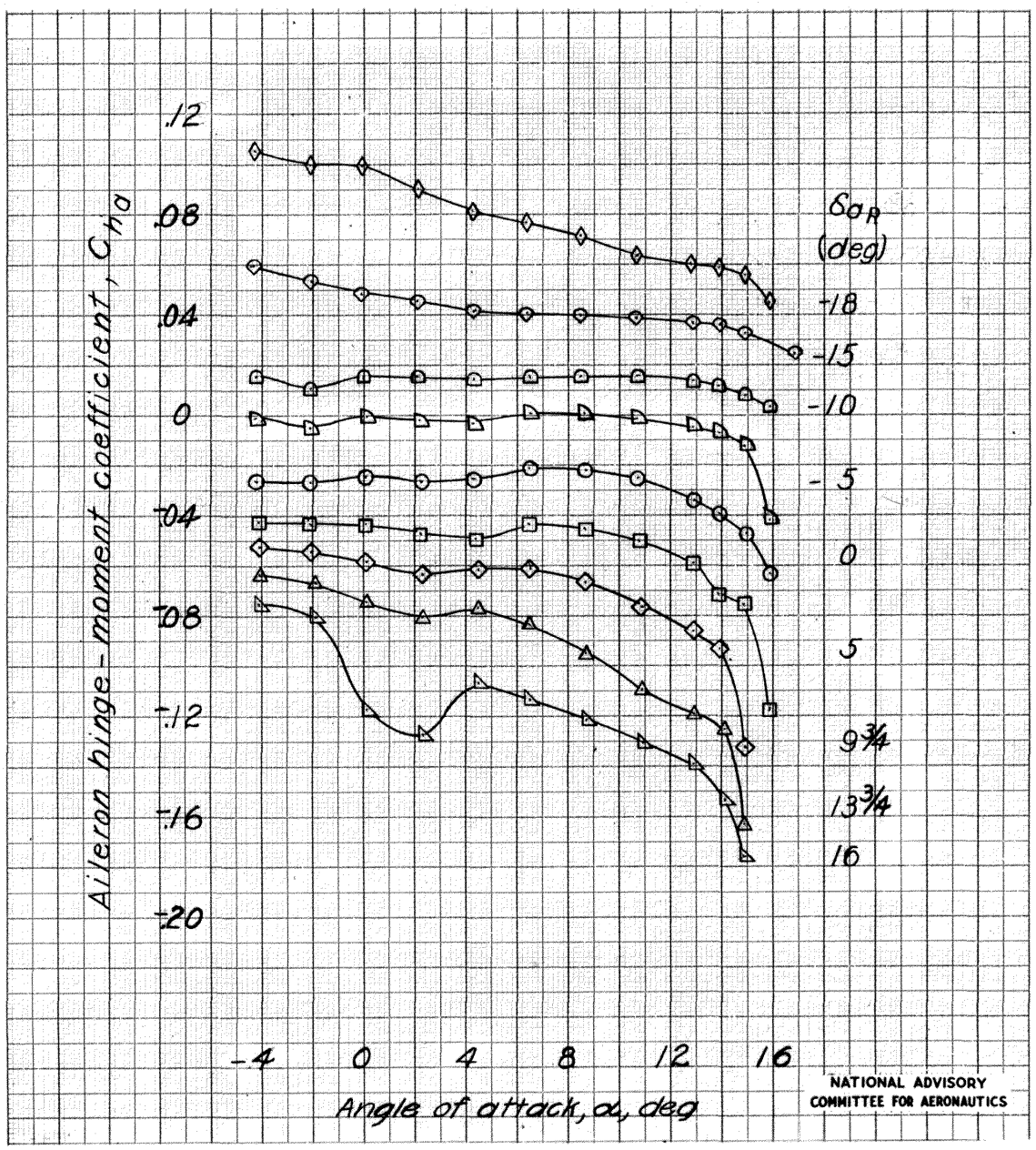

(a) Concluded.

Figure 23 : Continued.

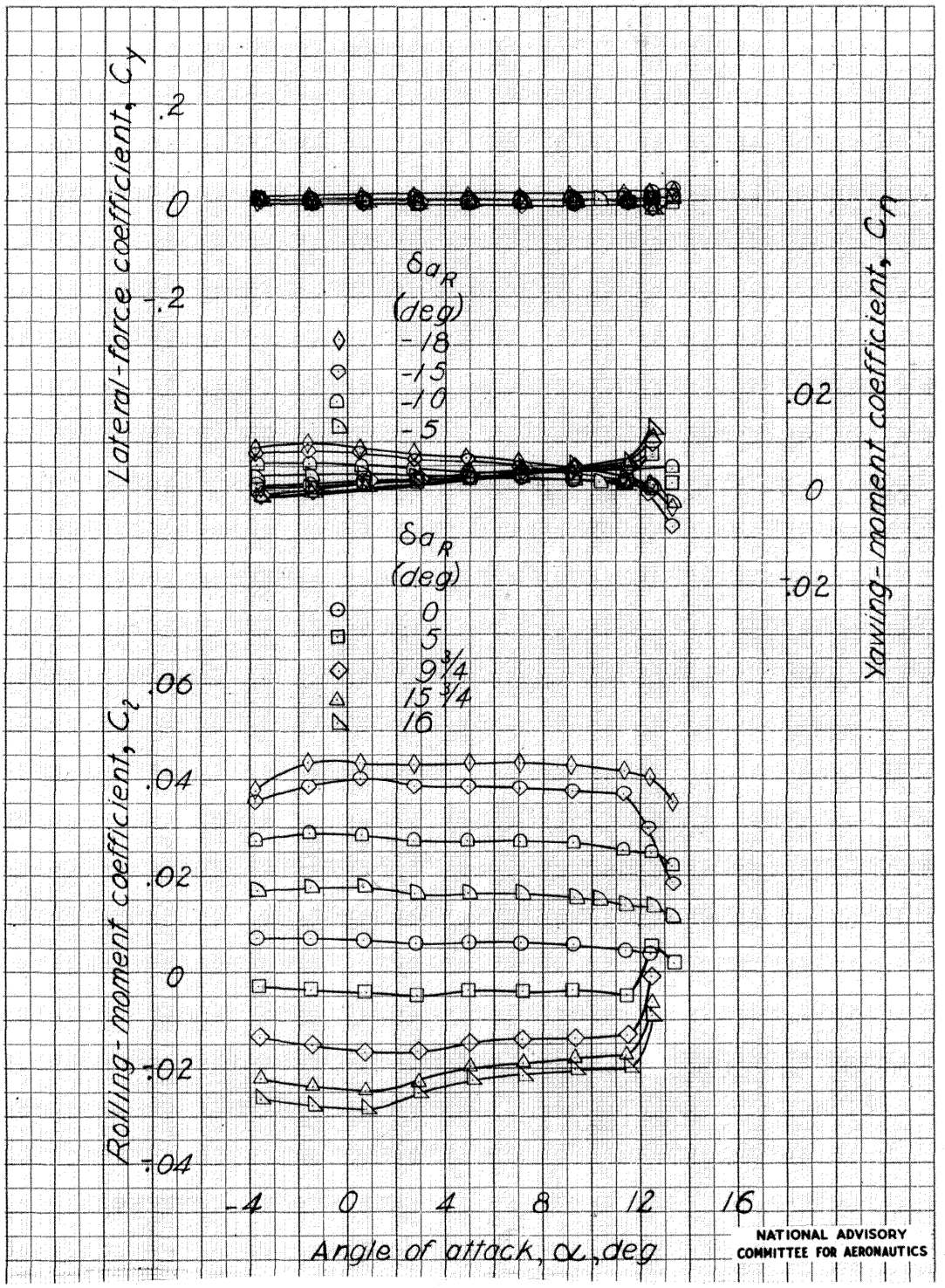

(b) Landing configuration.

Figure 23 :Continued.

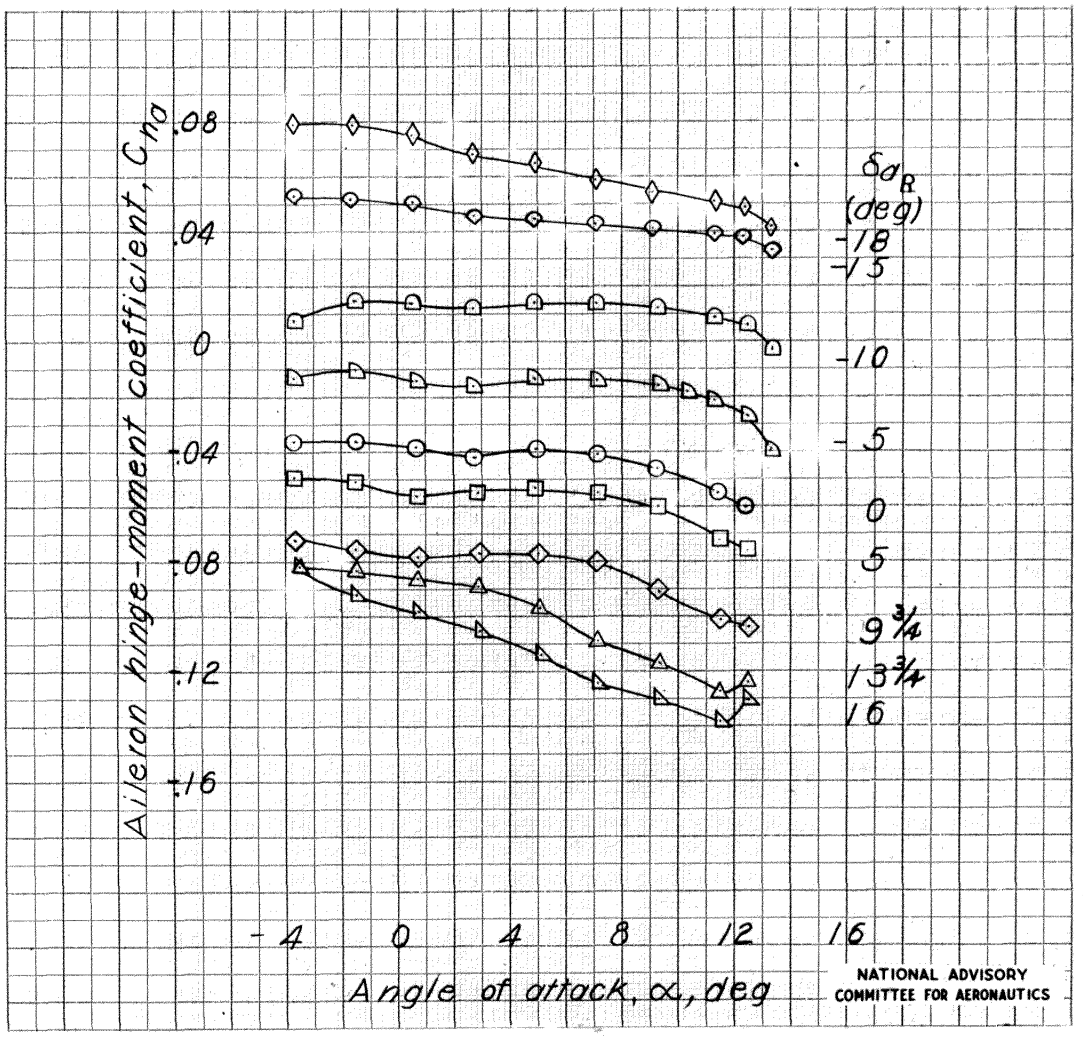

(b) Concluded.

Figure 23 : Concluded.

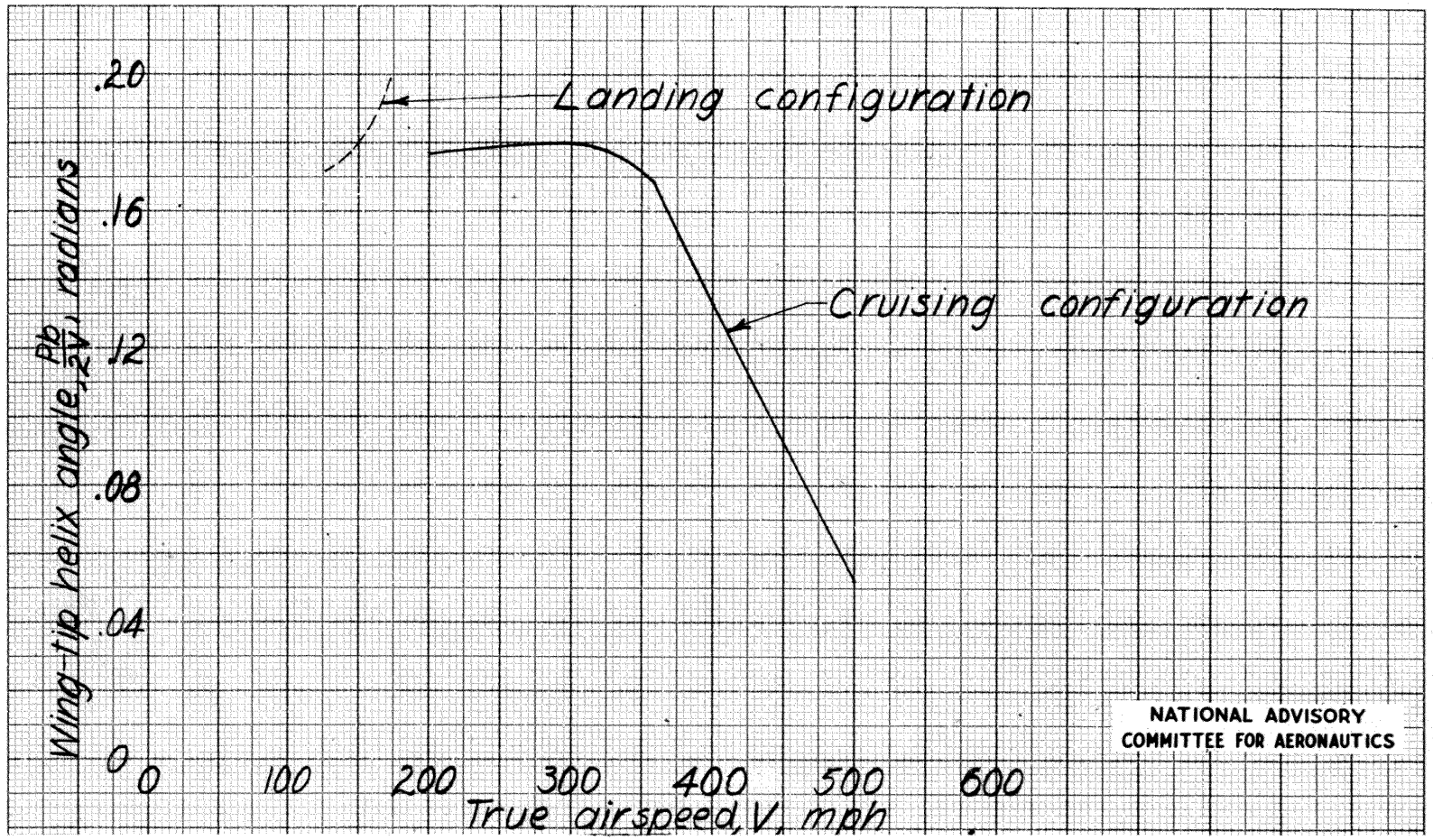

Figure 24: Estimated variation of wing-tip helix angle with airspeed at sea level for the full-scale Republic XP-84 airplane. Maximum aileron deflection with stick force limit of 30 lbs.; $\delta_r = 0$

End of Document